Valhalla U deposit

PREAMBLE

The Valhalla U deposit is an epigenetic, hydrothermal, structurally-controlled and albitite-hosted deposit of uranium, in which uraninite and coffinite are the most abundant uranium minerals, with lesser brannerite and mixed U-Zr-Si phases (Wilde et al, 2013). It is located within metabasalt and siltstone units of the Eastern Creek Volcanics, which form a thick rift sequence within the Leichhardt River Domain of the Mount Isa western succession (Figs 21.1 and 21.2).

Valhalla is the largest in a group of similar deposits in the region, none of which have been mined (Figs 21.3 and 21.4). The combined resources of in the Valhalla region of approximately 60,000 tonnes of U_3O_8 constitute Australia's third largest resource of uranium after Olympic Dam and Jabilkua.

Table 21.1. Published JORC Resources for uranium mineralisation in the Valhalla area (from Paladin website)

NATURE OF MINES

None of the uranium deposits in the area have been mined

PRODUCTION AND RESOURCES

Mineralised Bodies

Mineralisation in the Valhalla area is under thin alluvial/colluvial cover (Fig 21.5) and occurs in plunging shoots within discordant albitite bodies hosted within a variably-chloritised sequence of metabasalts and metasiltstones.

Dimensions

The main Valhalla shoot defines an elongate body plunging approximately 45° toward 165° with a long axis of approximately 600 metres, a subvertical intermediate axis of approximately 120 metres, and a subhorizontal short axis of approximately 60 metres. At Valhalla, there are two smaller but similarly-oriented shoots, all lying within a plane with an approximate orientation of 85° toward 255°.

Additional bodies to the south of the main Valhalla lodes (Valhalla South) and to the north (Odin) show similar plunges. The plunging shoot at Valhalla South has an approximate length of 200 metres, while the main shoot at Odin has an approximate length of 500 metres (Fig 21.51)

The Skal and Bikini deposits also show an association with discordant structures. In the case of the Bikini deposit, the mineralisation lies along a 1km-long structure striking 045°, and the single published cross section shows two 75° east-dipping zones with a downdip extent of about 250 metres each. At Skal, mapped zones of albitite trend between NE and NS and are mainly discordant to layering. Reported drill intersections appear to define a subvertical dip to the mineralised zones, which extend to a depth of approximately 200 metres. Reported significant intercepts appear to faintly define a southerly-plunge similar to that seen at Valhalla. No information was found relating to the geometry and dimensions of mineralised bodies at Mirrioola.

Deposit	Cut-off ppm U308	Measured				Indicated				Inferred				Total			
		Mt	Grade ppm	Tonnes U3O8	Mlb U3O8	Mt	Grade ppm	Tonnes U3O8	Mlb U3O8	Mt	Grade ppm	Tonnes U3O8	Mlb U3O8	Mt	Grade ppm	Tonnes U3O8	Mlb U3O8
Valhalla	230	16	820	13,120	28.9	18.6	840	15,624	34.5	9.1	640	5,824	12.8	43.7	792	34,610	76.2
Skal	250					14.3	640	9,152	20.2	1.4	520	728	1.6	15.7	630	9,891	21.8
Odin	250					8.2	555	4,551	10	5.8	590	3,422	7.6	14	569	7,966	17.6
Bikini	250					5.8	495	2,871	6.3	6.7	490	3,283	7.3	12.5	495	6,188	13.6
Mirrioola	250									2	560	1,120	2.5	2	566	1,132	2.5

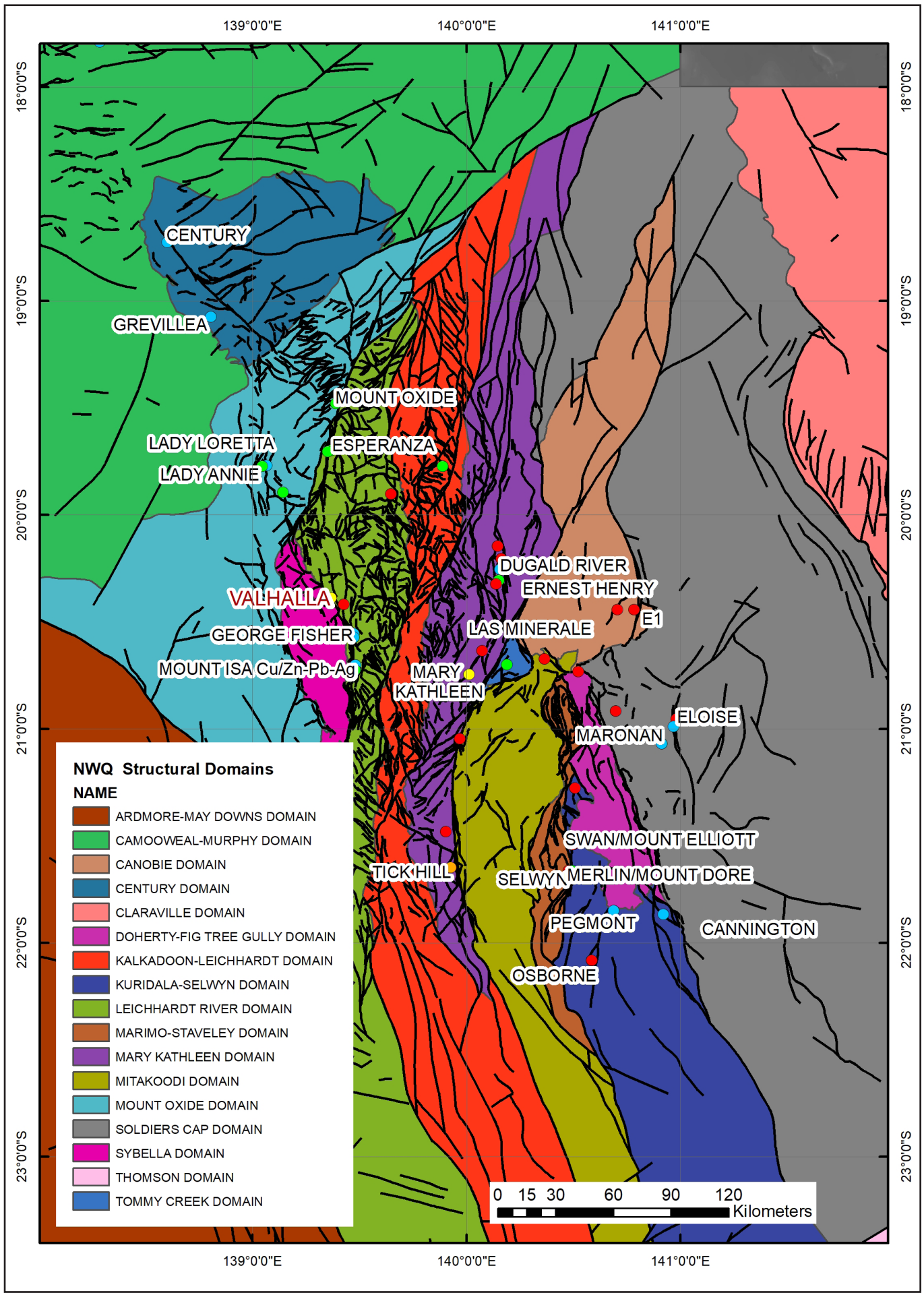

Figure 21.1. Regional location of Valhalla shown with respect to the Mount Isa Structural Domain Map from the 2010 NWQMEP GIS

Mineral Resources

Mineral resources reported by Paladin are summarised in Table 21.1. Together, the reported resources constitute Australia's third largest uranium resource after Olympic Dam and Jabiluka. Uranium is the only commodities for which resources have been estimated.

HOST ROCKS

Local Stratigraphy

Uranium mineralisation in the Valhalla region is predominantly hosted in metabasalts and metasiltstones of the Eastern Creek Volcanics (ECV) (Fig 21.4). The ECVs are indirectly dated at approximately 1779±4Ma based on maximum depositional age of the Lena Quartzite member (GSQ, 2011). In the Valhalla area, mineralisation occurs within basalts and fine-grained metasediments of the Cromwell Metabasalt Member, which is the lower of the two main volcanic packages within the Eastern Creek Volcanics.

Major Host Rock

Polito et al (2009) reported three main rock-types as hosts to the Valhalla deposit: metabasalt (ECV); weakly altered clastic sediments (WACS); and moderately altered fine-grained sediment (MAFS).

Metabasalt

Polito et al (2009) report that the ECVs are composed of varying amounts of epidote, actinolite, albite, calcite, sphene, chlorite and magnetite. Variants of this assemblage exposed in drilling at Valhalla include:

- Fine-grained calcite, albite and magnetite cut by fine chlorite veins and coarser quartz veins;
- Medium-grained equigranular albite-chlorite-magnetite ± biotite rock cut by quartz and calcite veins
- Fine-grained hematite-quartz-sphene with elongate albite grains and epidote-filled amygdales

Weakly altered clastic sediments

This rocktype consists of fine-grained sandstones and gritty siltstones with grains of feldspar, quartz, biotite, muscovite and variable amounts of Fe-, Mg-silicates, hematite and (titano)magnetite (Polito et al 2009). Polito et al (2009) report the presence of chlorite which is sometimes overprinted by anastomosing veinlets of illite. These sediments are recognised in a series of four interbedded zones labelled IJ, JK, KL and LM by Wilde et al (2013).

Moderately altered fine-grained sediment

Polito et al (2009) report the presence of MAFS at the margins of mineralisation, in which the original sedimentary rock is replaced by albite, calcite, minor amphibole and traces of red hematite.

INTRUSIVE ROCKS

Granitoids

There are no granitoid bodies mapped in the region of the deposit, though the Sybella Batholith is located approximately 10 kilometres to the southwest of the Valhalla deposit.

Mafic Intrusives

Regional mapping shows a series of layer-parallel and concordant dolerite dykes and sills, particularly in the Leander Quartzite immediately to the northeast of the Valhalla deposit. The actual host sequence to the mineralisation is poorly exposed, and it is difficult to trace the dykes into the ECVs as the dykes in this area don't appear to have a strong magnetic signature.

METAMORPHISM

Rocks in the Western Succession in the area of the Valhalla deposit are reported to have reached greenschist facies metamorphic conditions. Heinrich et al (1993) estimate peak regional metamorphic conditions for the area to have reached 350°C and 2-3 kbar on the basis of interpreted equilibria of peak metamorphic mineral assemblages (albite-chlorite-actinolite-epidote-sphene-magnetite-quartz-biotite). This temperature estimate is in agreement with the estimate of Polito et al (2009) based on analysis of isotopic fractionation between cogenetic calcite and riebeckite, which indicates formation of the calcite-riebeckite assemblage at temperatures between 340 and 380°C.

STRUCTURAL CHARACTERISTICS

Structural Setting

Valhalla

Mineralisation at Valhalla occurs in a steeply southwest-dipping (approx. 70° toward 230°) and southwest-younging package of Cromwell metabasalt which lies on the west limb of the regional N-S Leichhardt anticline (O'Dea et al, 1997) (Figs 21.12, 21.13, 21.14). The Basalt

Figure 21.2. Regional location of Valhalla overlain on an image of total magnetic intensity from the GADDS data for the region

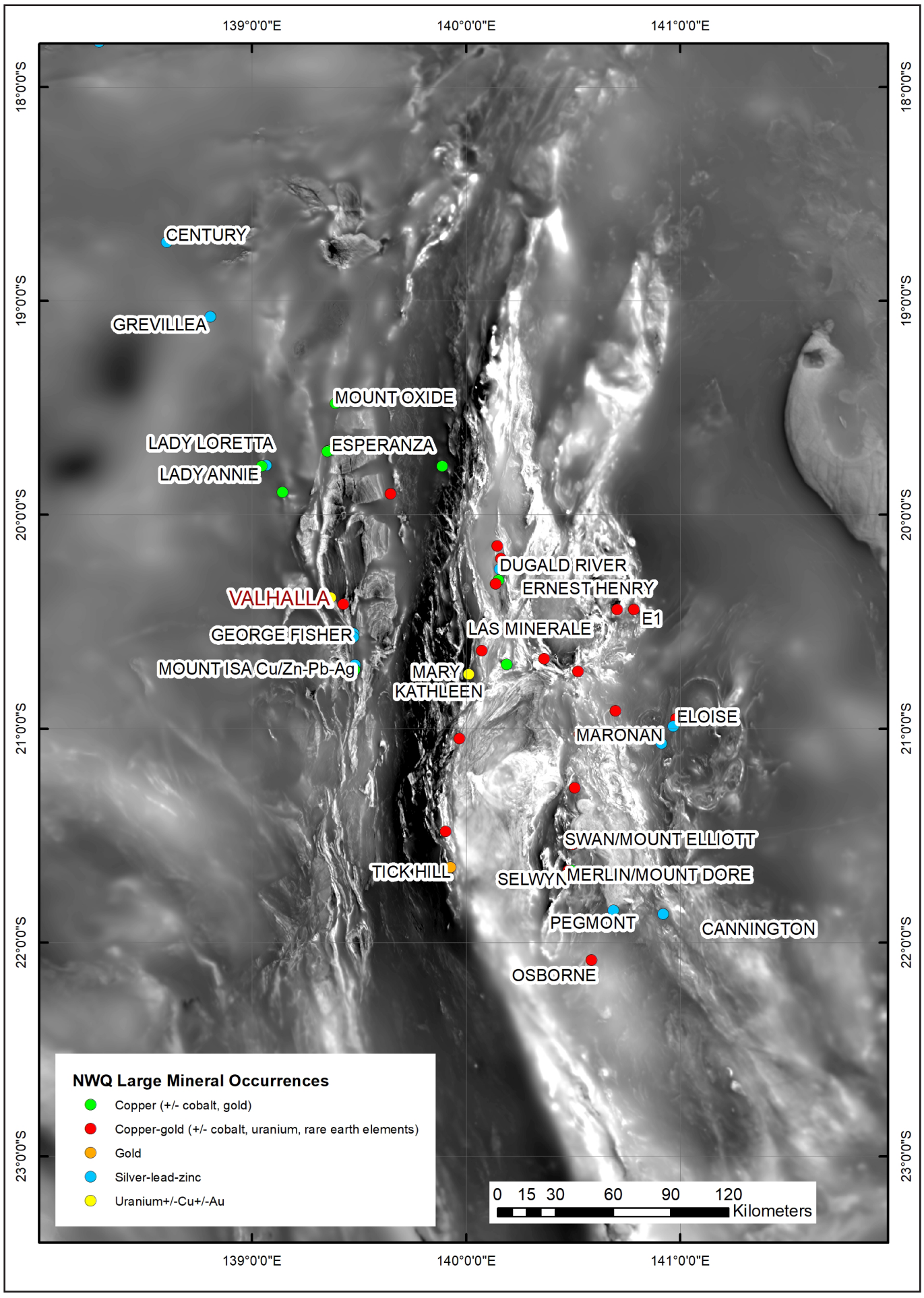

package appears to conformably overlie the Leander Quartzite to the northeast, but the NW-trending contact with the stratigraphically younger Myally Subgroup to the southwest appears to be slightly discordant in the magnetics.

Skal

Mineralisation at Skal is also hosted in the Cromwell metabasalt, but located on the eastern limb of the Leichhardt anticline and ESE-dipping and younging. Mineralised structures are discordant, striking NE, and both bedding and mineralised structures are cut and displaced sinistrally by NW-striking faults with displacements of up to several hundred metres.

Bikini

Mineralisation at Bikini is hosted in a NW-dipping and younging package of Cromwell metabasalt which is cut by closely-spaced NW-trending apparent sinistral faults, and the zone of more intense magnetisation which appears to be associated with mineralisation is rotated slightly clockwise from the strike of layering and is also displaced by the NW-trending apparent-sinistral faults.

Structural History

The structural history of the Leichhardt River domain has been well-studied (eg O'Dea et al, 1997a and b) (Figs 21.6 to 21.11). The ECVs and associated coarse clastic sequences were deposited in a roughly N-S zone (the Leichhardt River Domain) associated with E-W extension in a series of linked half graben. This sequence was then subjected to N-S extension, producing a series of north-tilted half graben and associated synchronous sedimentation which continued though the deposition of the mixed clastic-carbonate sequence of the Mount Isa Group. This architecture was then subjected to periods of N-S shortening (Isan D_1) and E-W shortening resulting in major N-S trending folds and associated reverse and strike-slip faults (Isan D_2) as well as more localised folding and later faulting (Isan D_3). In the area of the Valhalla, Skal and Bikini deposits, this history is manifest as a broad anticlinorium (the Leichhardt anticline which is cut by a series of N-S trending reverse faults, the main one of which is the Hero fault which cuts the eastern edge of the main body of Leander Quartzite to the east of the Valhalla deposit.

Structural Control on Mineralisation

Valhalla

Mineralisation at Valhalla is hosted in an albitite body which is discordant to stratigraphy within the ECV basalts and metasediments (Figs 21.38, 21.39, 21.51). The albitite body is spatially coincident with a N-S trending zone of weak magnetite alteration in the regional magnetics, which trends northward into a zone with small apparent sinistral displacement on markers within the ECVs. The albitite body has an

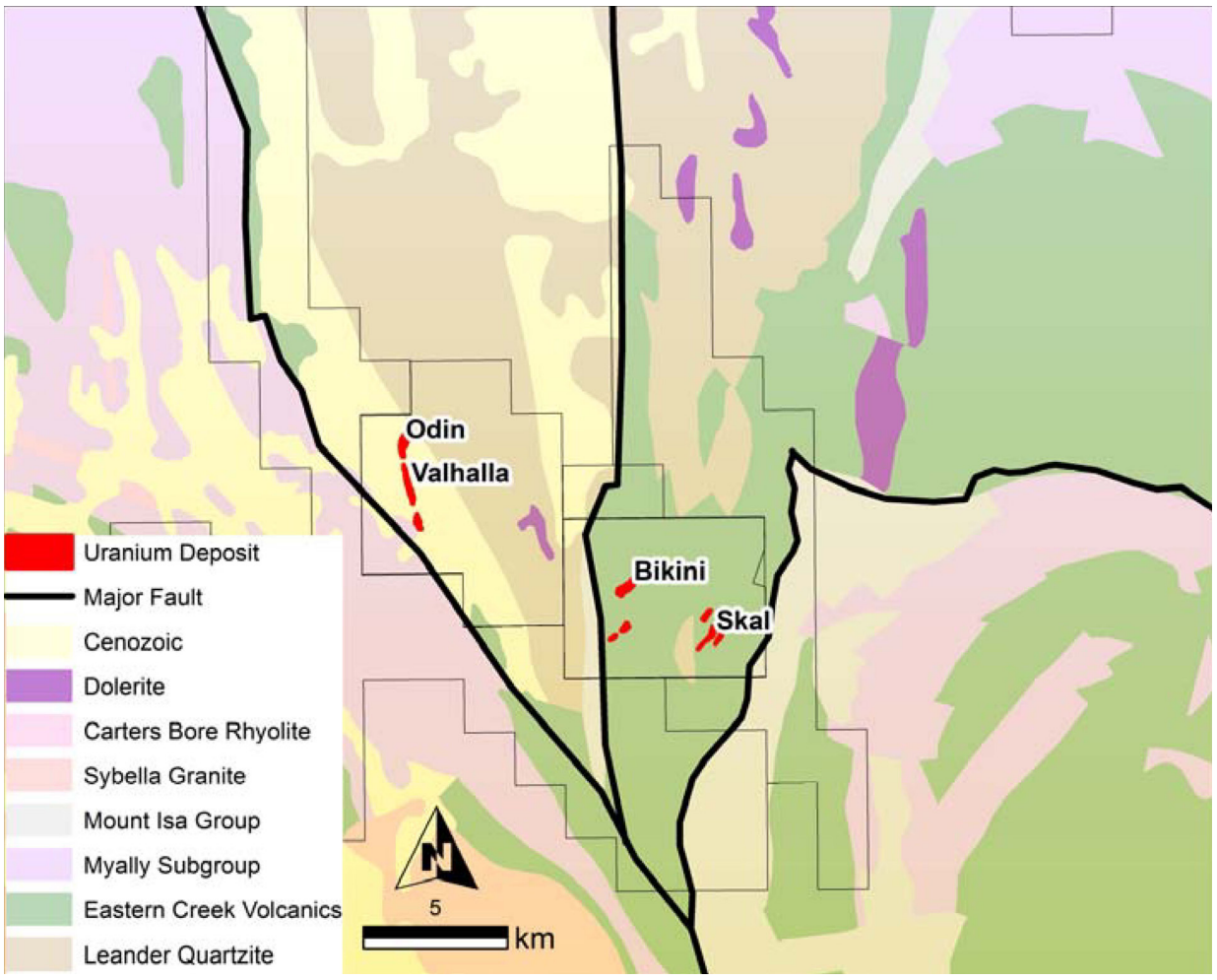

Figure 21.3. Regional location map of Valhalla region U deposits over regional geology.

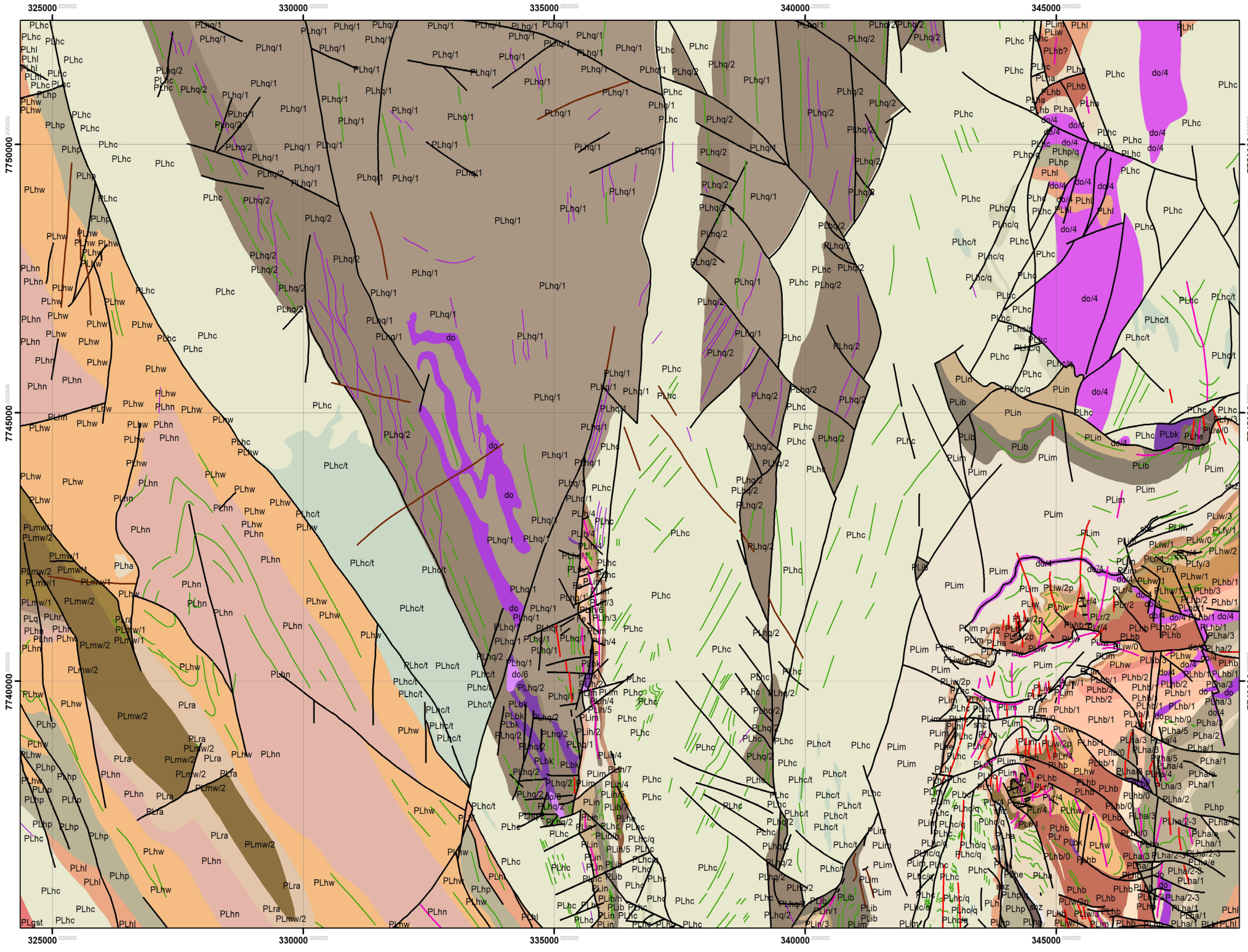

Figure 21.4. Geological map extracted from data provided by the Geological Survey of Queensland - legend on facing page. Note - the prefix “P” in the legend is labelled as “PL” on the map. Map Projection GDA94, MGA54.

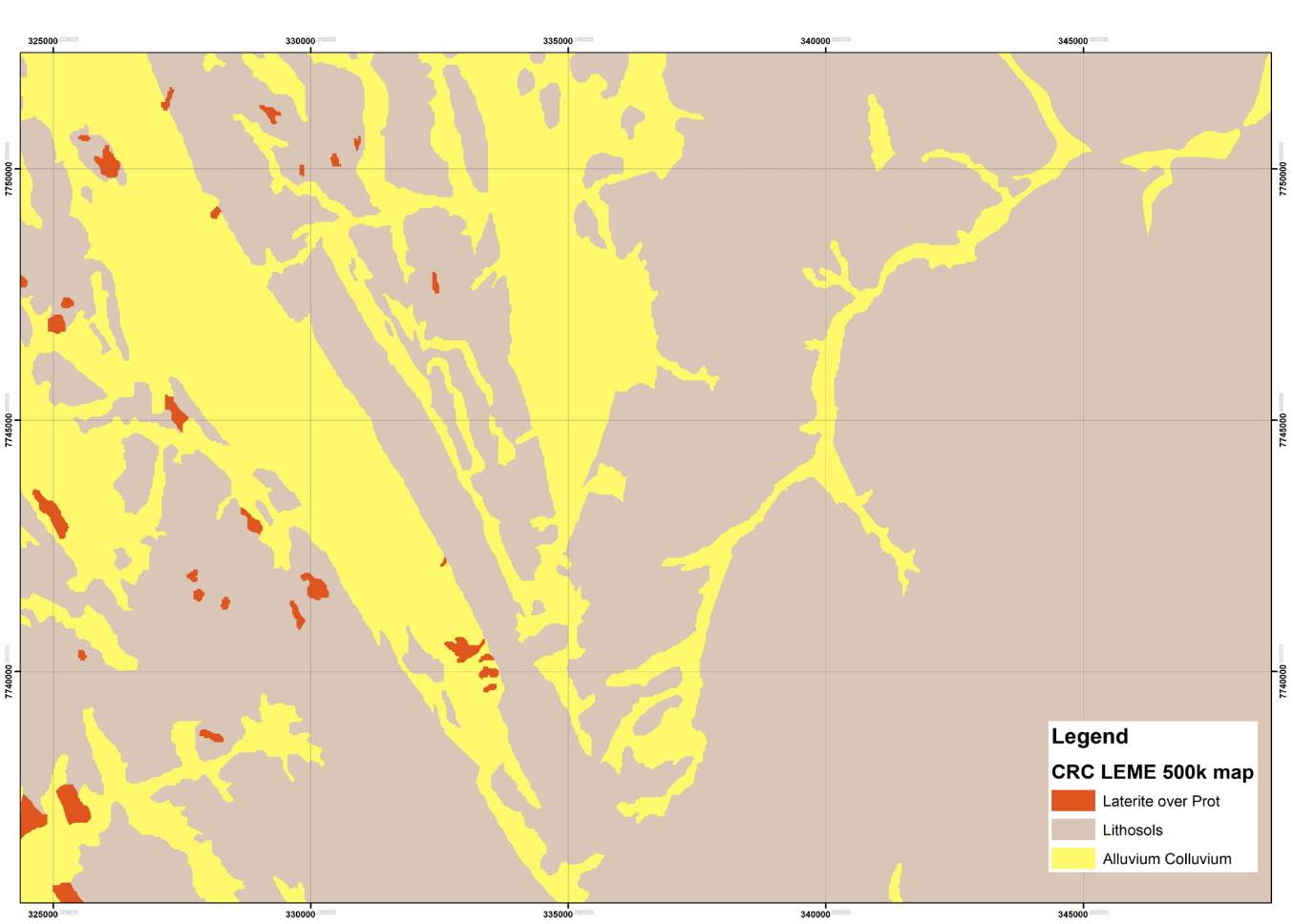

Figure 21.5. Extract of Mount Isa Region 1:500,000 regolith map, sourced from CRC LEME http://crcleme.org.au/Pubs/MAPS/mt_isa_500k.pdf. Map Projection GDA94, MGA54.

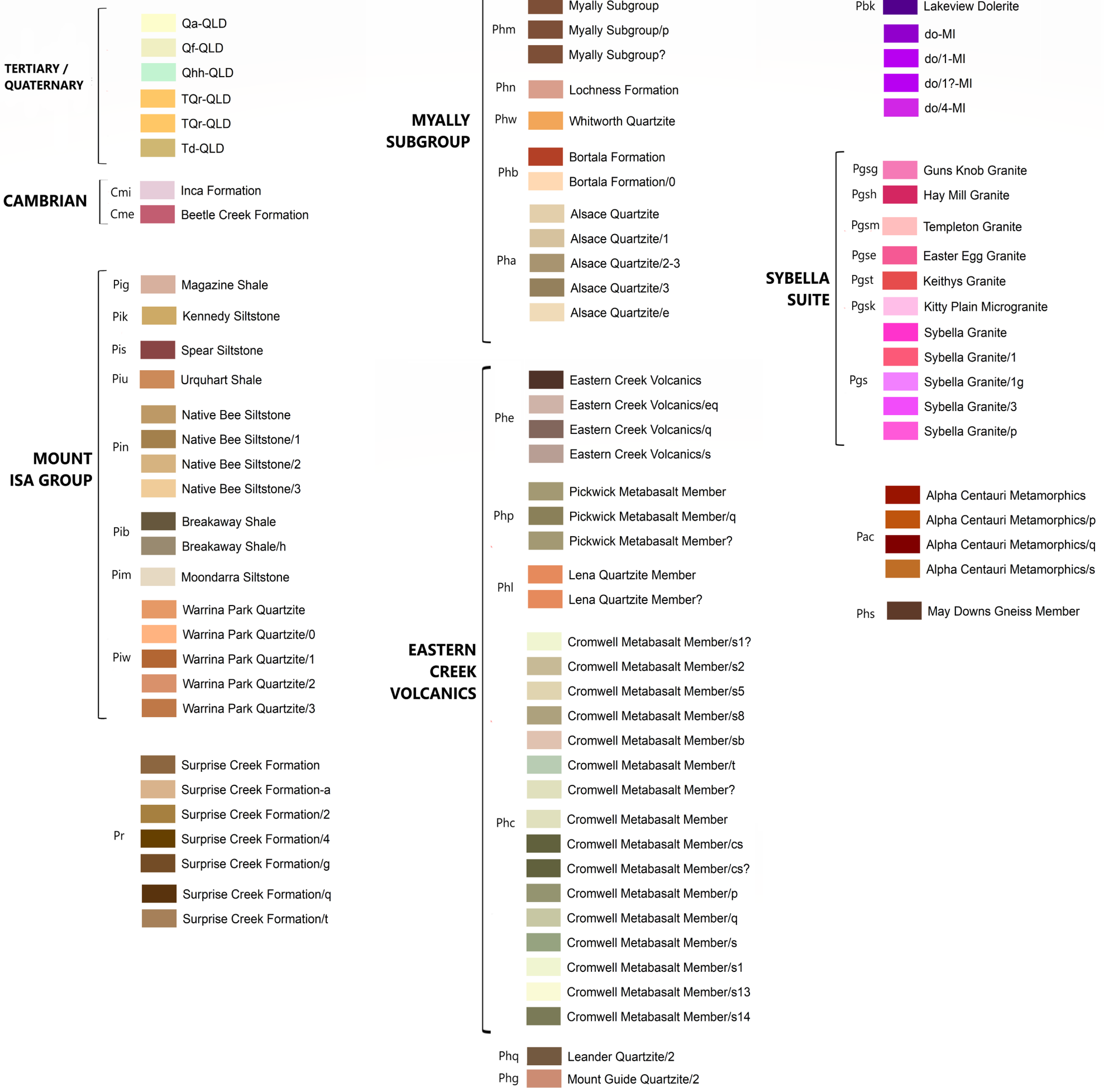

orientation of 85° toward 256°, and the intersection between this orientation and the orientation of bedding defines a southerly plunge which is parallel to the orientation of higher grade shoots within the Valhalla deposit. The lowermost and largest shoot is localised where the LM metasedimentary layer intersects the fault and associated albitite, suggesting that higher grade shoots at Valhalla were localised by the intersection between metasedimentary layers and the main controlling fault for the mineralisation.

MINERALISATION

General Characteristics

Uranium mineralisation at Valhalla is hosted within a subvertical and discordant body of albitite which shows a stable assemblage of albite-zircon-apatite-amphibole-magnetite.

Ore Mineralogy

Figs 21.43 to 21.49

Valhalla – based on QEMSCAN analysis (Wilde et al, 2013), approximately 50% of the Uranium is hosted in Uraninite and Coffinite, with the remainder hosted in Uranium-silicate and Uranium-carbonate intergrowths, as well as minor Brannerite and Zircon

Skal – based on QEMSCAN analysis (Wilde et al, 2013), approximately 50% of the Uranium is hosted in Brannerite, with about 30% in Uranium-silicate intergrowths, 15% in coffinite, and the remainder in Uraninite and Uranium-carbonate intergrowths

Bikini – based on QEMSCAN analysis (Wilde et al, 2013), approximately 75% of the Uranium is hosted in Brannerite, with most of the remainder in Coffinite and Uranium-silicate intergrowths, as well as trace Uranium – Fe-Oxide intergrowths.

Gangue Mineralogy

Analysis of gangue mineralogy by Wilde et al (2013) at Valhalla shows that albite and amphibole make up about 54% of the sample mineralogy. These occur along with approximately 8.9% carbonates comprising a mixture of calcite, dolomite and ankerite; as well as high contents of hydrothermal apatite (approximately 8%) and zircon (approximately 5.6%).

Paragenesis

Two detailed studies of paragenesis exist for Valhalla and associated deposits. Polito et al (2009) studied a single drillhole (V39) from the Valhalla deposit, and Wilde et al (2013) studied selected samples from Valhalla, Skal, and Bikini, and supplemented traditional petrographic studies with QEMSCAN and high resolution electron microprobe. Both studies

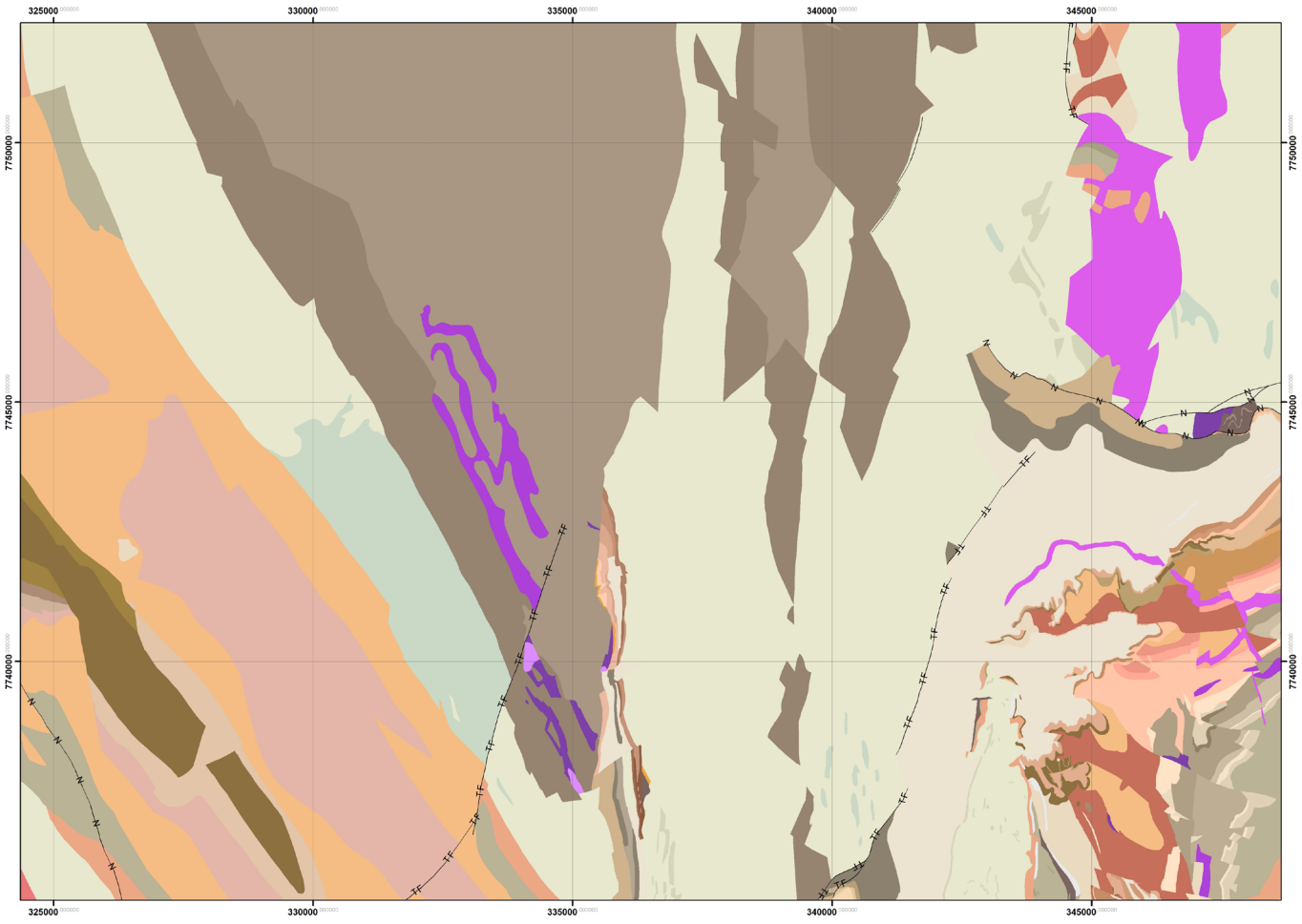

Figure 21.6. Wonga-age timesliced structures from the 2010 DNRME NW Mineral and Energy Province GIS. Map Projection GDA94, MGA54.

Figure 21.7. OP1-age timesliced structures from the 2010 DNRME NW Mineral and Energy Province GIS. . Map Projection AGD84, AMG54.

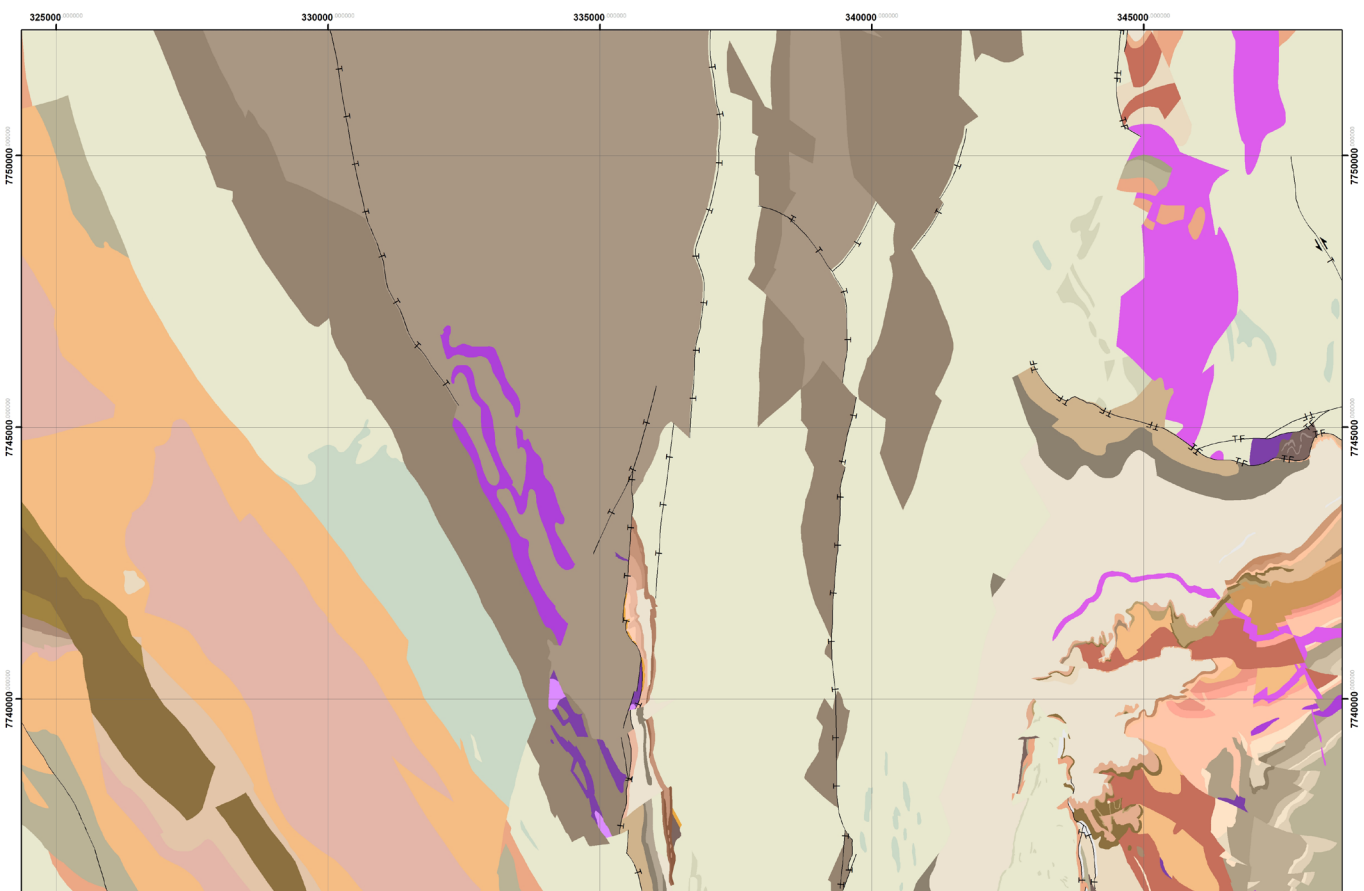

Figure 21.8. D1640-1620-age timesliced structures from the 2010 DNRME NW Mineral and Energy Province GIS. . Map Projection GDA94, MGA54.

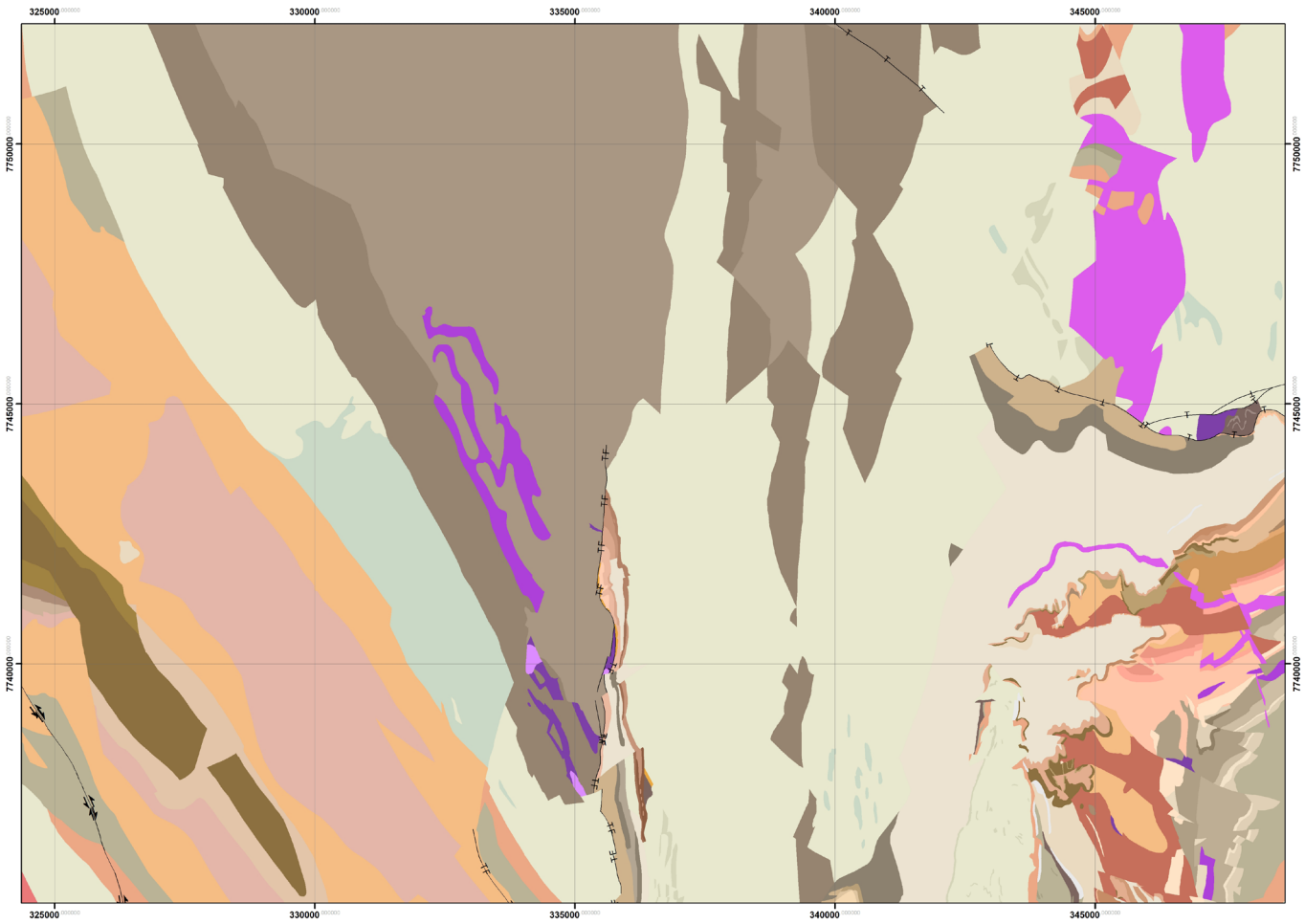

Figure 21.9. Isa D1-age timesliced structures from the 2010 DNRME NW Mineral and Energy Province GIS. . Map Projection GDA94, MGA54.

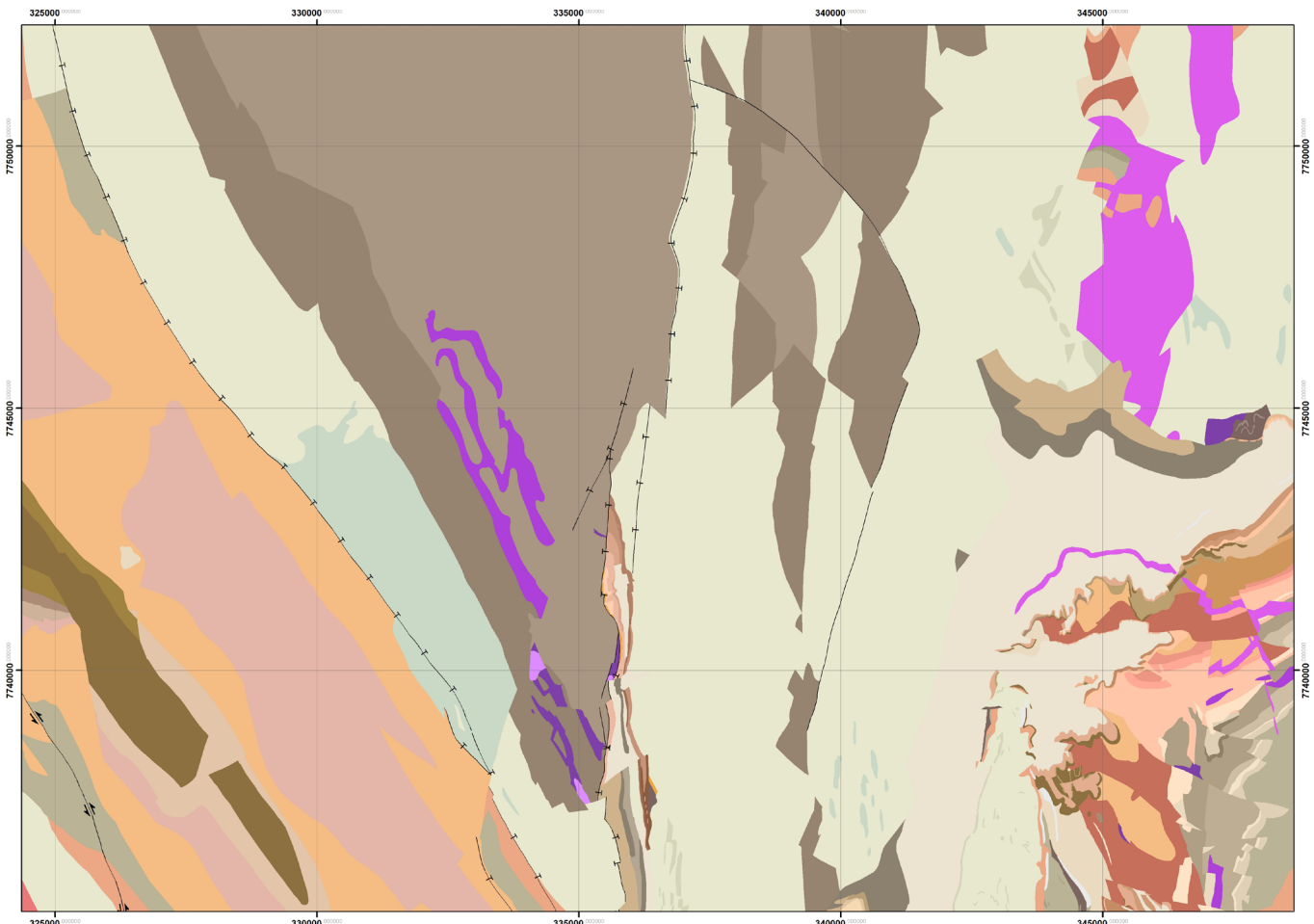

Figure 21.10 Isa D2-age timesliced structures from the 2010 DNRME NW Mineral and Energy Province GIS. . Map Projection GDA94, MGA54.

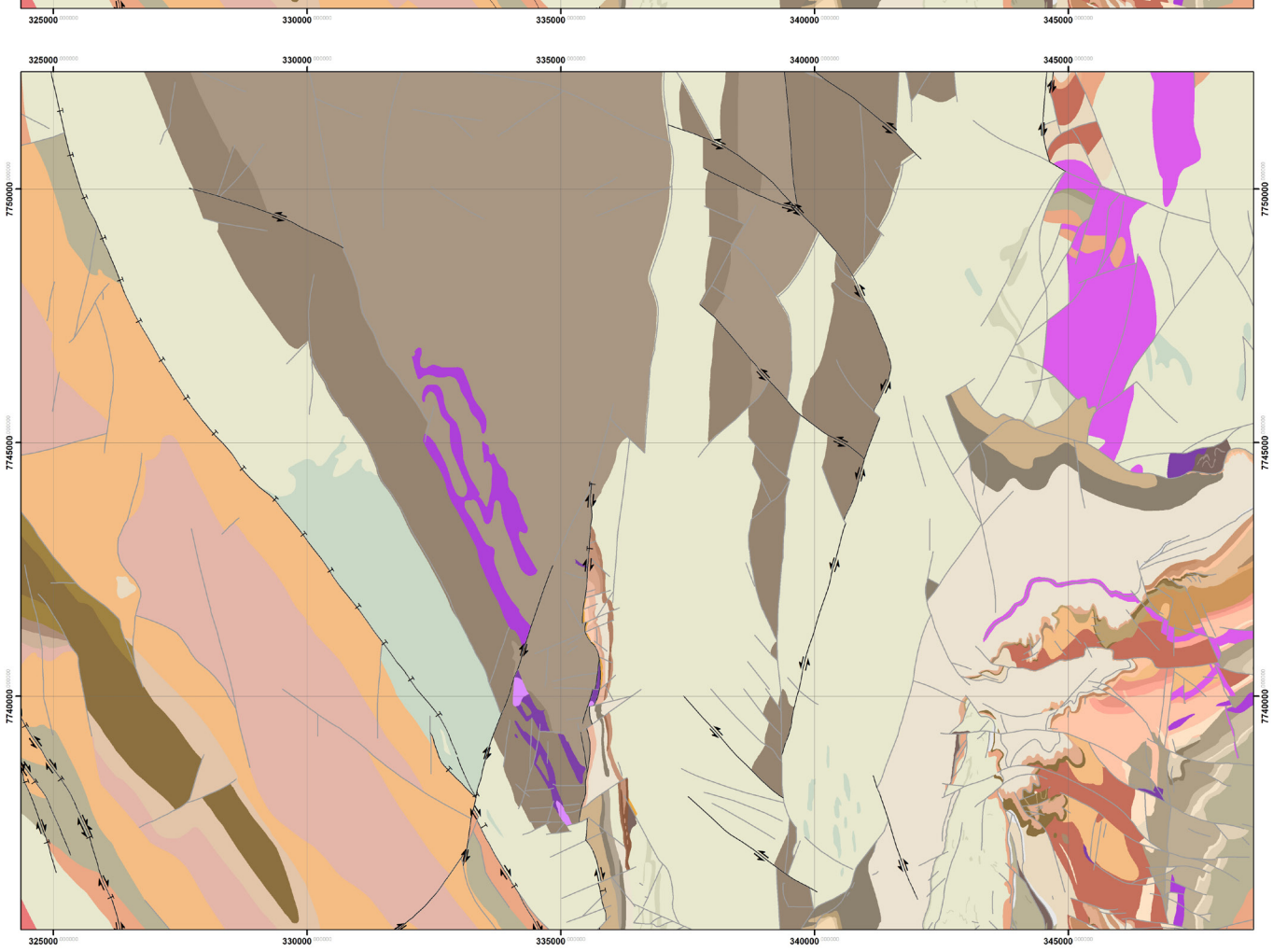

Figure 21.11. Isa D3-age timesliced structures from the 2010 DNRME NW Mineral and Energy Province GIS. . Map Projection GDA94, MGA54.

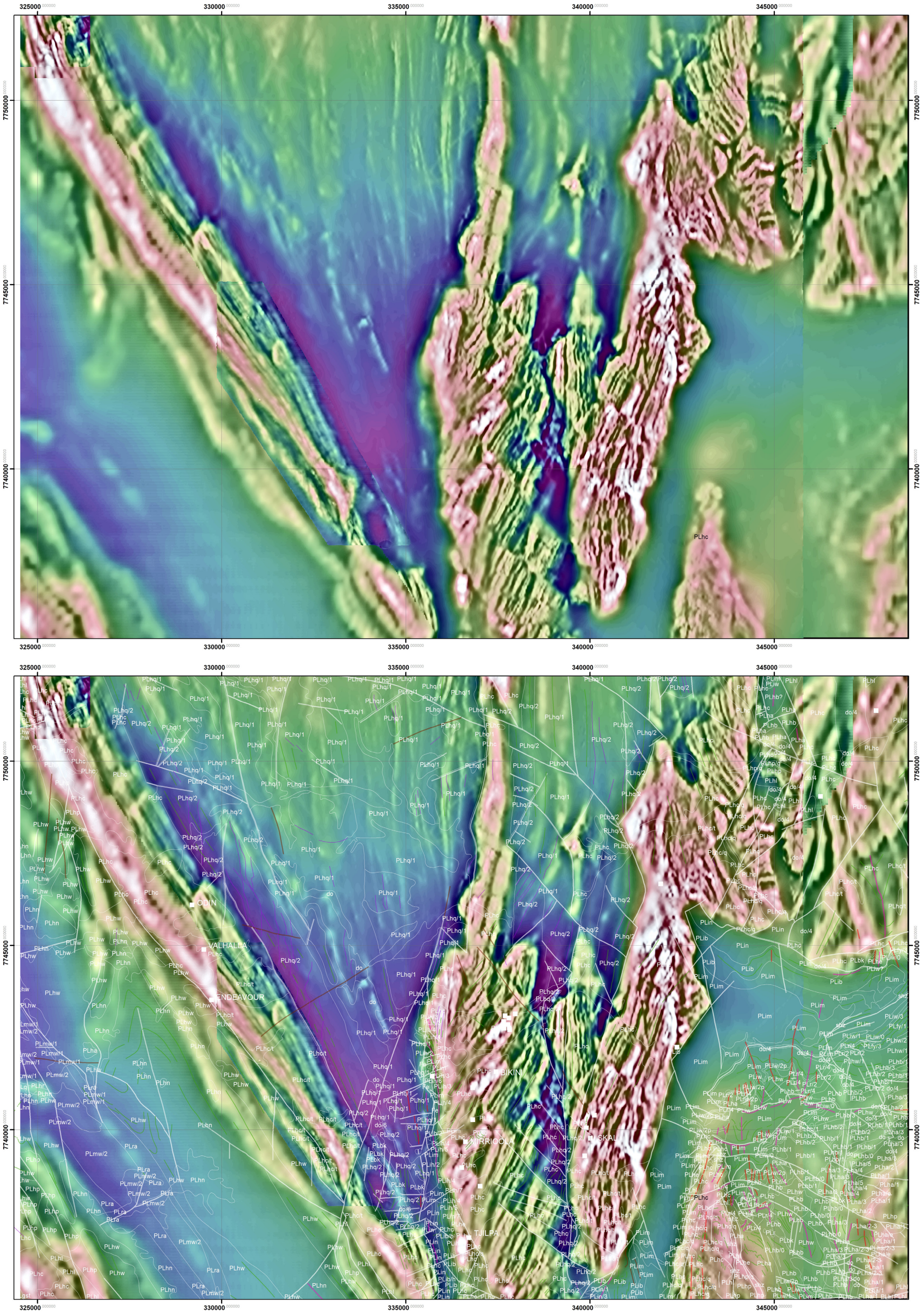
325000
330000
335000
340000
345000
7750000
7745000
7740000
PLhc
ODIN
VALHALLA
ENDEAVOUR
BIKINI
MIRRIOOLA
SKAL
TJILPA

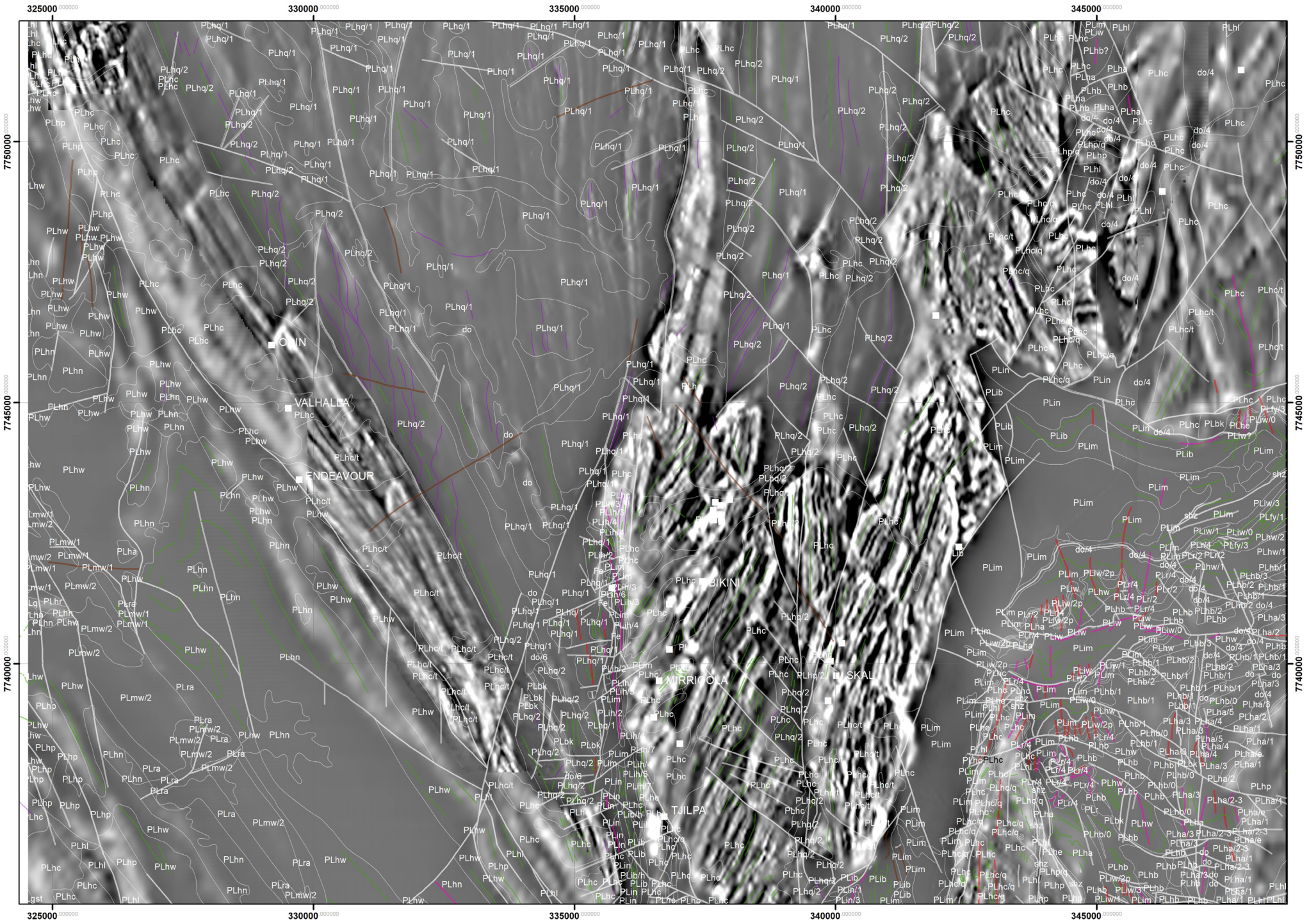

Figure 21.14. Geological boundaries and unit codes superimposed on greyscale first vertical derivative of RTP. Map Projection GDA94, MGA54.

Figure 21.12. Facing page, upper frame. Merged open file magnetic datasets from the Valhalla area - colour Reduced to Pole (RTP) of greyscale first vertical derivative of RTP. Map Projection GDA94, MGA54.

Figure 21.13. Facing page, lower frame. Geological boundaries and unit codes superimposed on merged open file magnetic datasets from the Valhalla area - colour Reduced to Pole (RTP) of greyscale first vertical derivative of RTP. . Map Projection GDA94, MGA54.

recognise an early synmetamorphic sodic alteration assemblage, but differ slightly on details. Polito et al (2009) define the following:

- an early stage of albite, riebeckite, calcite and dolomite with minor hematite, brannerite and uraninite;
- the main stage of mineralisation associated with brannerite, apatite, uranoan zircon, hematite and anatase; and
- a late stage of hematite, uraninite, chlorite, calcite, pyrite, dolomite, chalcopyrite, galena, vein quartz and sulphides

On the other hand, Wilde et al (2013) define a slightly different paragenesis comprising

- Early sodic – albite; riebeckite; aegirine; apatite; zircon and magnetite
- Main stage mineralisation in potassic microveins - K-feldspar; biotite; coffinite; brannerite; rare uraninite; ilmenite and rutile
- Late stage – Calcite; epidote and sulphide veinlets

A significant difference between the two interpretations is the observation in Wilde et al (2013) that the main stage of uranium mineralisation is spatially associated with K-feldspar and biotite, though the two potassic minerals are not sufficiently volumetrically significant to affect lithogeochemical patterns.

ALTERATION HALO

General Characteristics

Mineralisation at Valhalla is hosted in a broad zone of albitite which extends between 0-20 metres to the hangingwall and footwall of mineralised shoots but may persist several hundred metres away in the plane of the body.

Inner Halo

The inner halo is defined by the presence of increased albite, calcite, minor amphibole and hematite dusting (Polito et al 2009). Wilde et al (2013) note that the two minerals which most clearly characterise the halo to Valhalla are albite and chlorite.

Albitite halo

They also state that such albitites are relatively rare when not associated with uranium mineralisation. Albitites are the main host to the mineralisation, but are also more laterally extensive along and across strike of the hosting structure. It is difficult to assess the full extent of the resulting halo based on the limited drilling available, but the radiometric and magnetic response attributable to known albitite bodies suggests that these bodies are relatively extensive, mappable and good potential guides to mineralisation.

Chlorite halo

The definition of chlorite schist is less clear as descriptions of unaltered ECV metabasalts show that chlorite is often present in the groundmass. However, lithogeochemical

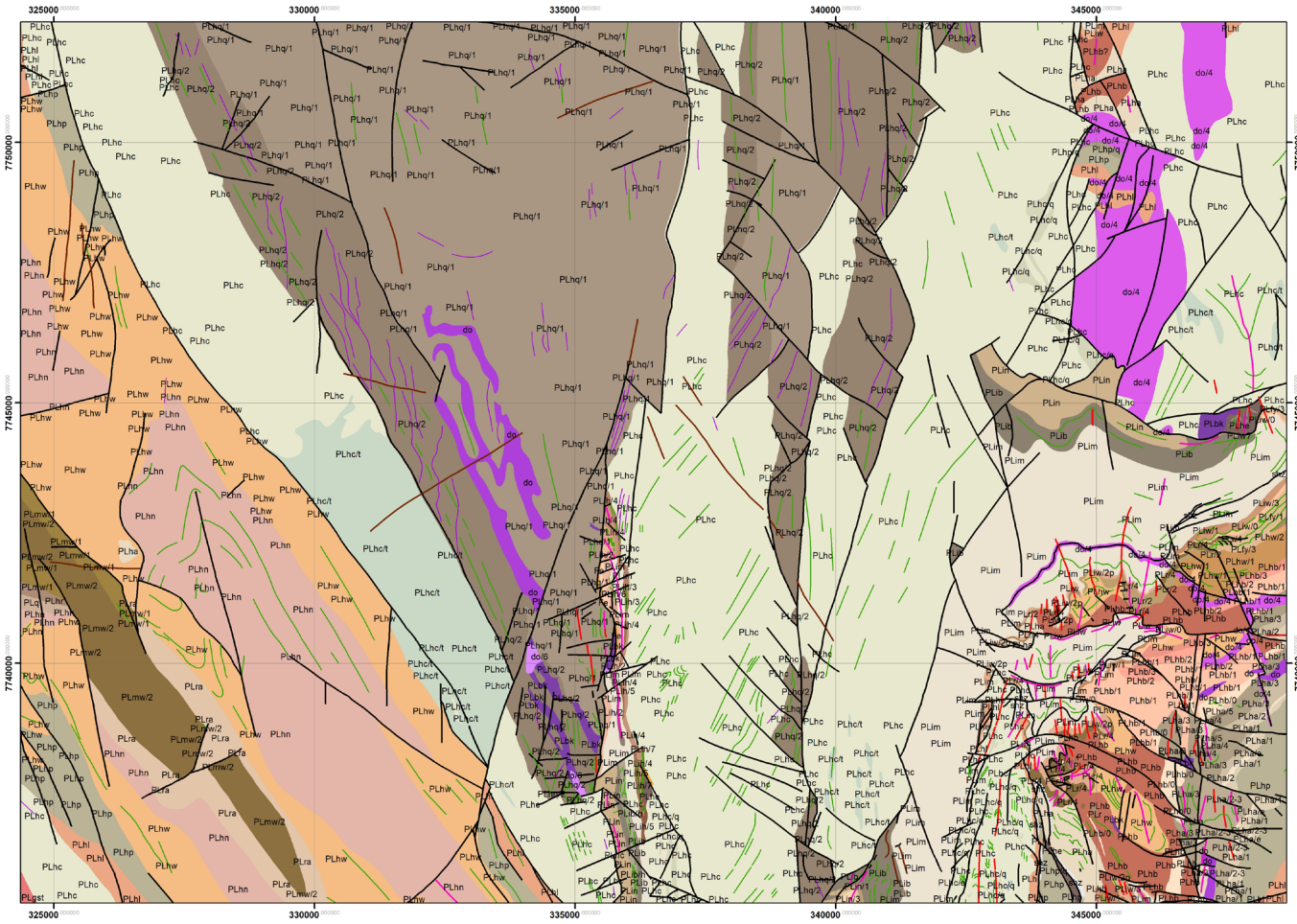

Figure 21.15. Geological map extracted from data provided by the Geological Survey of Queensland - legend on facing page. For reference for other figures on page. Map Projection GDA94, MGA54.

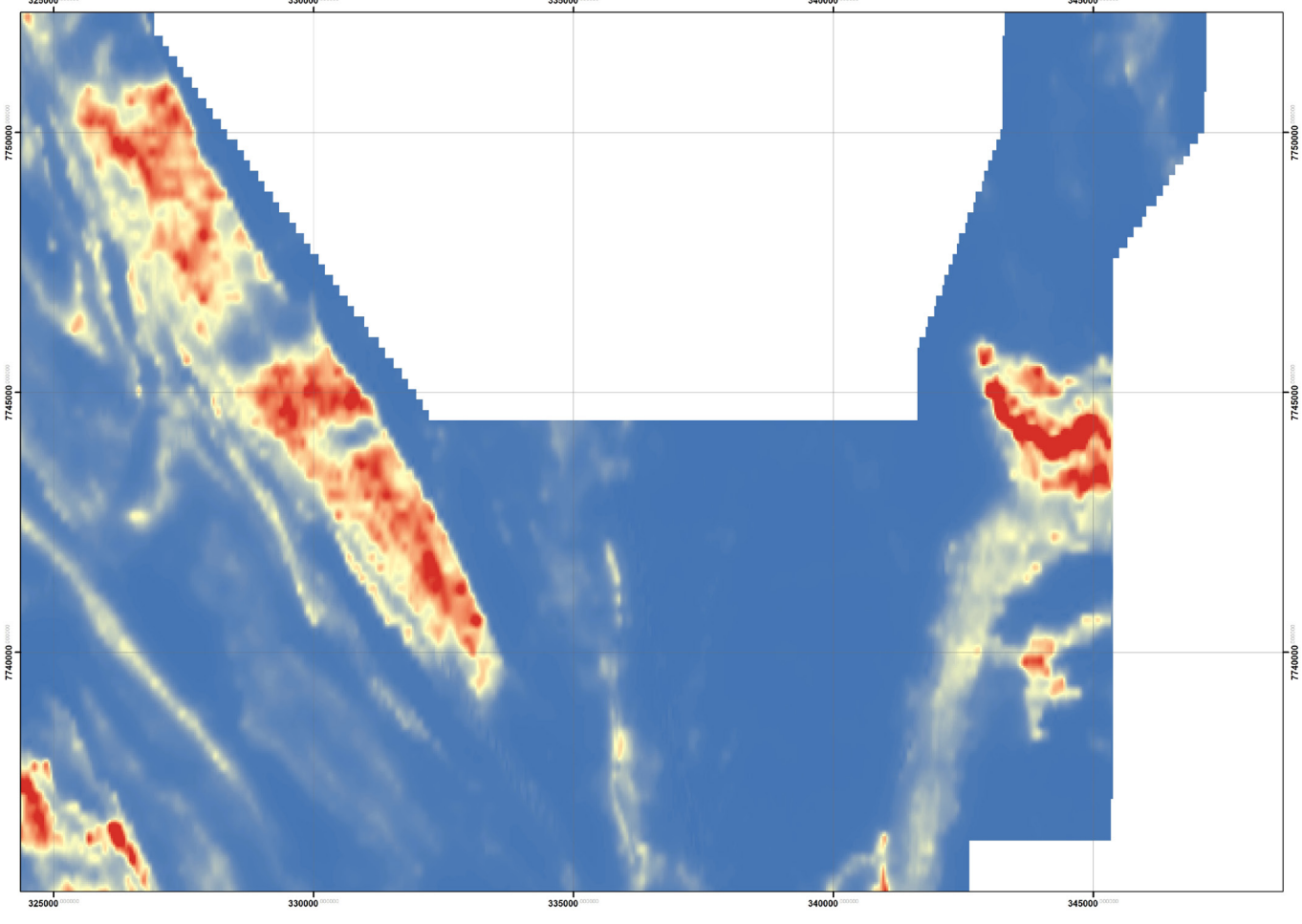

Figure 21.18. Facing page - upper. Merged radiometric data from the Valhalla area - RGB image with Red-K; Green-Th; Blue - U. Geological units and prospects overlain in white. Map Projection GDA94, MGA54.

Figure 21.16. Helicopter VTM EM data from the open file Calton survey (QDEX1249). Image of Channel 10 B-field, which is designed to enhance highly conductive sources (Smith and Annan, 1998). Map Projection AGD84, AMG54.

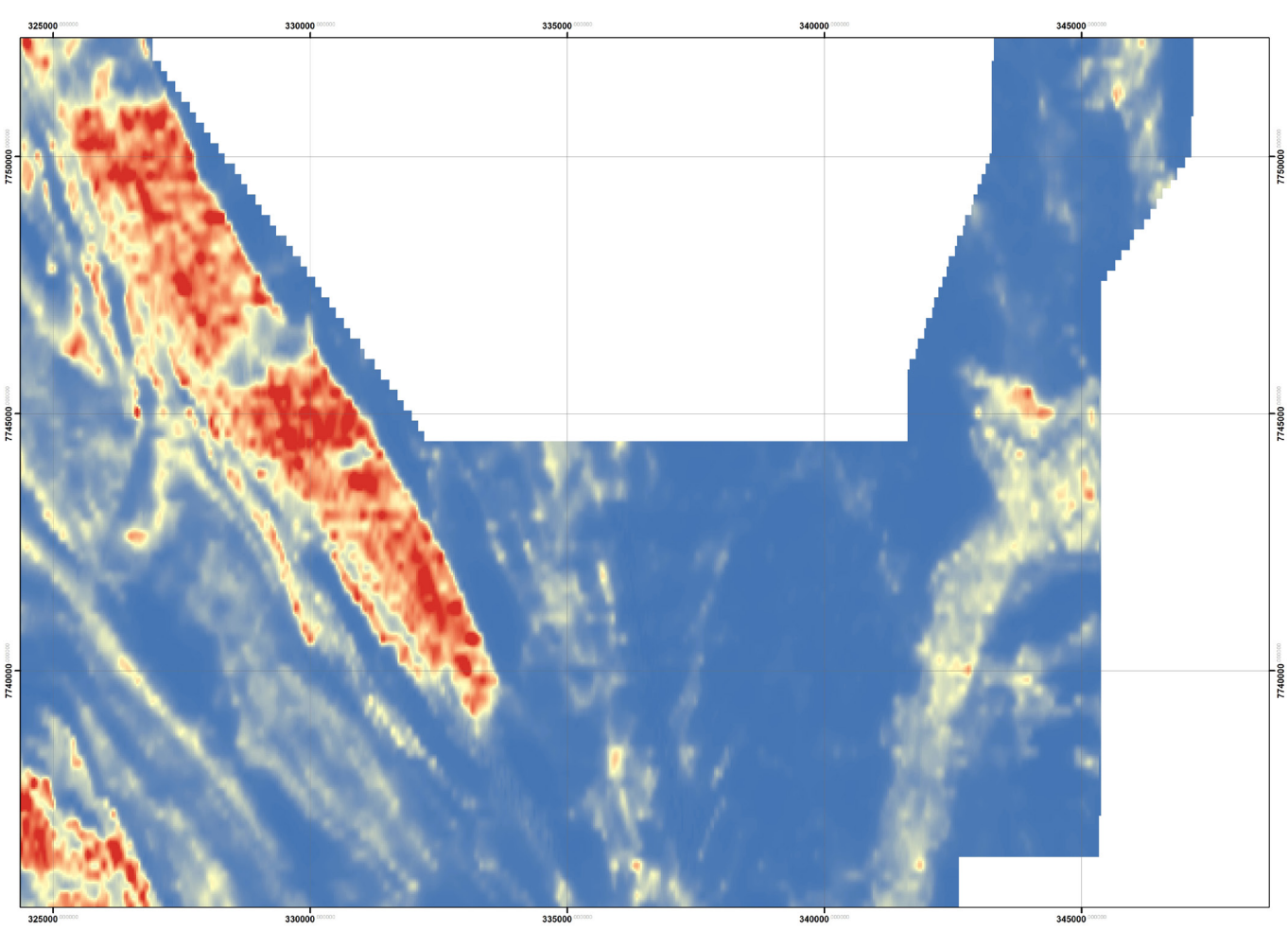

Figure 21.19. Facing page - lower. Merged radiometric data from the Valhalla area - RGB image with Red-K; Green-Th; Blue - U. Map Projection GDA94, MGA54.

Figure 21.17. Helicopter VTM EM data from the open file Calton survey (QDEX1249). Image of Channel 10 dB/dt, which is representative of conductance in low to moderate conductance sources (Smith and Annan, 1998). Map Projection GDA94, MGA54.

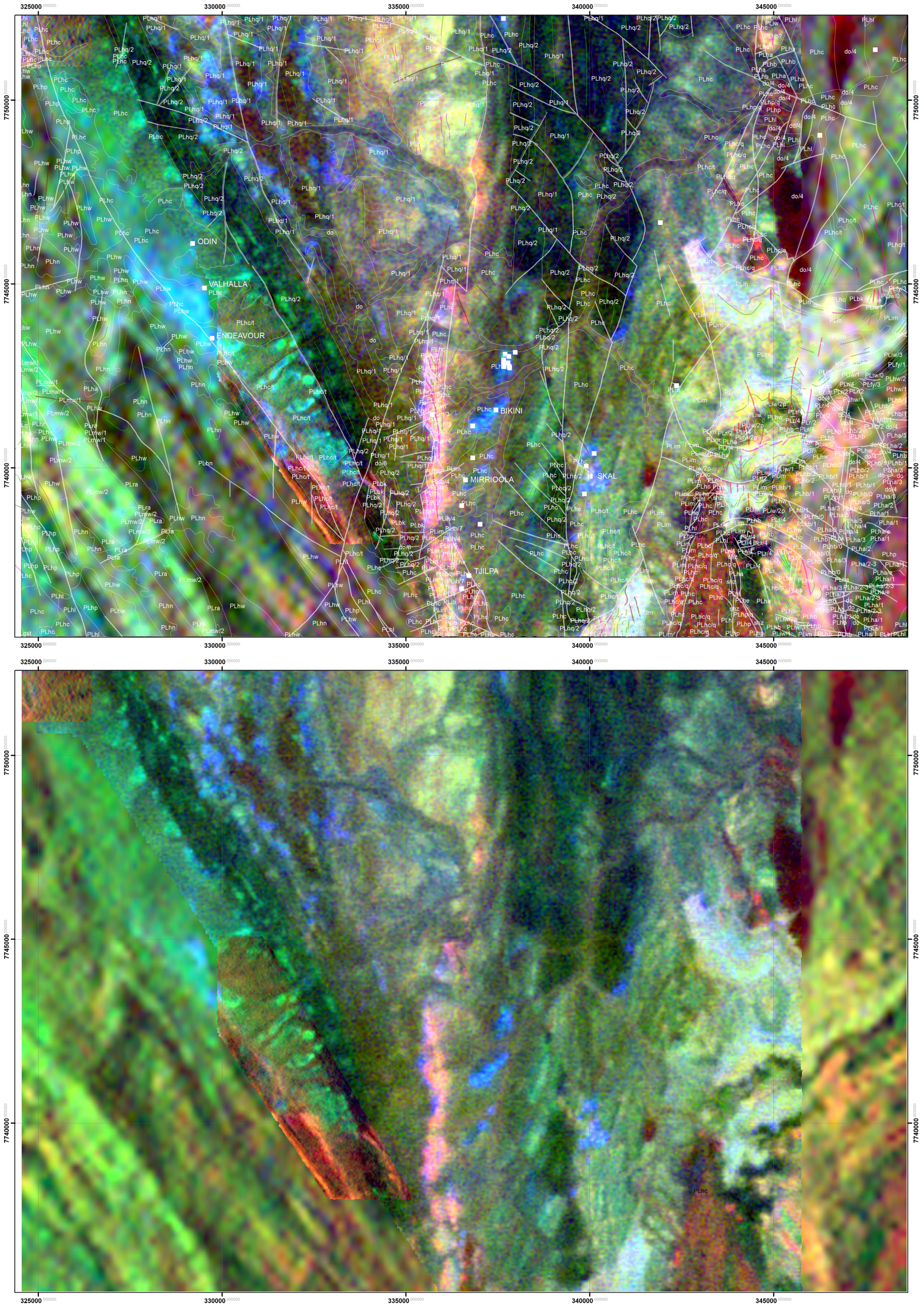
325000
330000
335000
340000
345000
7750000
7745000
7740000
ODIN
VALHALLA
ENDEAVOUR
BIKINI
MIRRIOOLA
TJILPA
SKAL
PLhc

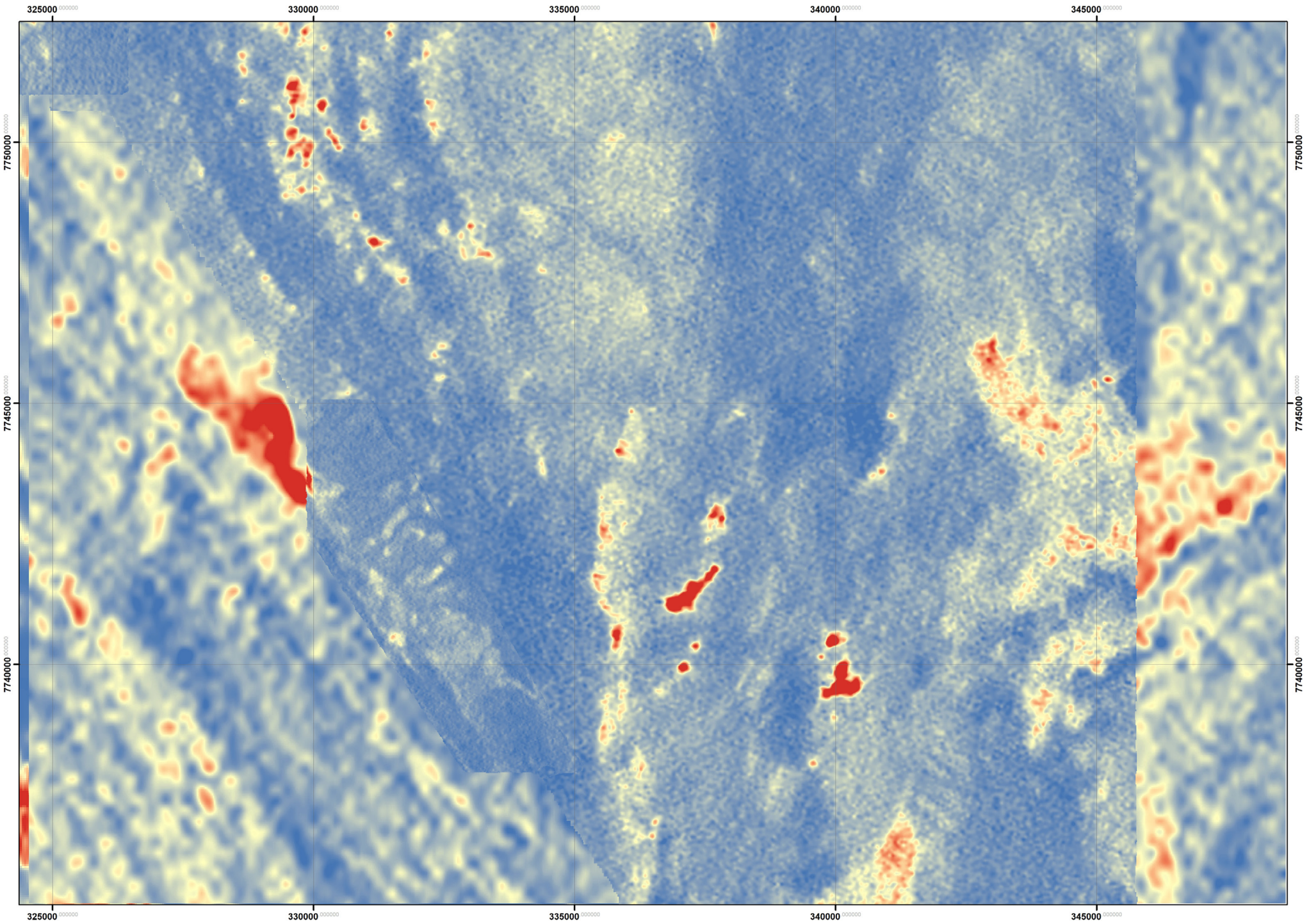

Figure 21.20. Merged radiometric data from the Valhalla area - U counts image. Map Projection GDA94, MGA54.

analysis (Wilde et al 2013) shows that chlorite schist alteration has a distinctive geochemical signature when compred to unaltered metabasalt. Chlorite schist is much less commonly associated with mineralisation, but assessment of the Valhalla drill dataset shows that logged chlorite schist appears to be slightly more extensive across and along strike of the hosting structure. Chlorite schist is even more extensive at Bikini, where albitites and associated uranium mineralisation occur within bodies of chlorite schist up to 150 metres wide.

Lithogeochemical trends

Figs 21.24 to 21.28; 21.50

Polito et al (2009) observed the following lithogeochemical trends associated with mineralisation:

- Addition of Na, U, V, Zr, P, Sr, Y
- Depletion of K, Si, Rb and Ba

Wilde et al (2013) analysed a broader range of samples from Valhalla and other uranium occurrences in the region, and reached the following conclusions:

- A strong bulk gain in Na and bulk loss of K
- A loss in Si in metasediments, though less pronounced in metabasalts
- Enrichment in Zr, Hf, Cu, and V
- Good correlation between U and Zr, Hf, HREE and Th

Neither study provided the information which would allow a spatial assessment of the lithogeochemical halo.

Outer Halo

There is little geological or geochemical information available to define an outer halo for the Valhalla, Skal and Bikini deposits. However, the expression of the mineralisation in magnetic and radiometric datasets is relatively distinctive, and defines zones of elevated magnetic and radiometric response that are significantly more extensive than the footprints of the actual deposits.

HYMAP DATA

HyMap data was acquired in 2006-2007 over the district as part of the Stage 2 Block E Mount Isa survey. Figures 18.12 to 18.16 are representative images of the HyMap data, which cover the Valhalla deposit and region. The spatial resolution of the HyMap sensor is 3-10m depending on flight height.

The data was flown on behalf of the Geological Survey of Queensland and CSIRO, and imagery is available at: https://qdexdata.dnrme.qld.gov.au/gdp/search

The principal reference for the program is Cudahy et al (2008).

The images presented in this document are as follows:

False colour image: with RGB representing the reflectance bands 750nm, 650nm, 550nm, respectively (Figure 21.29).

Ferric oxide abundance: Attempts to map hematite, goethite, 'limonite', and Fe3+ pyroxenes, olivines and carbonates by using the normalized depth of the 900nm absorption feature. Blue to red represents low (~10% Fe2O3) to high (~60% Fe2O3) abundance. High confidence (Figure 21.30).

Ferrous iron and MgOH: Attempts to map Fe^{2++}-bearing minerals like actinolite, some chlorites, ankerite and siderite. Blue to red represent low to high content of ferrous iron in pixels with MgOH (+carbonate) mineralogy (black is below threshold). Moderate confidence. There is a zone with anomalous appearance at the south end of the Valhalla trend. (Figure 21.31).

Kaolin composition: deep blue approximates dickite, blue-green is halloysite and/or poor-

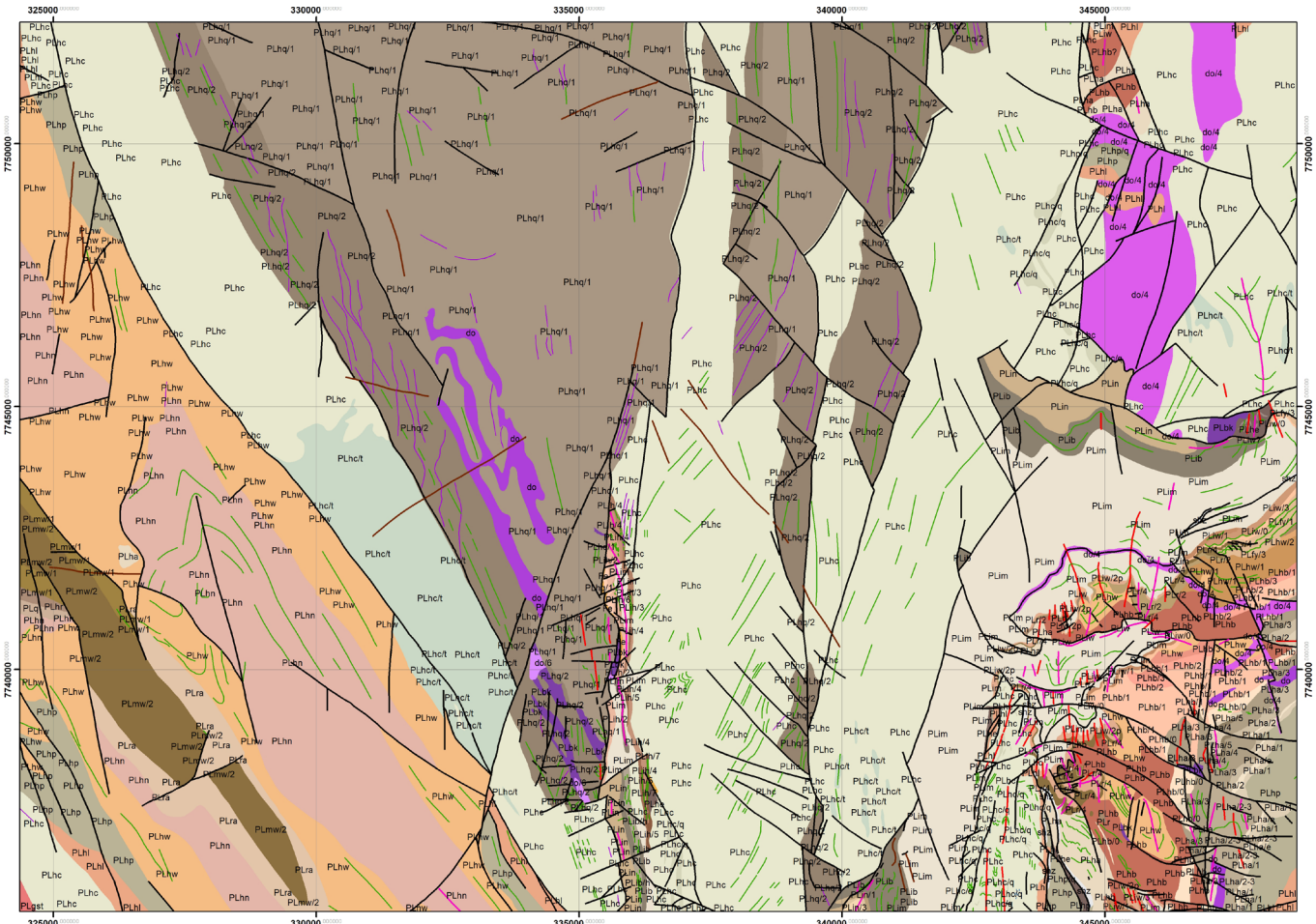

Figure 21.21. Geological map extracted from data provided by the Geological Survey of Queensland - legend on facing page. For reference for other figures on page. Map Projection GDA94, MGA54.

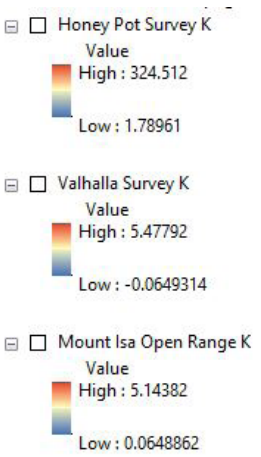

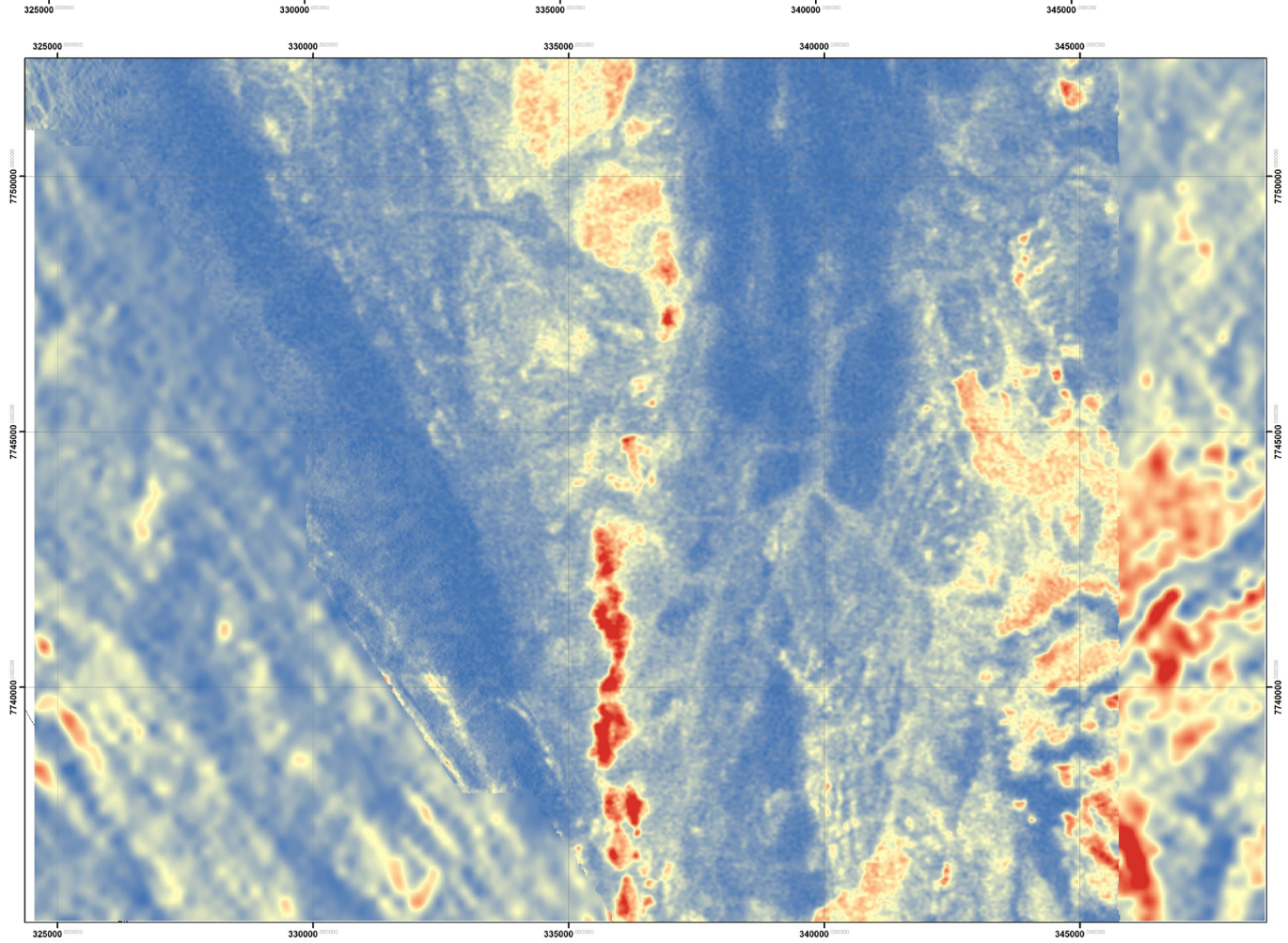

Figure 21.22. Merged radiometric data from the Valhalla area - K counts image. Map Projection GDA94, MGA54.

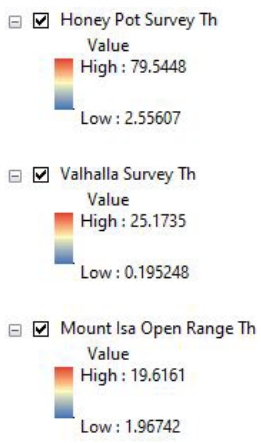

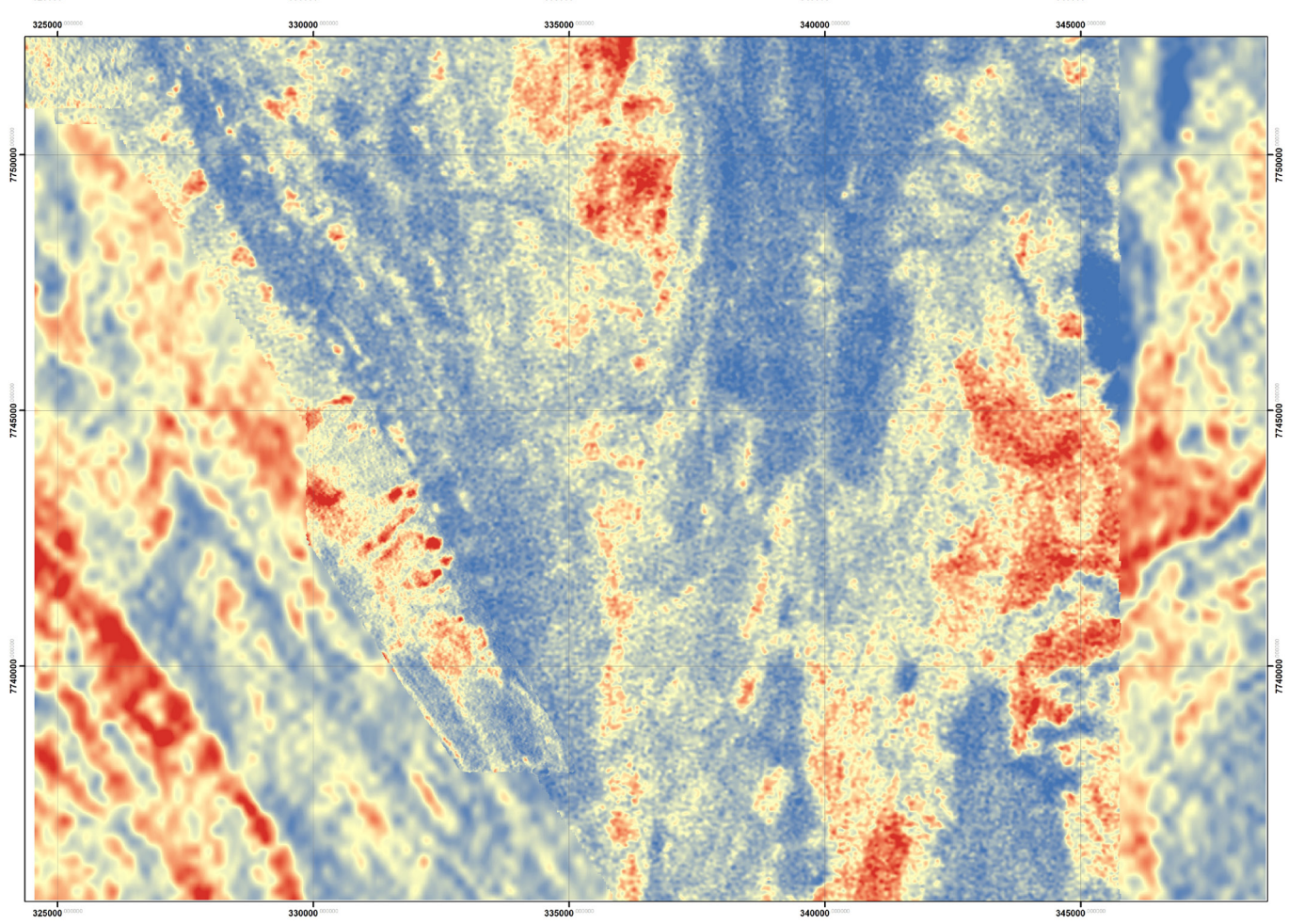

Figure 21.23. Merged radiometric data from the Valhalla area - Th counts image. Map Projection GDA94, MGA54.

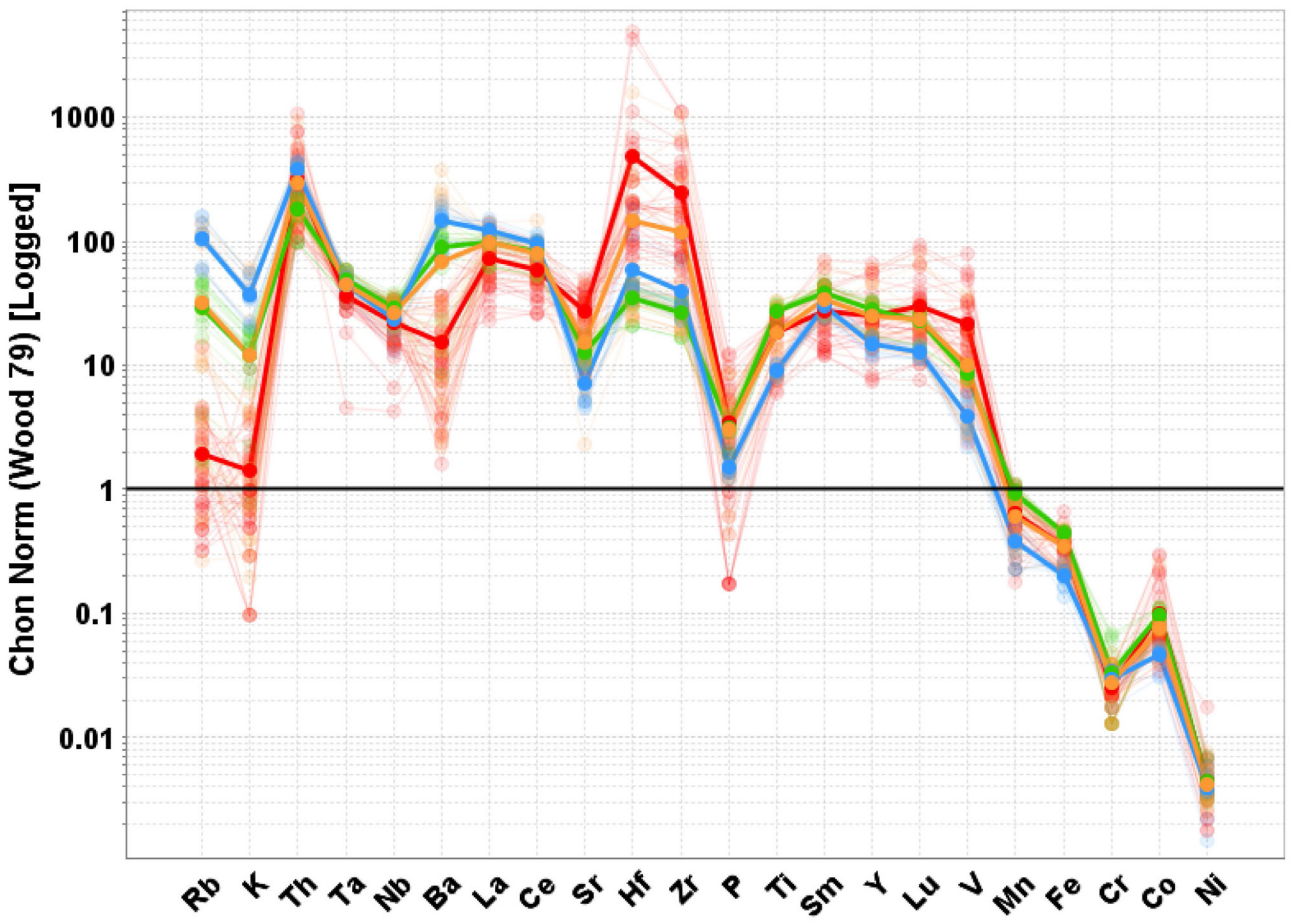

Figure 21.24. Elemental spidergram showing patters for Valhalla rocktypes - colour legend same as figure 21.25. From Wilde et al (2013).

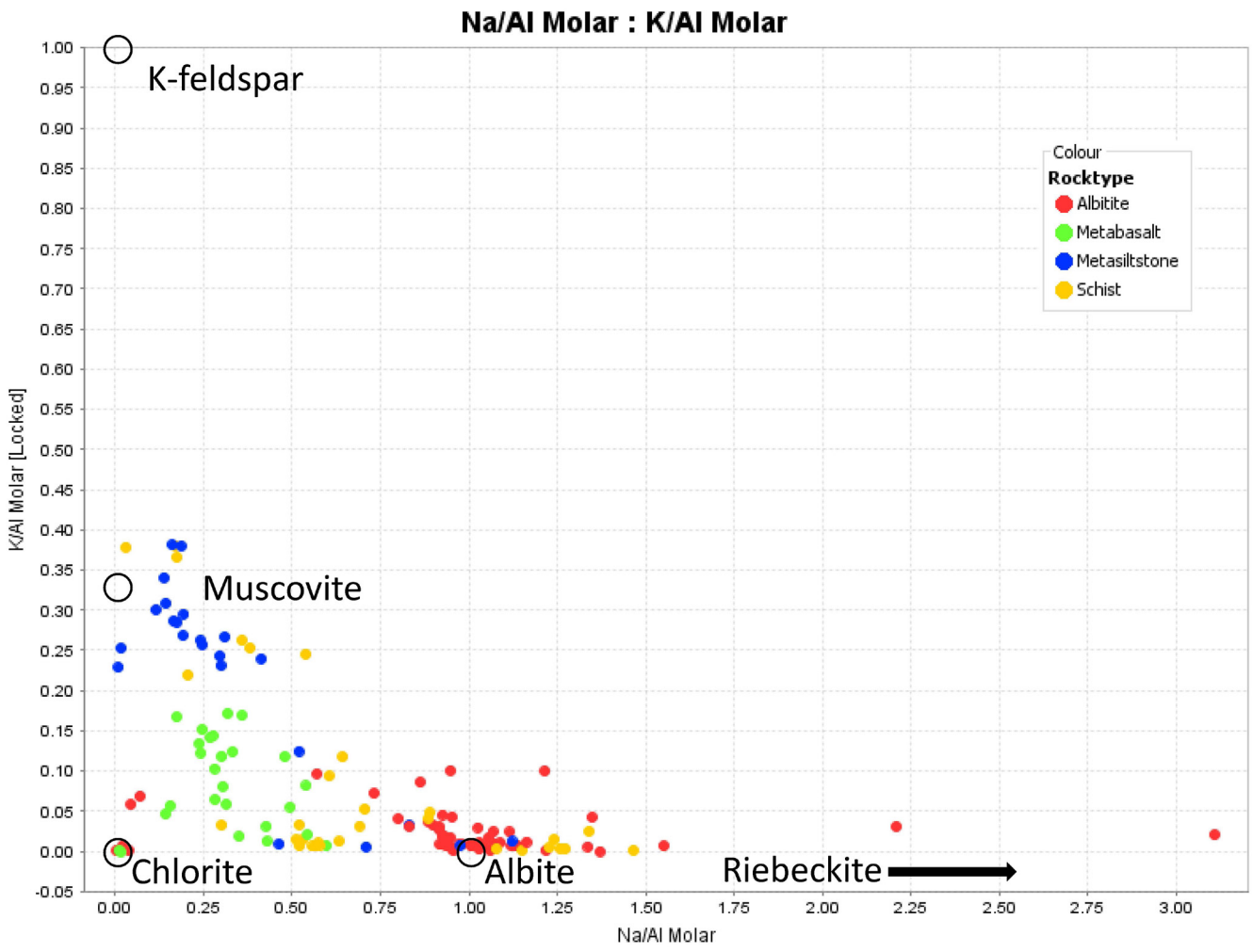

Figure 21.25. K/Al vs Na/Al plot of Valhalla rocktypes with mineralogical points displayed.

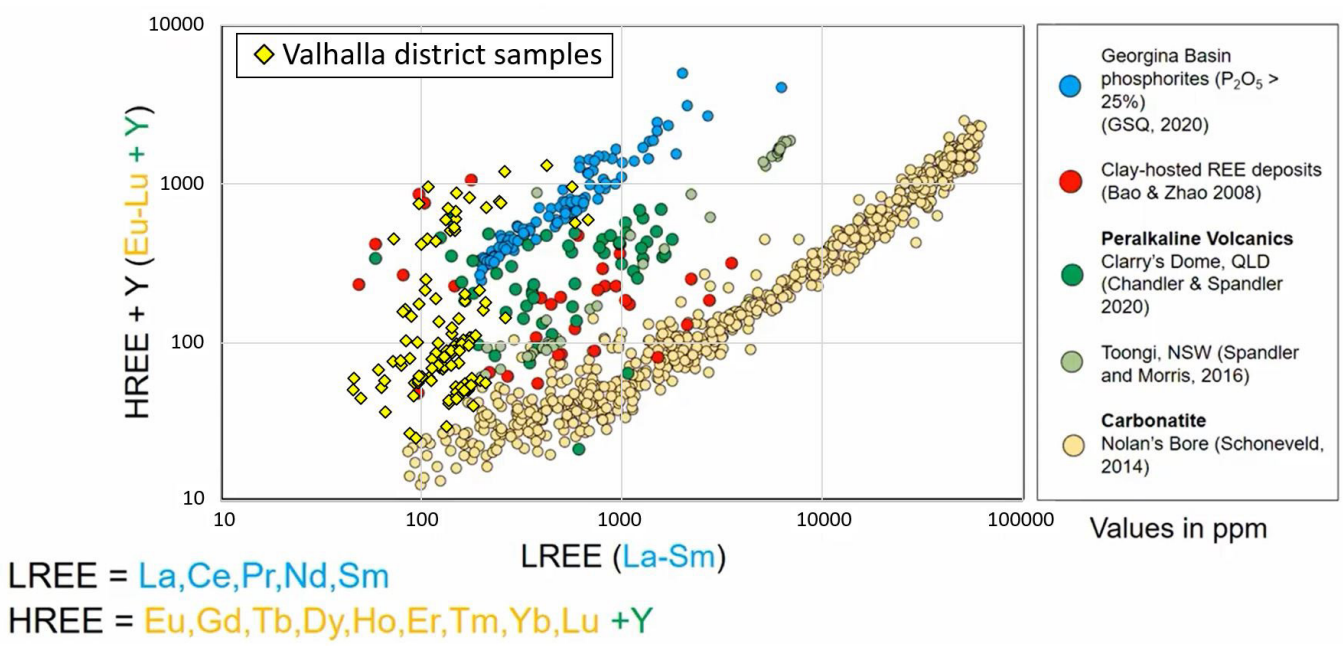

Figure 21.26. Heavy (HREE) and light (LREE) element concentrations for Valhalla district mineralisation samples (Wilde et al, 2013), plotted against a background of other REE-bearing mineralisation types, compiled by Valetich, M (GSQ 2020).

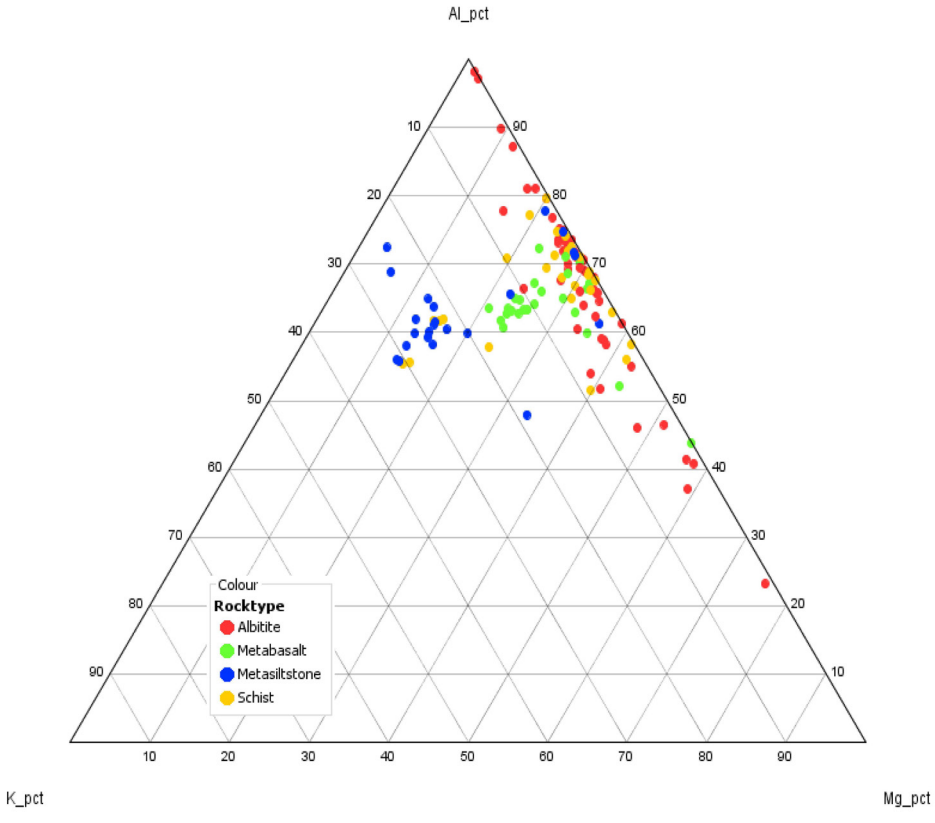

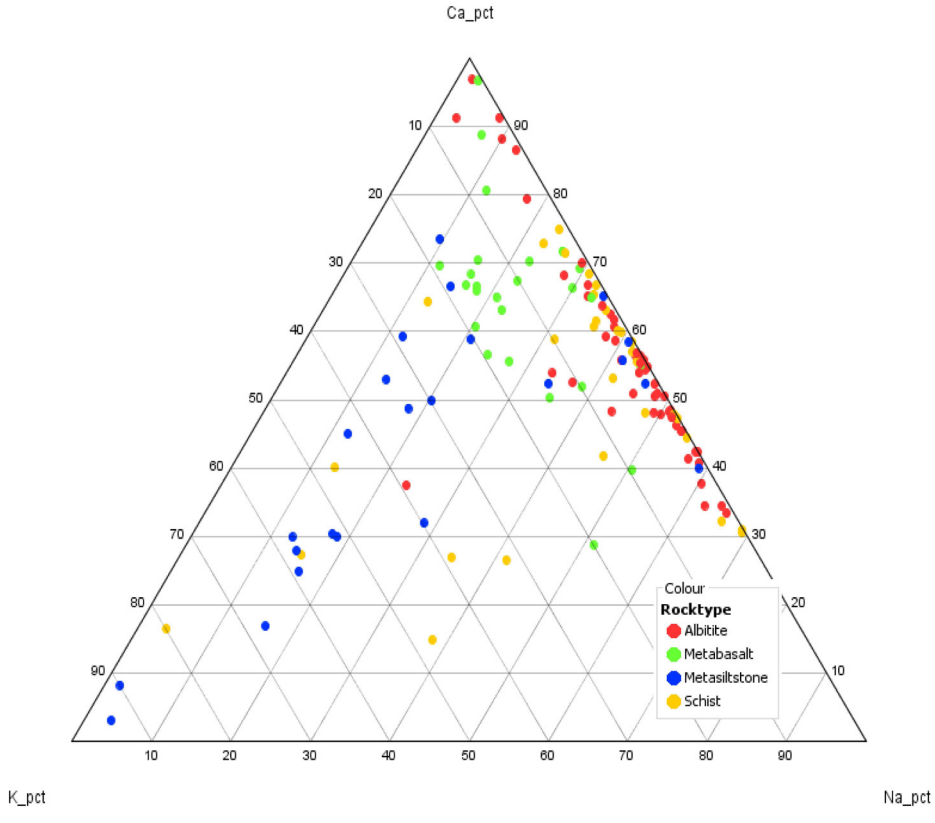

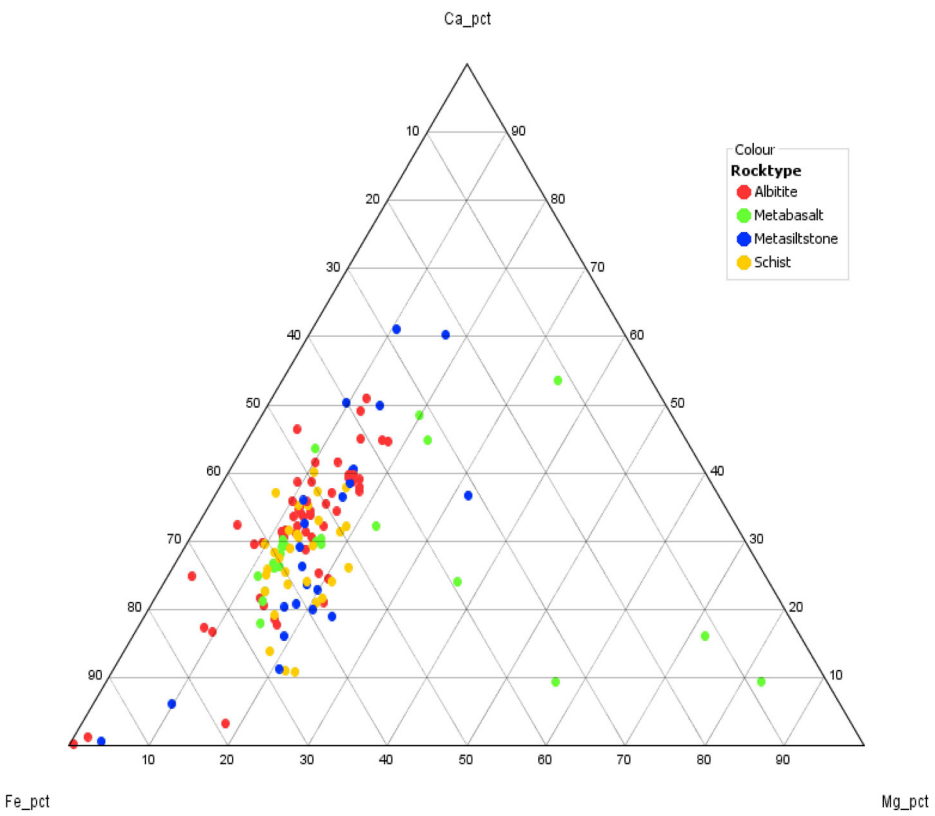

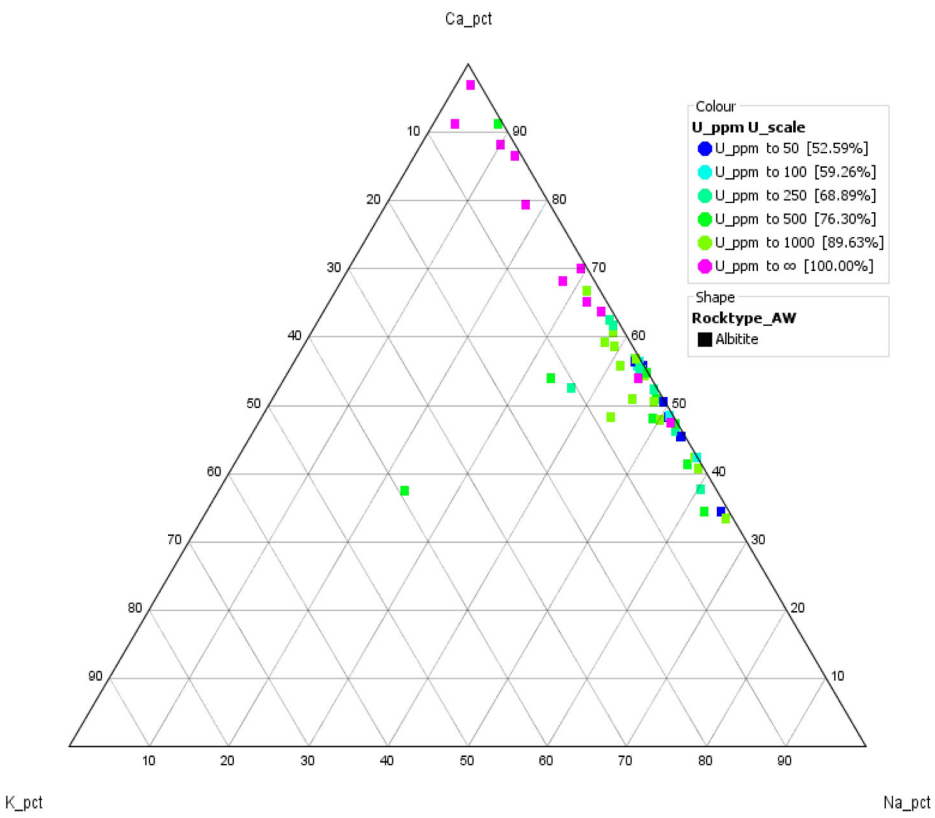

Figure 21.27. Elemental ternarty plots for Valhalla and distric rocktypes. Data from Polito et al (2009) and Wilde et al (2013).

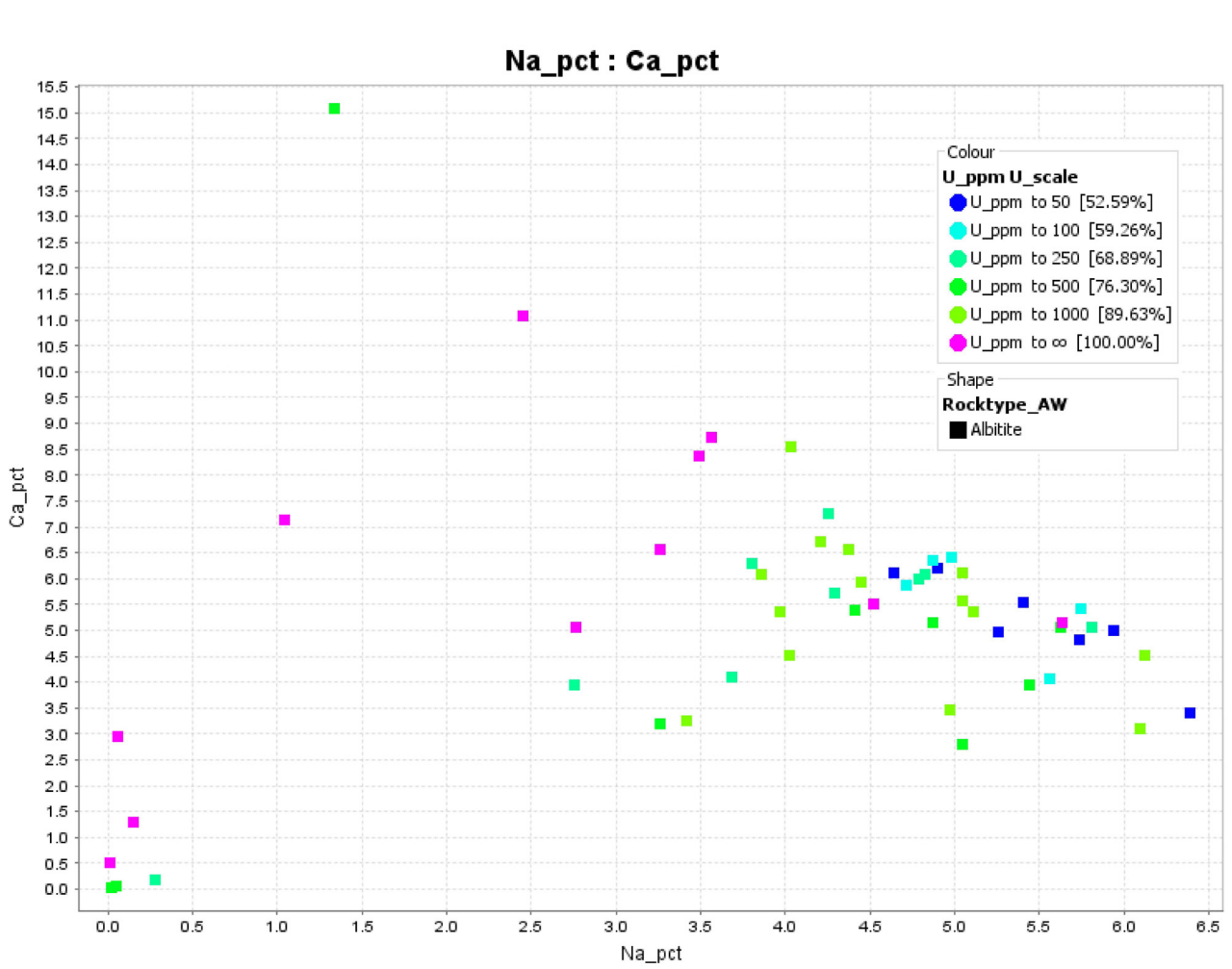

Figure 21.28. Ca vs Na plot of Valhalla samples colour coded by uranium grade, showing a correlation between uranium grade and Ca/Na (data from Wilde et al, 2013).

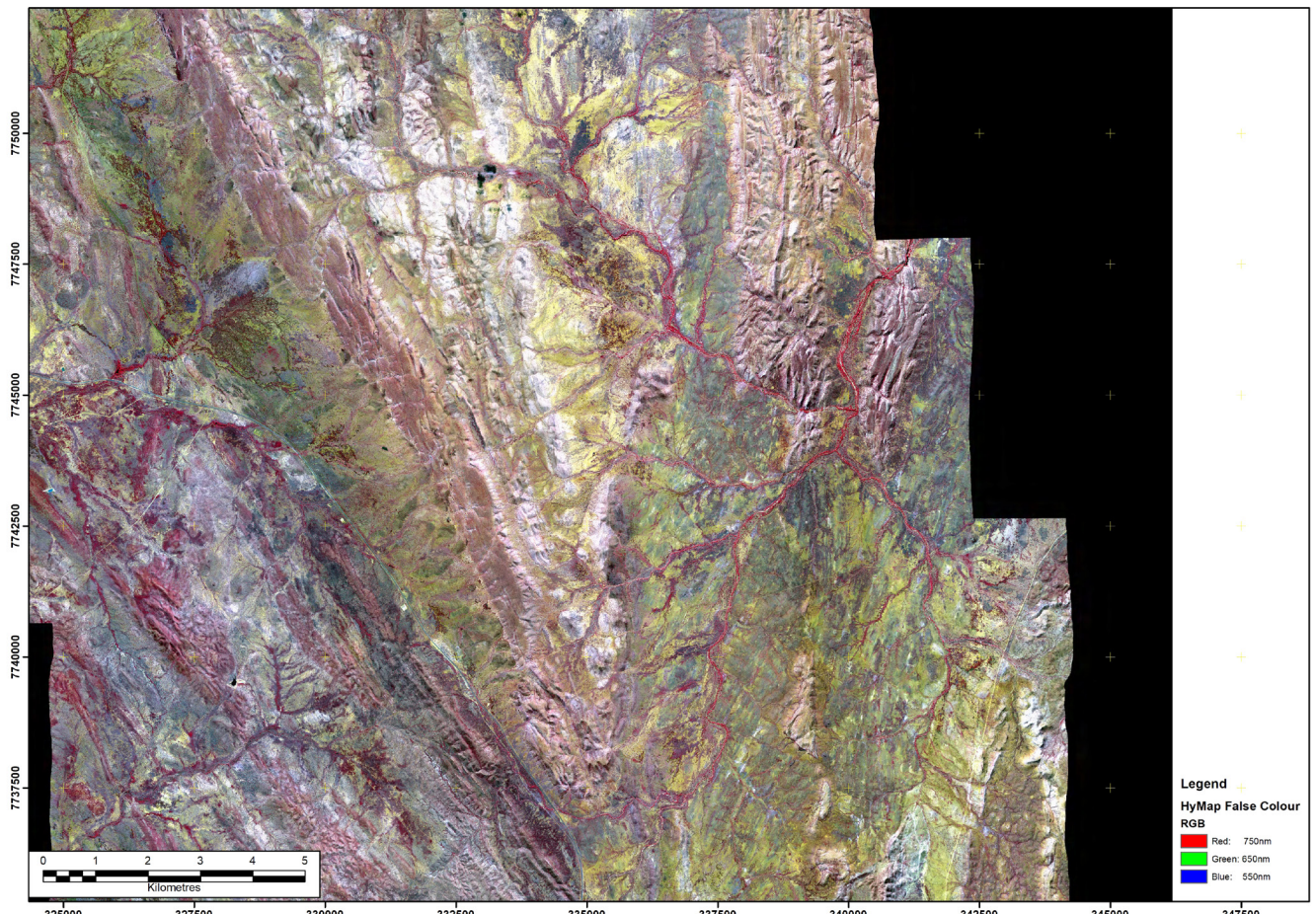

Figure 21.29. Hymap data - False colour image: with RGB representing the reflectance bands 750nm, 650nm, 550nm, respectively. Map Projection GDA94, MGA54.

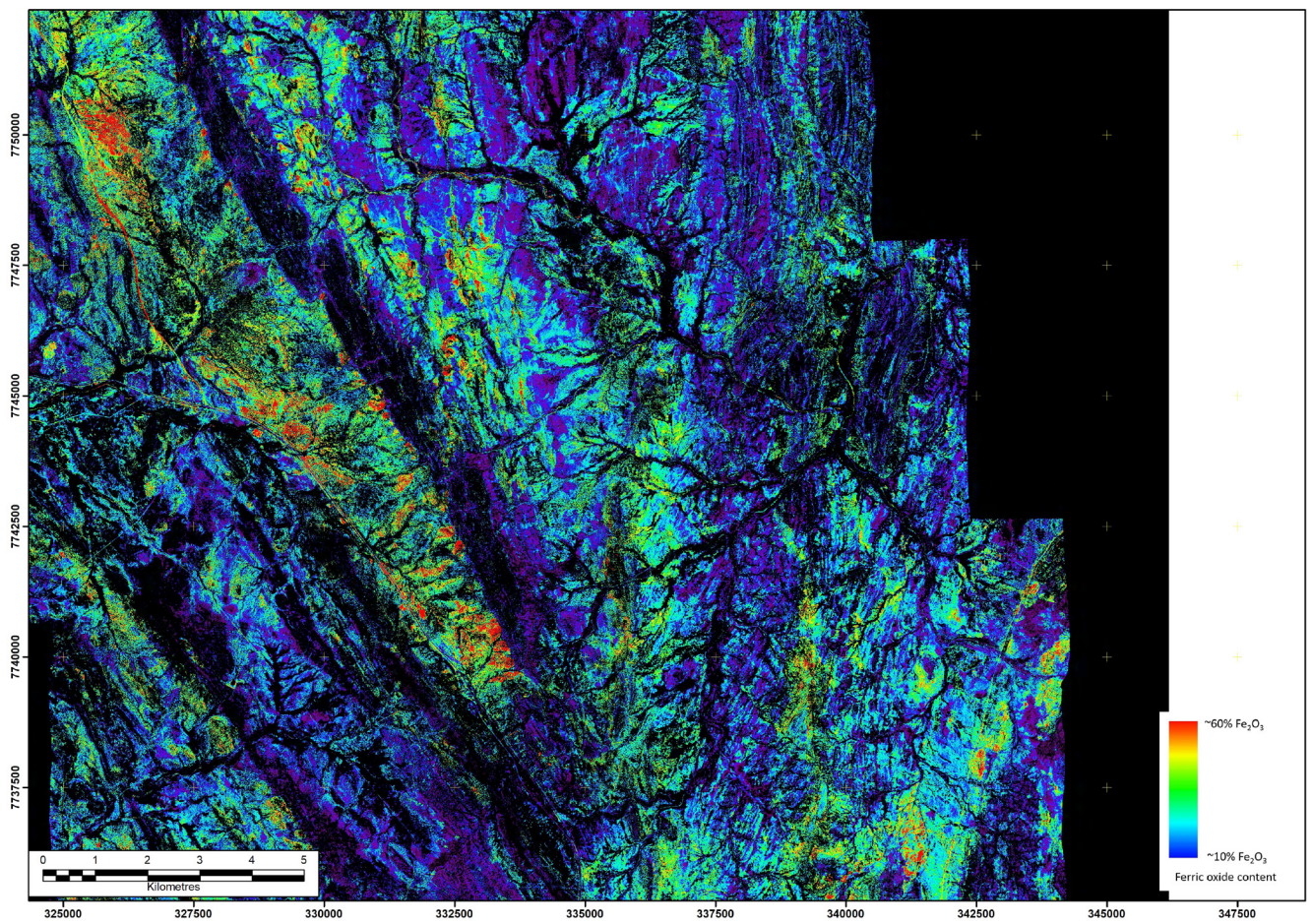

Figure 21.30. Hymap data - Ferric oxide abundance: Attempts to map hematite, goethite, 'limonite', and Fe3+ pyroxenes, olivines and carbonates by using the normalized depth of the 900nm absorption feature. Blue to red represents low (~10% Fe2O3) to high (~60% Fe2O3) abundance. High confidence Map Projection AGD84, AMG54.

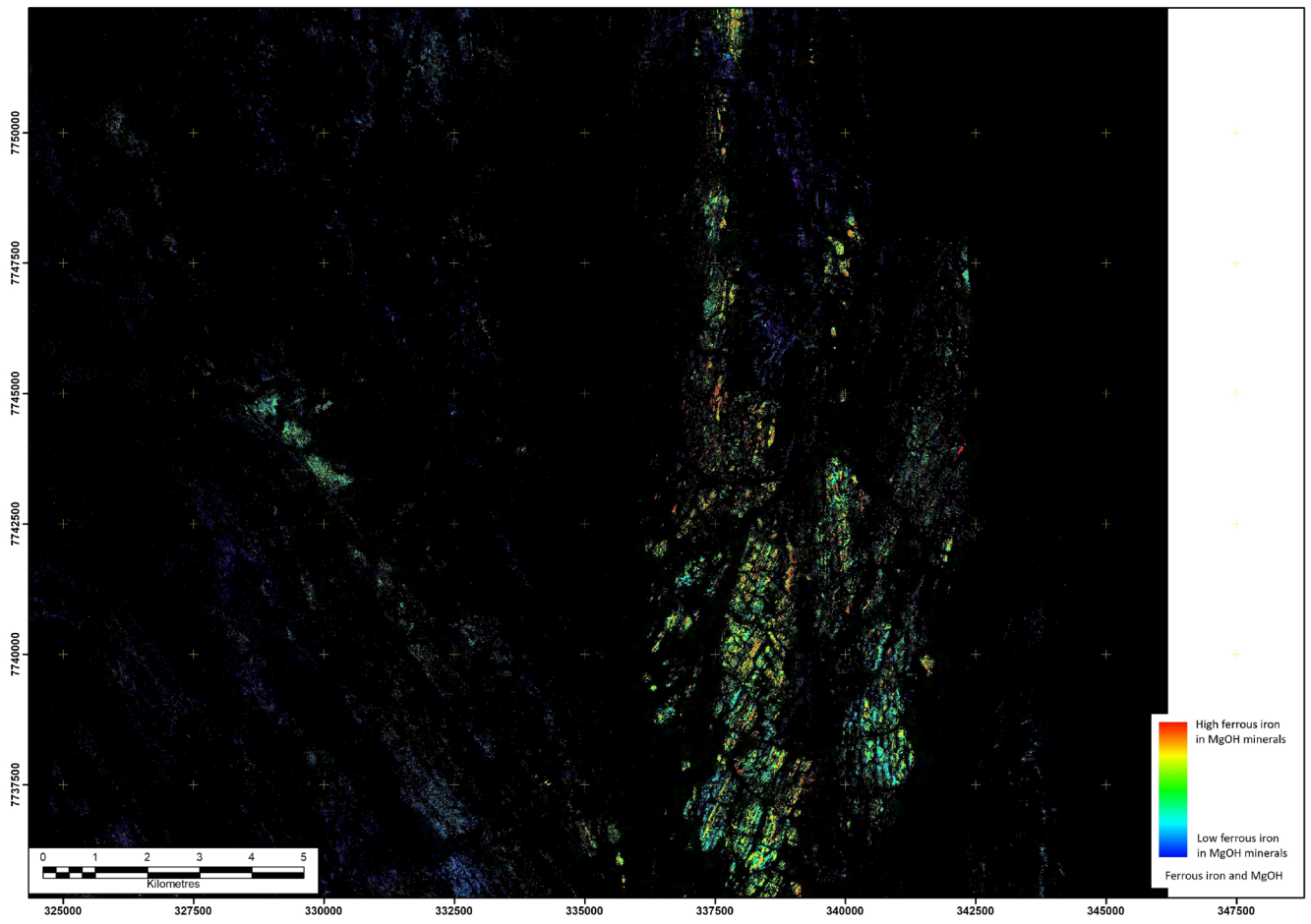

Figure 21.31. Hymap Data - Ferrous iron and MgOH: Attempts to map Fe^{2++}-bearing minerals like actinolite, some chlorites, ankerite and siderite. Blue to red represent low to high content of ferrous iron in pixels with MgOH (+carbonate) mineralogy (black is below threshold). Moderate confidence. There is a zone with anomalous appearance at the south end of the Valhalla trend. Map Projection GDA94, MGA54.

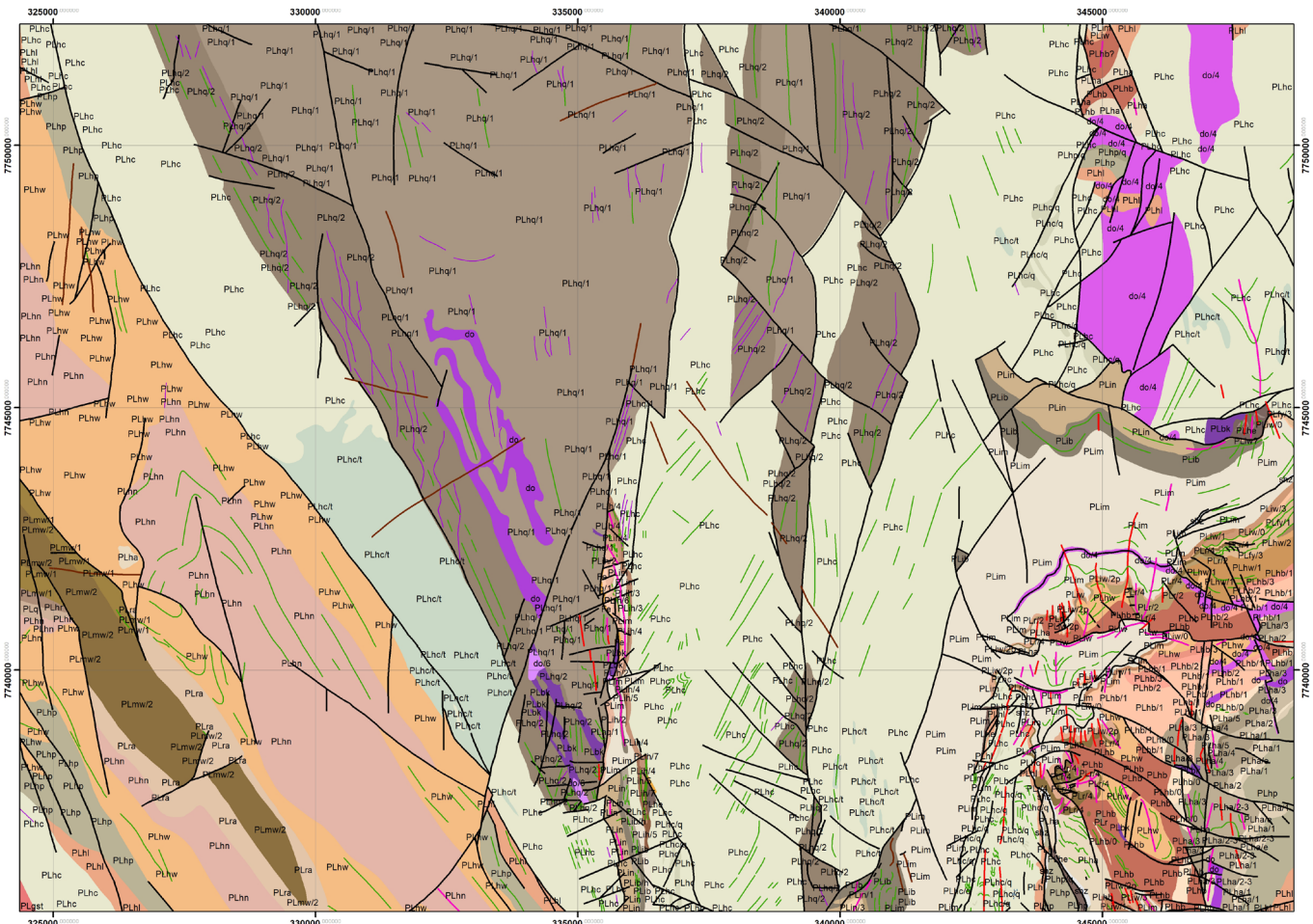

Figure 21.32. Geological map extracted from data provided by the Geological Survey of Queensland - legend on facing page. For reference for other figures on page. Map Projection GDA94, MGA54.

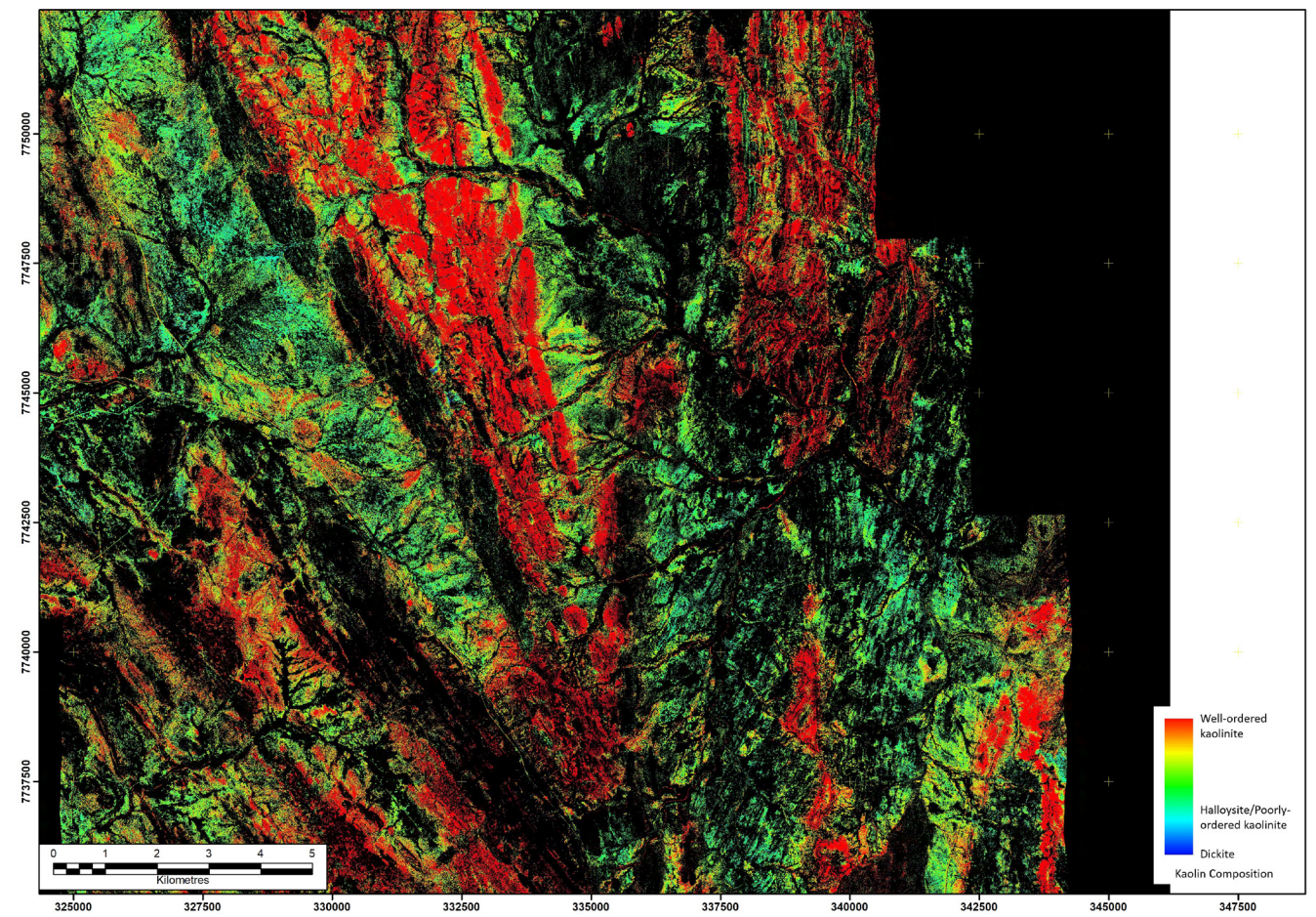

Figure 21.33. Hymap data - Kaolin composition: deep blue approximates dickite, blue-green is halloysite and/or poorly-ordered kaolinite and red approximates well-ordered kaolinite. This product attempts to separate kaolin group minerals based on the formula [(R2138+ R2173)/R2156]/[(R2156+R2190)/R2173] where R is relflectance at wavelength x. Moderate product confidence.Map Projection GDA94, MGA54.

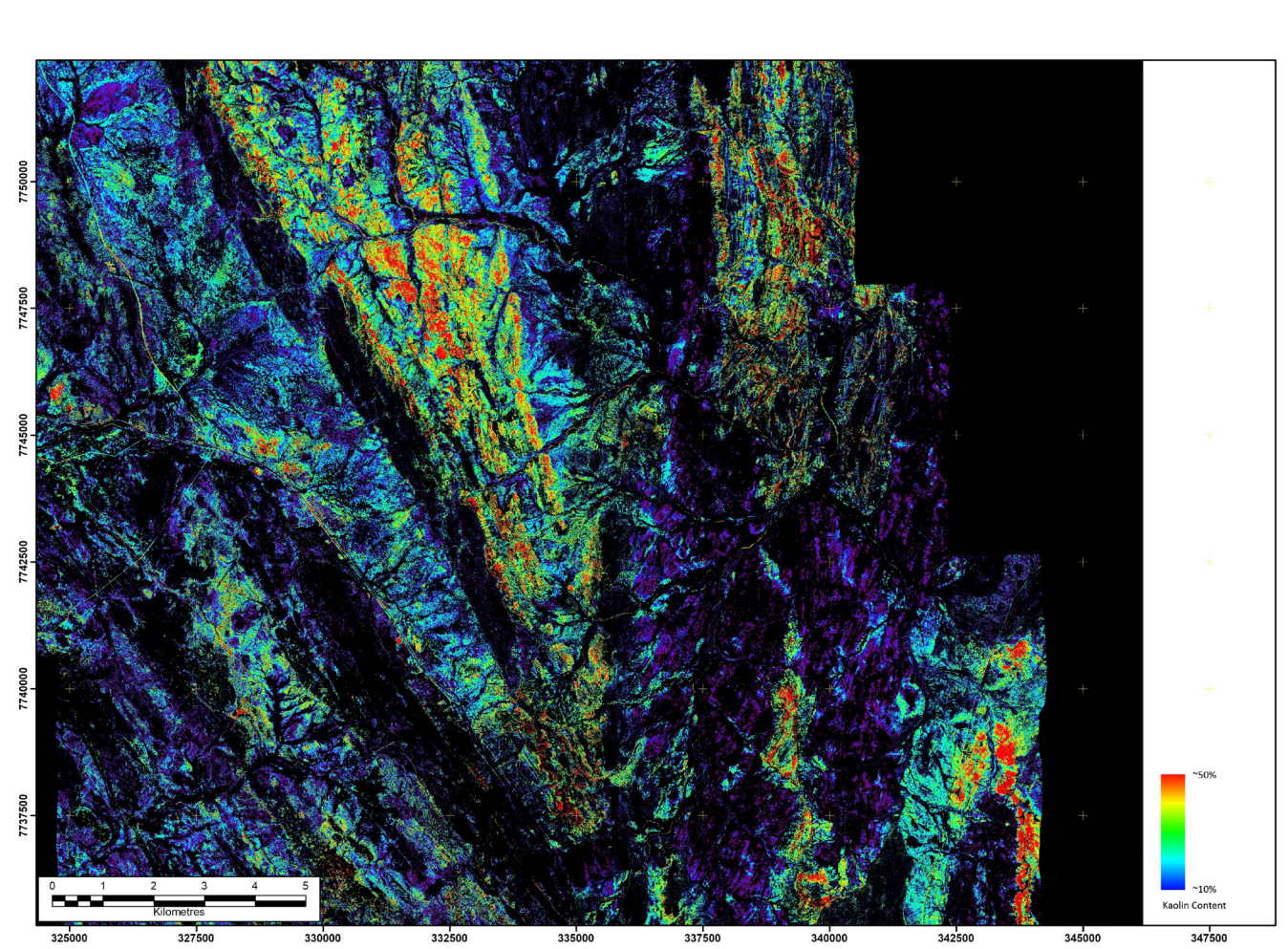

Figure 21.34. Hymap data - Kaolin content: Blue to red represents low (~10%) to high (~60%) abundance. It utilizes the normalised depth of a fitted 4th order polynomial between 2120 and 2245 nm, with moderate product confidence. Map Projection GDA94, MGA54.

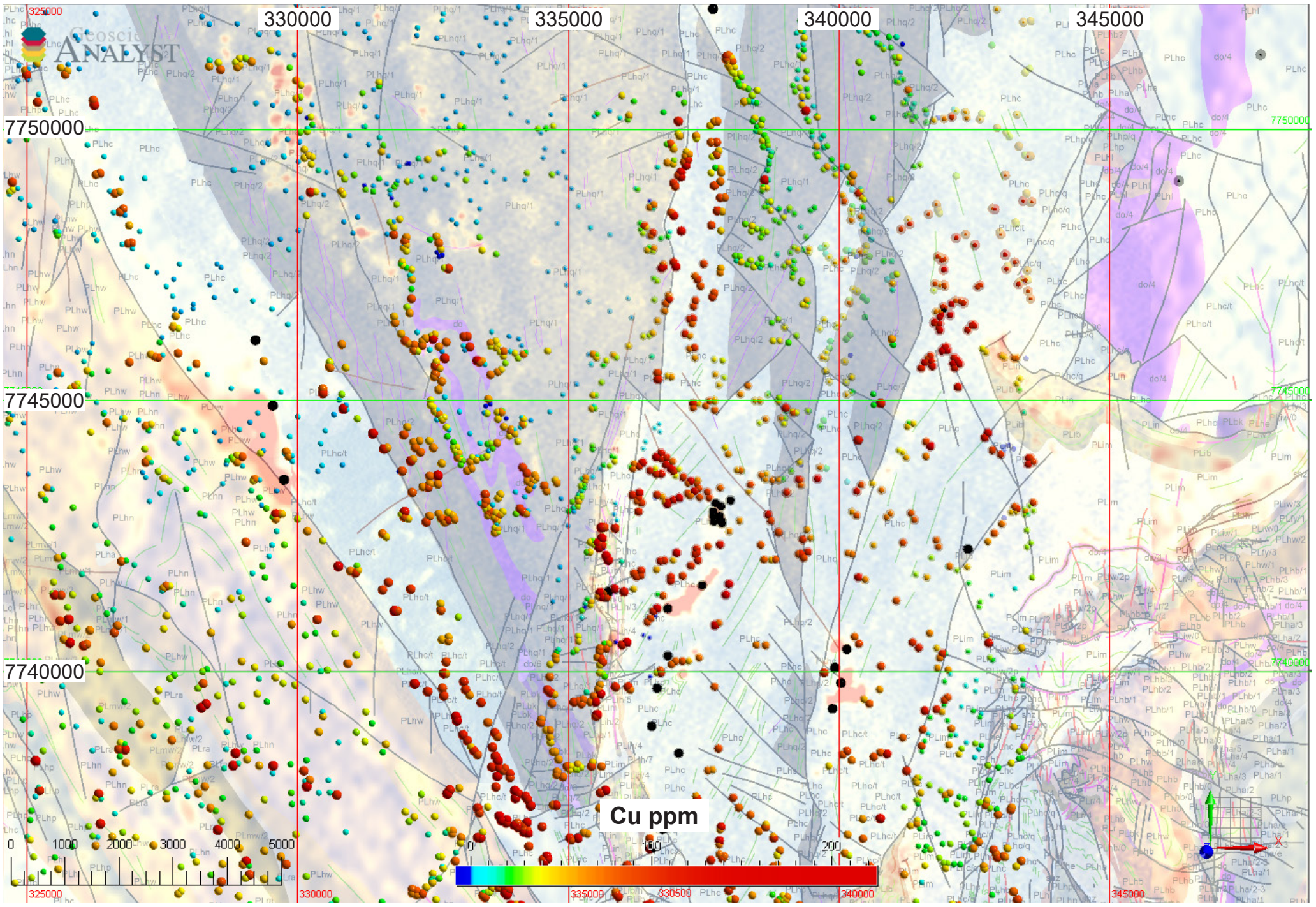
325000
330000
335000
340000
345000
7750000
7745000
7740000
Cu ppm
0
1000
2000
3000
4000
5000
0
100
200

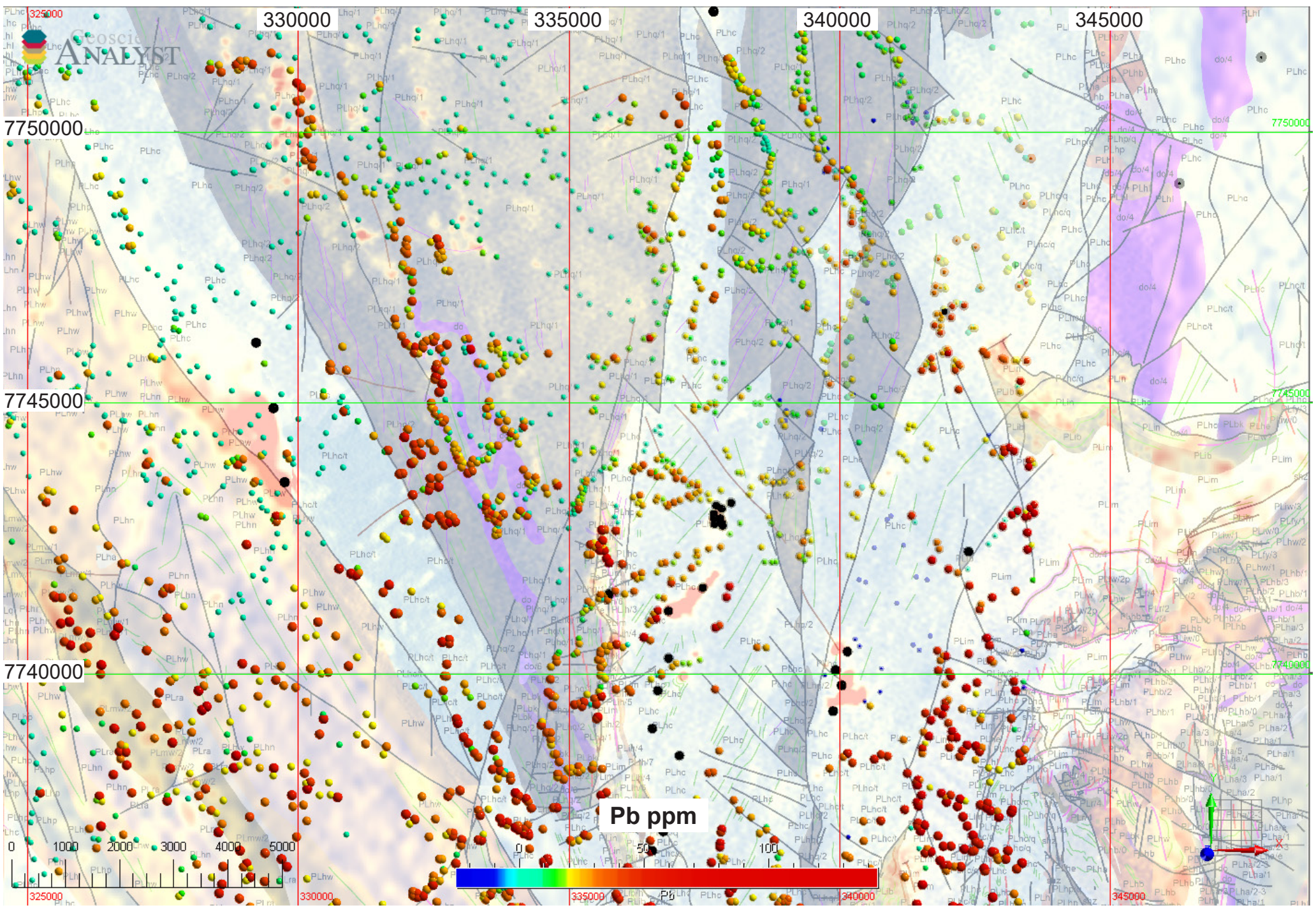
325000
330000
335000
340000
345000
7750000
7745000
7740000
Pb ppm
0
1000
2000
3000
4000
5000
0
50
100
Pb

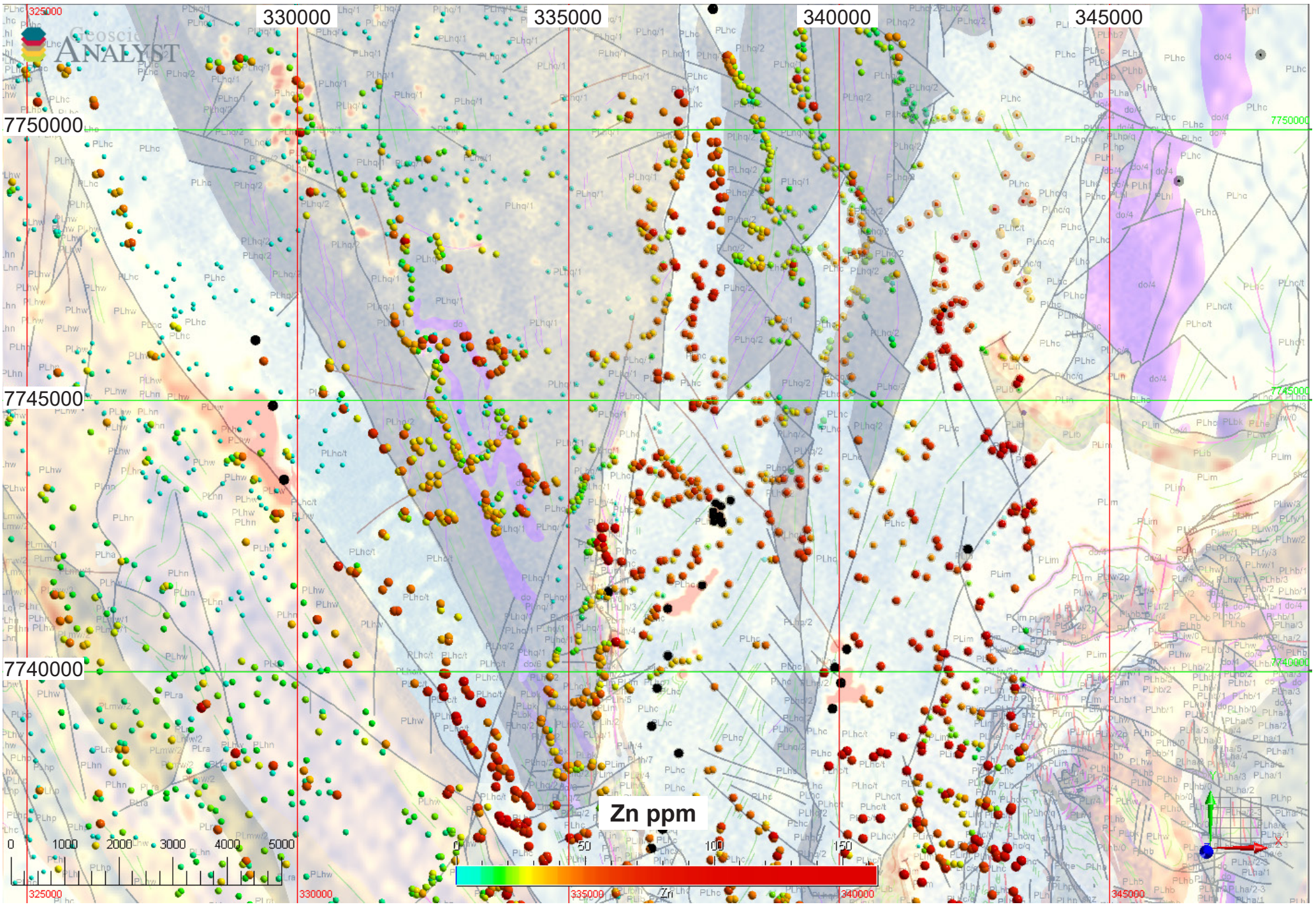

Figure 21.37. Zn stream sediment geochemistry plotted over the geological map (see fig 21.4 for legend) merged with a U radiometric image (see fig 21.20 for legend). Map Projection GDA94, MGA54.

Figure 21.35. Facing page, upper. Cu stream sediment geochemistry plotted over the geological map (see fig 21.4 for legend) merged with a U radiometric image (see fig 21.20 for legend). Map Projection GDA94, MGA54.

Figure 21.36. Facing page, lower Pb stream sediment geochemistry plotted over the geological map (see fig 21.4 for legend) merged with a U radiometric image (see fig 21.20 for legend). Map Projection GDA94, MGA54.

ly-ordered kaolinite and red approximates well-ordered kaolinite. This product attempts to separate kaolin group minerals based on the formula [(R2138+ R2173)/R2156]/[(R2156+R2190)/R2173] where R is relflectance at wavelength x. Moderate product confidence. (Figure 21.33)

Kaolin content: Blue to red represents low (~10%) to high (~60%) abundance. It utilizes the normalised depth of a fitted 4th order polynomial between 2120 and 2245 nm, with moderate product confidence. (Figure 21.34)

PETROPHYSICAL PROPERTIES

No petrophysical data was found for the deposits or the region.

GEOPHYSICAL EXPRESSION

Valhalla

Whilst there are no high resolution radiometrics available for the Valhalla deposit, it does have a clear and strong Uranium response in the Mount Isa Open Range Survey (Figs 21.20, 21.53). The uranium anomaly associated with Valhalla and Valhalla South is parallel to the hosting structure and has the dimensions of 2100m along the structure and 550m along the structure. It is part of a broader zone of elevated uranium which has dimensions of 3500m by 1000m, and is oriented in a more NW-SE direction. In the magnetic data, the Valhalla South, Valhalla and Odin zones show a clear spatial association with a discordant zone of elevated magnetic response. This zone is interpreted to be the result of magnetite-additive early albitite alteration (Fig 21.52). The deposit does not appear to have any expression in EM or Hymap datasets.

Skal

Uranium mineralisation at Skal is associated with a group of clear and distinctive uranium radiometric anomalies (Figs 21.20, 21.57, 21.58). The Skal area is relatively well-exposed (Wilde et al 2013) and geological mapping shows that the zones of albitite and uranium mineralisation are displaced across a NW-trending sinistral fault with approximately 500m of displacement (Fig 21.42). Uranium anomalies exist on both sides of this fault. Mineralisation at Skal is also associated with a slightly elevated magnetic signature interpreted to be albitite. Removal of late fault displacements on the ECV sequence hosting the Skal deposit suggests that the zone of albitite hosting uranium mineralisation may persist for up to 4 km to the north and up to 1 km to the south, and appears to be associated with an apparent dextral shear zone (Fig 21.55). The deposit does not appear to have any expression in EM or Hymap datasets.

Betatron – Bikini – Mirrioola zone

There are a number of occurrences in a zone that runs form Mirrioola South at the south end to a group of occurrences at the north end including Betatron, with the largest occurrence in this belt being Bikini (Fig 21.40). Most of the uranium occorrences in the belt have distinctive radiometric anomalies which are

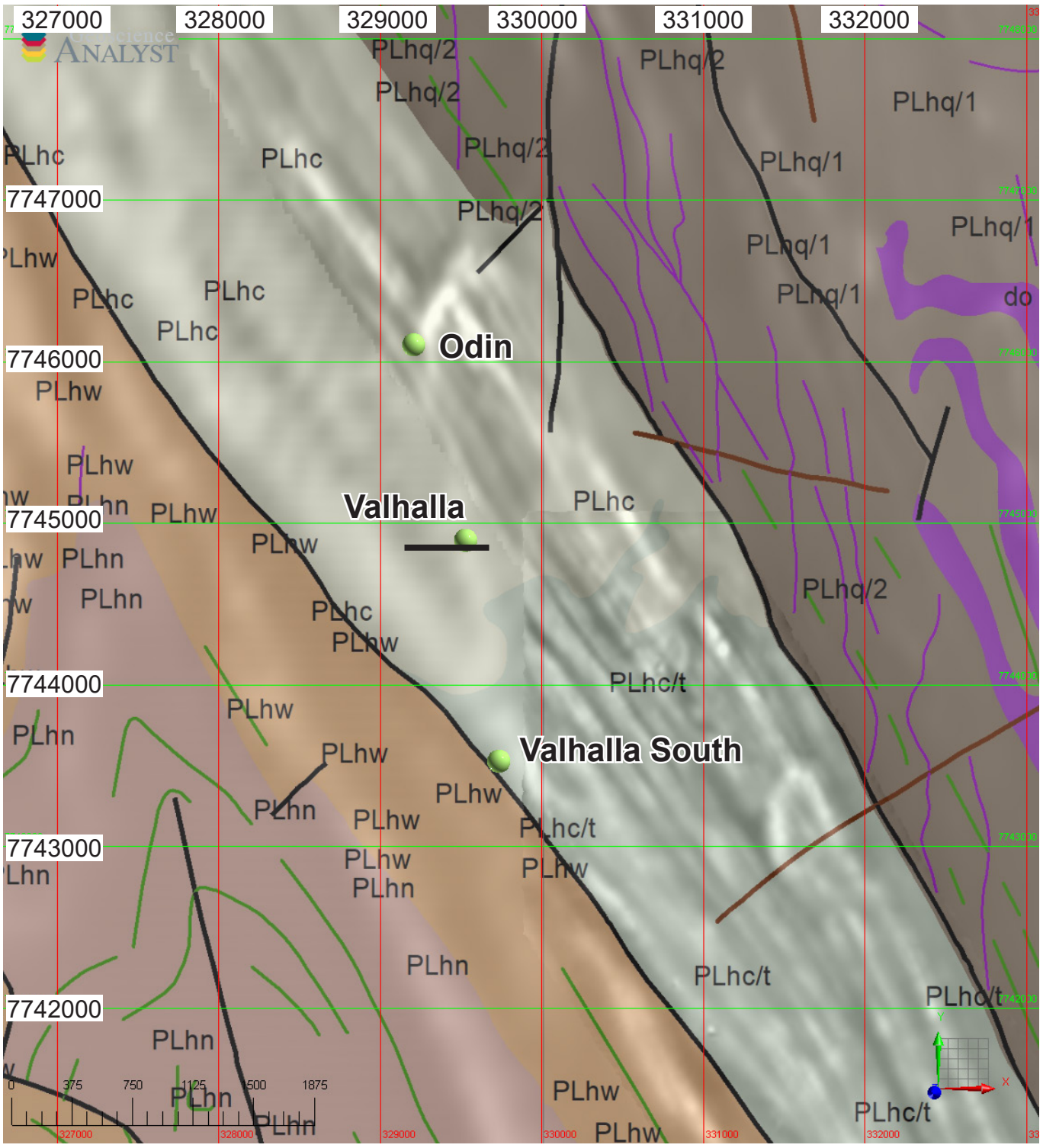

Figure 21.38. Geological map showing the location of deposits in the immediate area of Valhalla. The black line near Valhalla shows the location of the figure in section 21.39. Map Projection GDA94, MGA54.

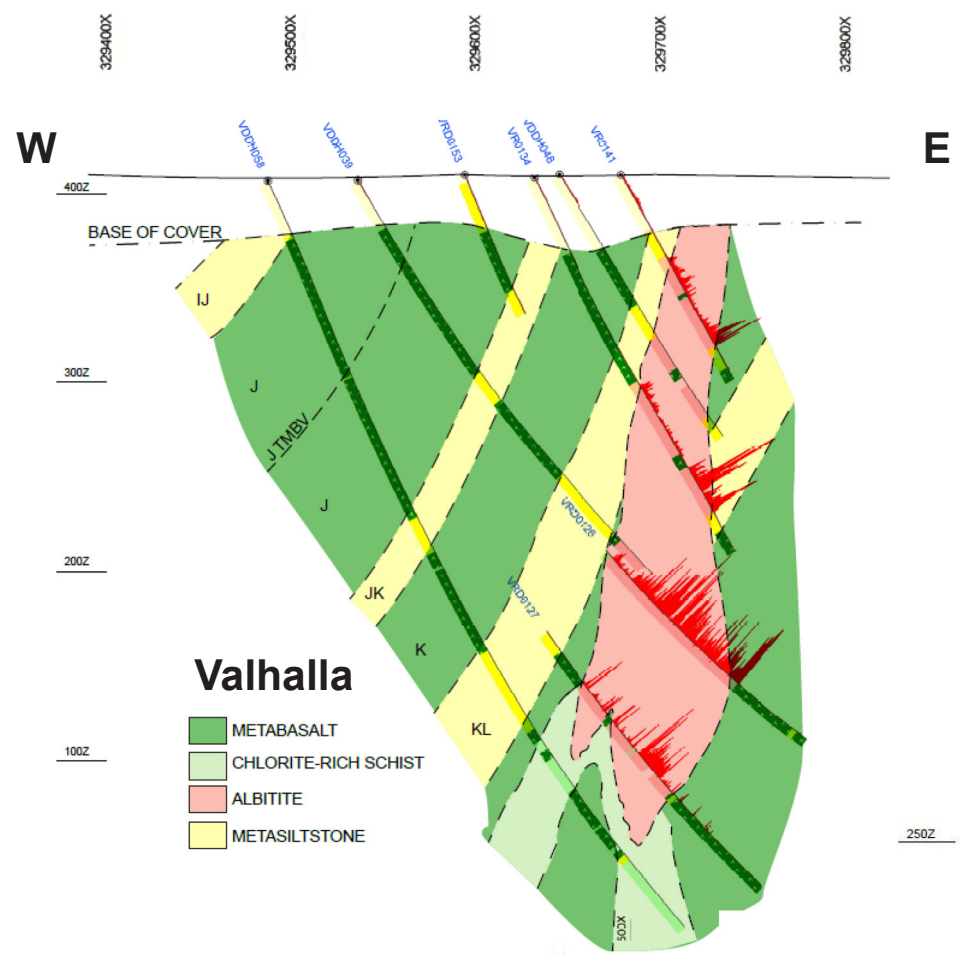

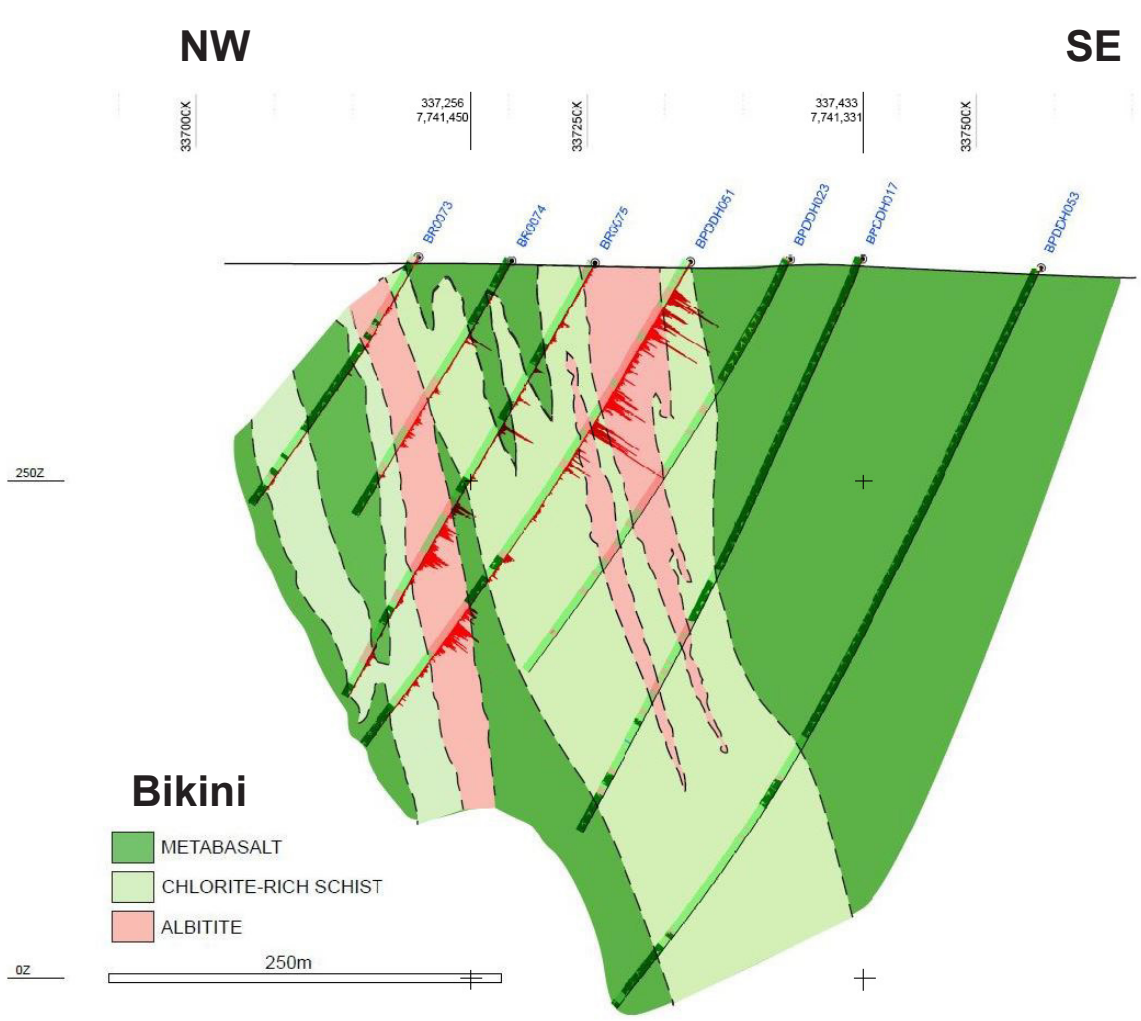

Figure 21.39. E-W drill section through Valhalla, from Wilde et al (2013). See fig 21.38 for section location. Map Projection GDA94, MGA54.

relatively restricted in extent (Fig 21.58). The largest anomaly is associated with the Bikini resource, which has a NW-oriented uranium anomaly with dimensions of 1250m in a NE-SW direction and 250m in a NW-SE direction. This zone also has a distinctive elevated magnetic signature which after removal of younger faults has a strike length of approximately 5km (Fig 21.55). The zone does not appear to have any expression in EM or Hymap datasets.

EXPLORATION GEOCHEMISTRY

Stream Sediment Geochemistry

Open file stream sediment geochemical data are available in the area for Cu, Pb, and Zn, but no data are available for U (Figs 21.35, 21.36, 21.37). The deposits have no obvious expression in the base metal stream sediment geochemical datasets.

Soil Geochemistry

No soil geochemical data are available for the area.

TIMING OF MINERALISATION

Relative Timing

Wilde et al (2013) established through QEM-SCAN and Hyperprobe analysis that Uranium in associated with a relatively late potassic (K-feldspar and biotite) overprint of early albitic alteration. The early albitic alteration is interpreted to be synchronous with the more penetrative D_2 deformation and is texturally associated with the development of penetrative foliations in the rock. The overprint interpreted to have brought in the bulk of the uranium mineralisation is associated with more brittle features and interpreted to be synchronous with D_3 deformation.

Absolute Age

Polito et al (2009) performed direct U-Pb and Pb-Pb dating on Brannerite and obtained ages between 1,555 and 1,510 Ma. They also obtained $^{40}Ar/^{39}Ar$ ages of 1,533±9 Ma and 1,551±7 Ma from early and main-stage riebeckite. These dates are broadly in agreement with the relative timing derived from observations of mineralisation with respected to structures at various scales.

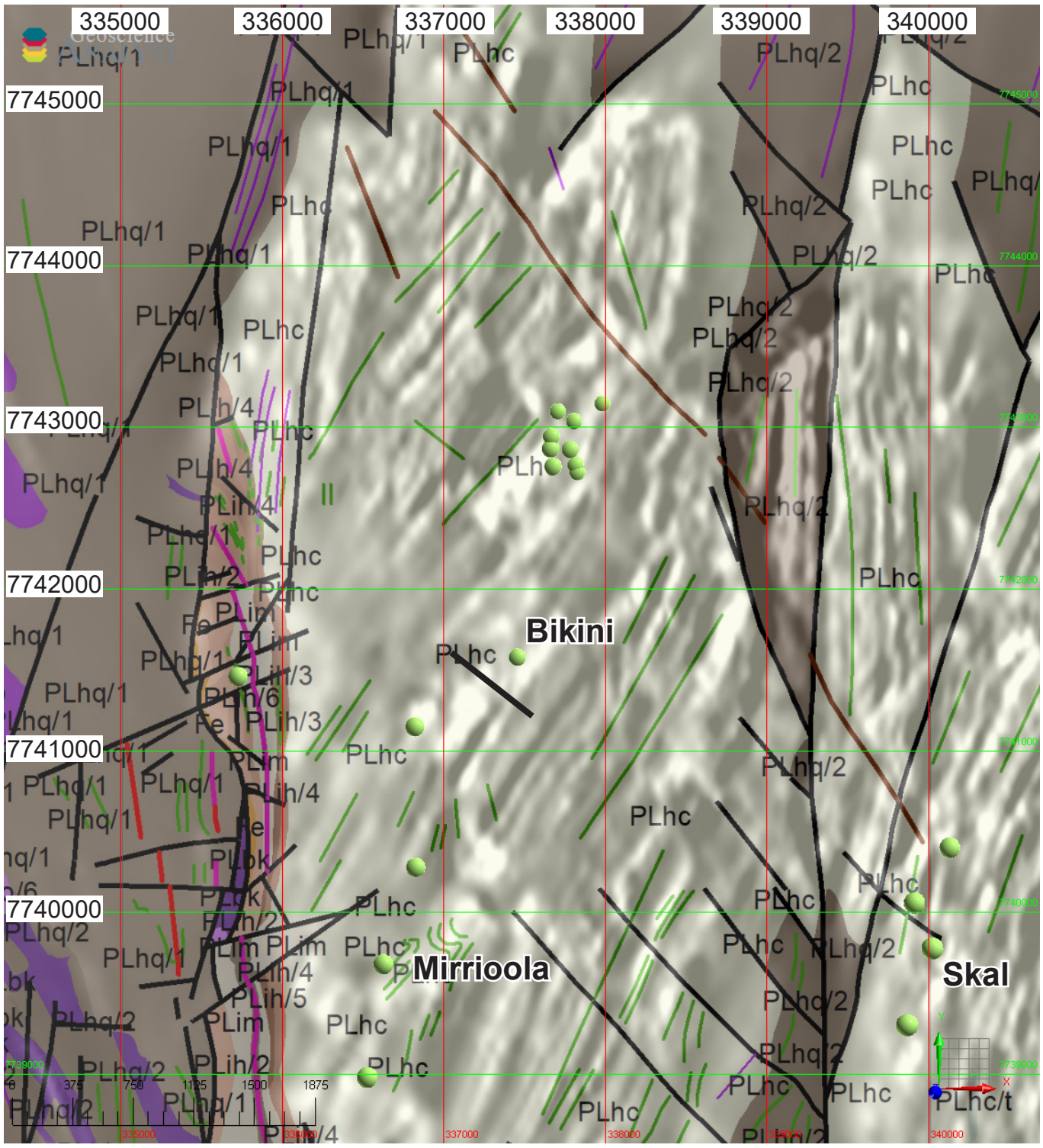

Figure 21.40. Geological map in the area of the Mirrioola, Bikini and Skal deposits. NW-SE Block line to the southwest of Bikini shows the position of the section in figure 21.41 Map Projection GDA94, MGA54.

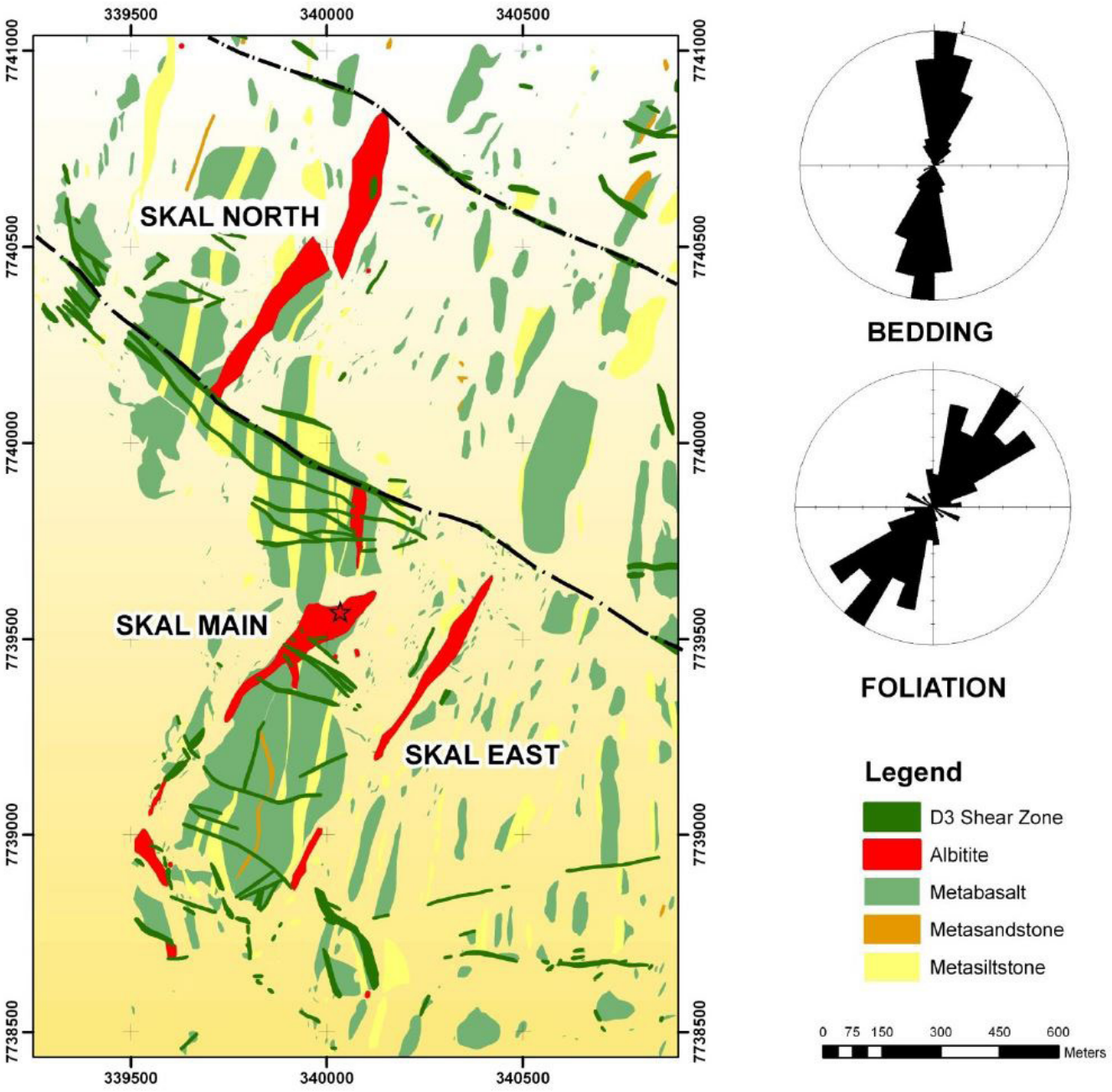

Figure 21.41. NW-SE drill section through Valhalla, from Wilde et al (2013). See fig 21.40 for section location. Map Projection GDA94, MGA54.

Figure 21.42. Geological map of the Skal area, from Wilde et al (2013). Map Projection GDA94, MGA54.

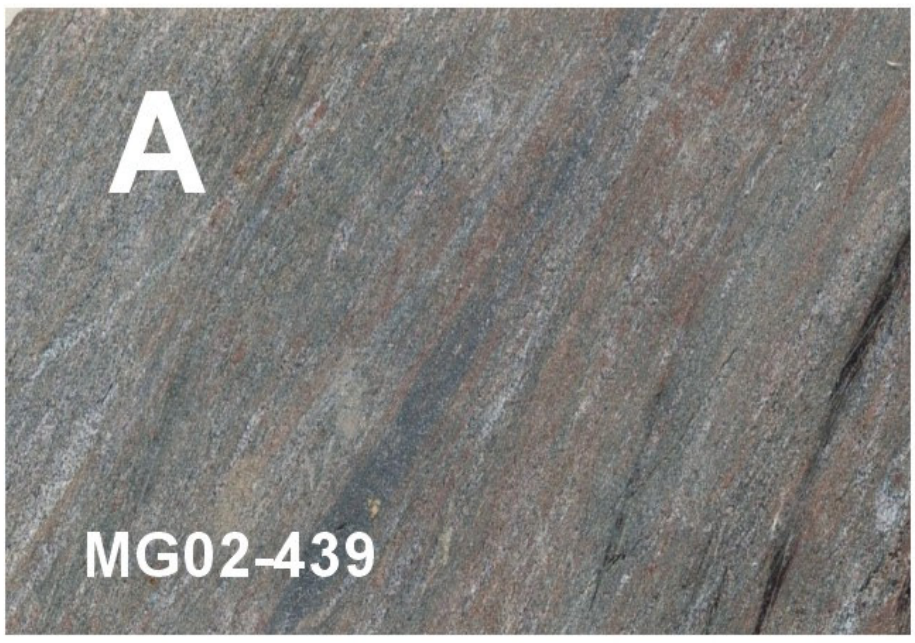
A
MG02-439

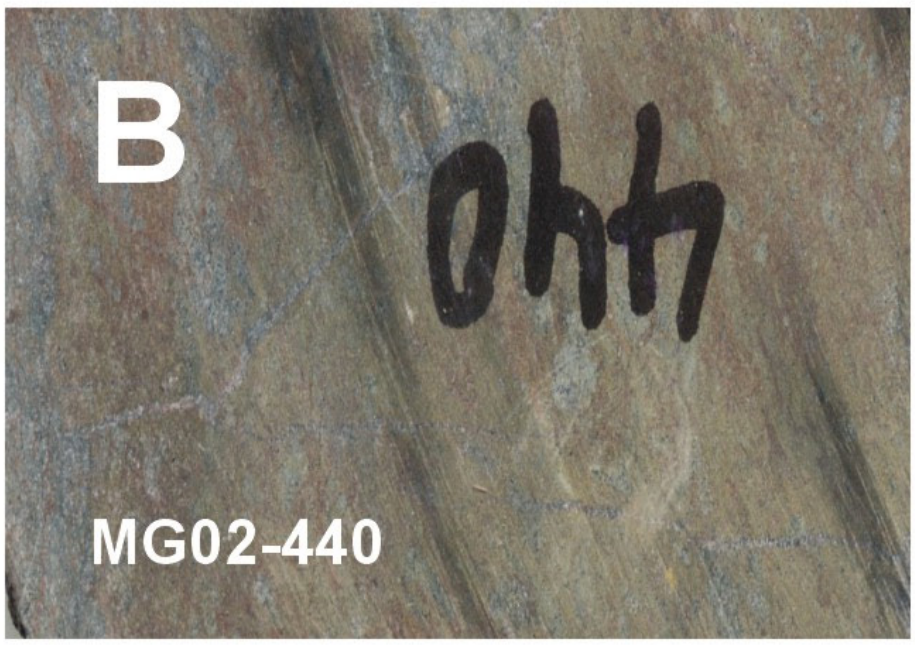
B
MG02-440


C
MG02-441


D
MG02-442


E
MG02-443


F
MG02-444


G
MG02-445

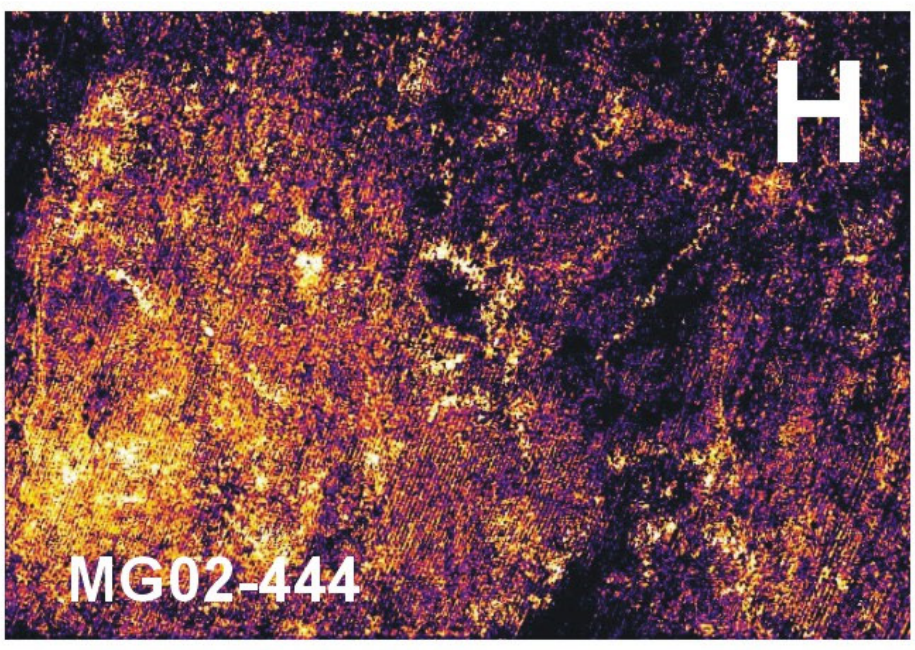
H
MG02-444

Figure 21.44. Rock photographs from the Valhalla region, from Wilde et al (2013) (A) Valhalla VRD185 232.1 m. Brecciated albitite (Ab) with matrix of dark red hydrothermal zircon (Zr). (B) Skal SD084 56.4 m. Breccia of rounded early quartz vein fragments in dark green riebeckite-rich matrix. (C) Typical laminated ore, Bikini BPDD024 169 m. Ab, Albitite. Cc, late calcite vein emplaced parallel to and transgressive to S2. (D) Bikini BPDH051 92 m. Boudinaged lithons of albitite (Ab) enveloped by spaced S2 domains defined mainly by riebeckite (Rb). Cc, calcite-rich area. (E) Mirrioola MIDDH012 109 m. Folded albitite (Ab) with partially transposed limbs. Riebeckite-rich matrix (Rb). (F) Queen's Gift QGDC008 81.5 m. Similar to (E), showing greater abundance of milky white carbonate (Cb) veinlets.

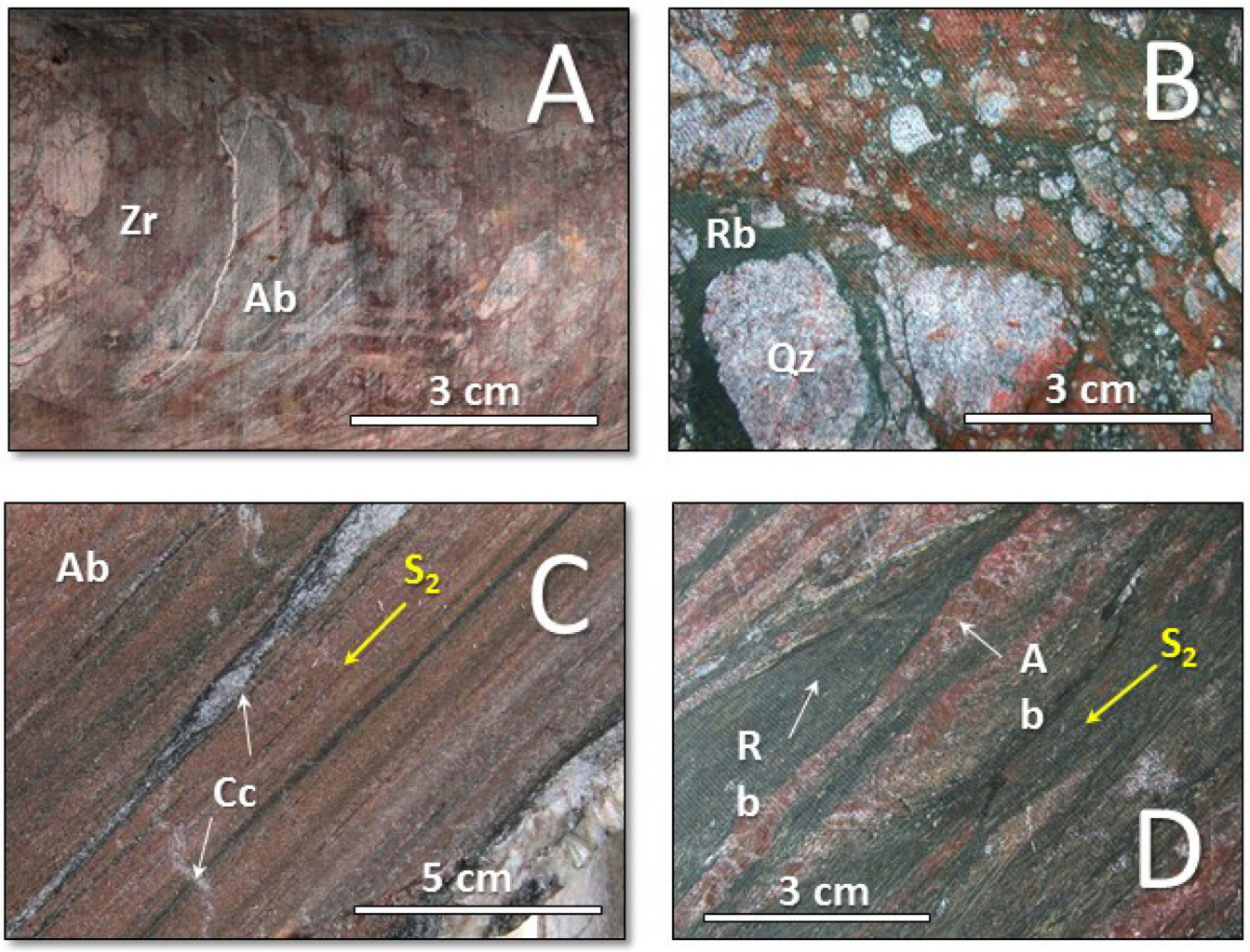

Figure 21.43. Facing page. Photographs of core samples from Valhalla. Each sample is approximately 10cm wide. From Wilde (2006) pmd*CRC I7 unpublished report).

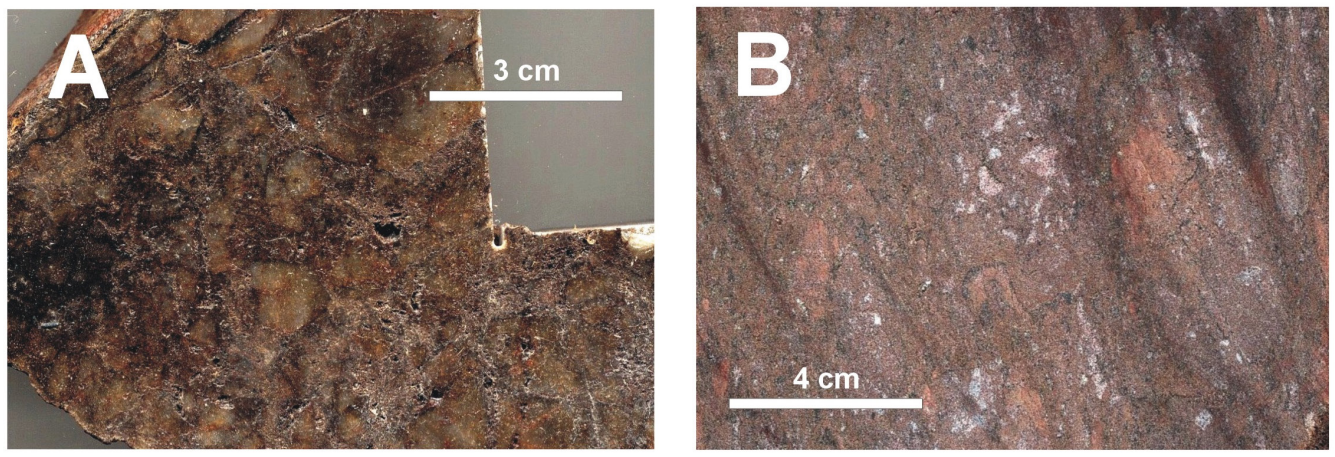

Figure 21.45. Photographs of core samples from Skal From Wilde (2006) pmd*CRC I7 unpublished report) .

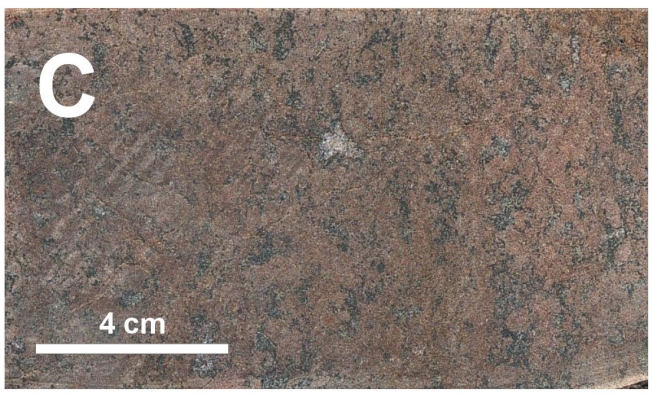

Figure 21.46. Thin section photographs from Polito et al (2009). a. foliated albitite; b. close-up of a showing disseminated magnetite; c. brecciated and uranium-mineralised albitite; d. zircon-rich alteration; e. late-stage uraninite-dominated mineralisation.

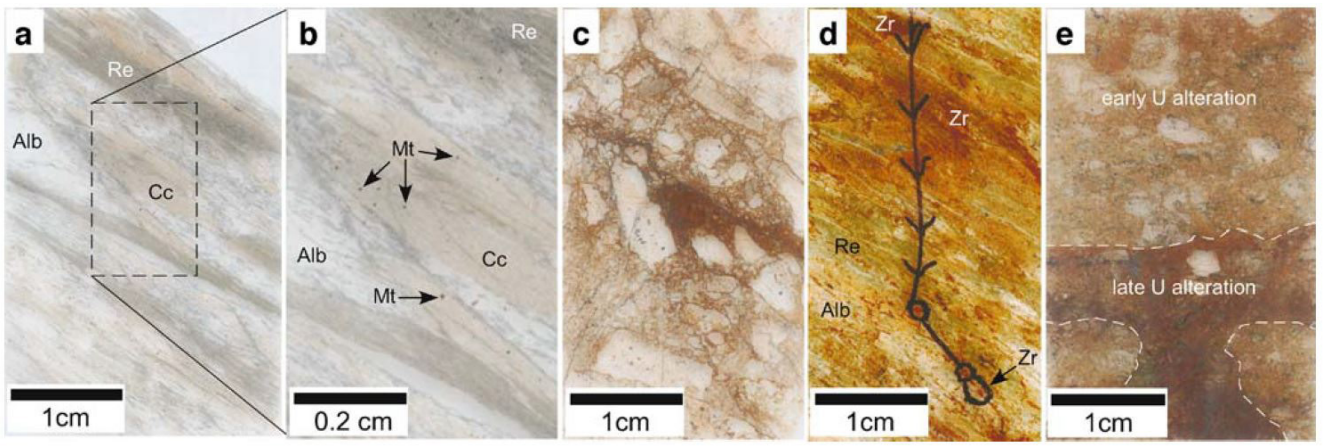

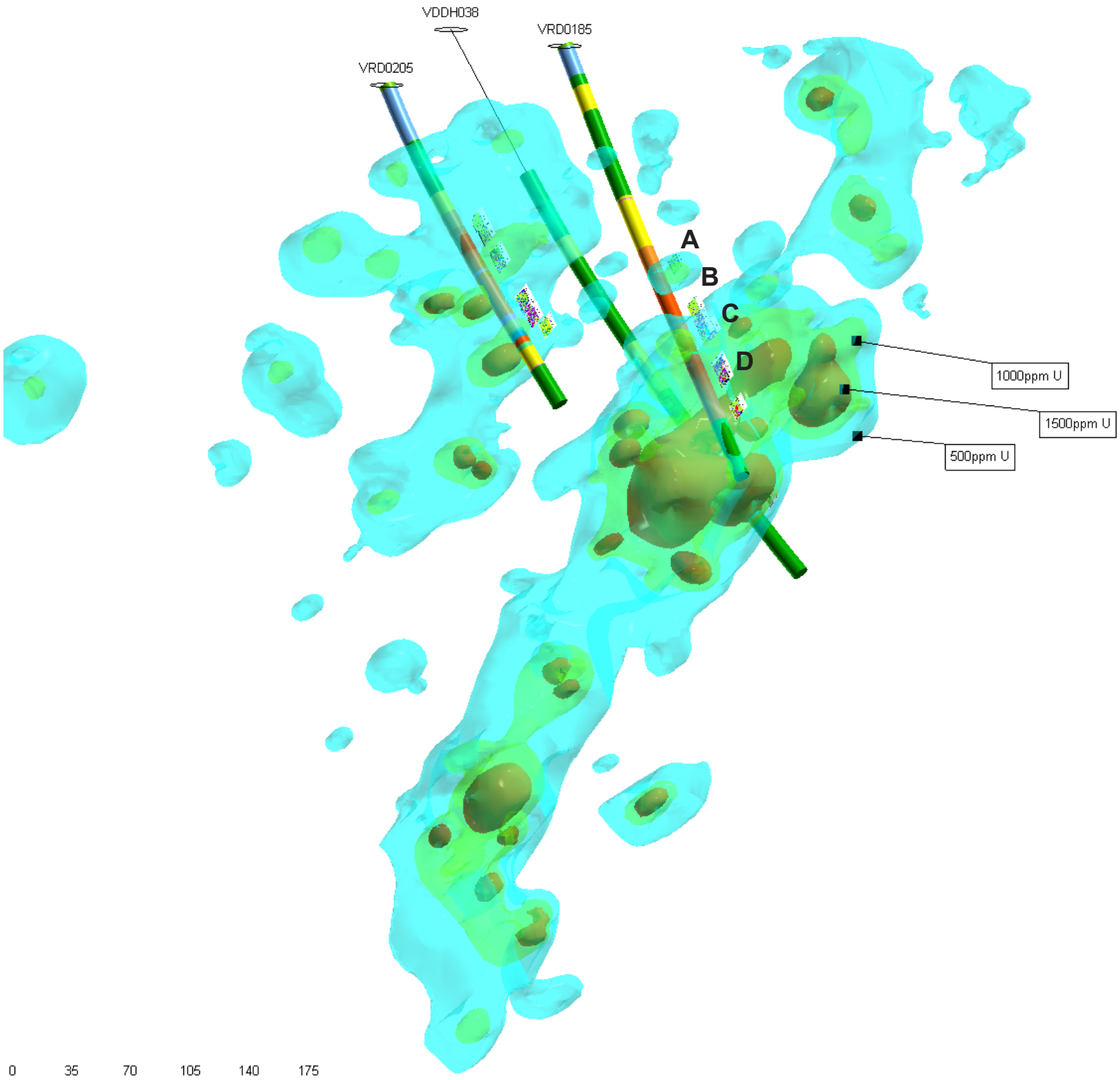

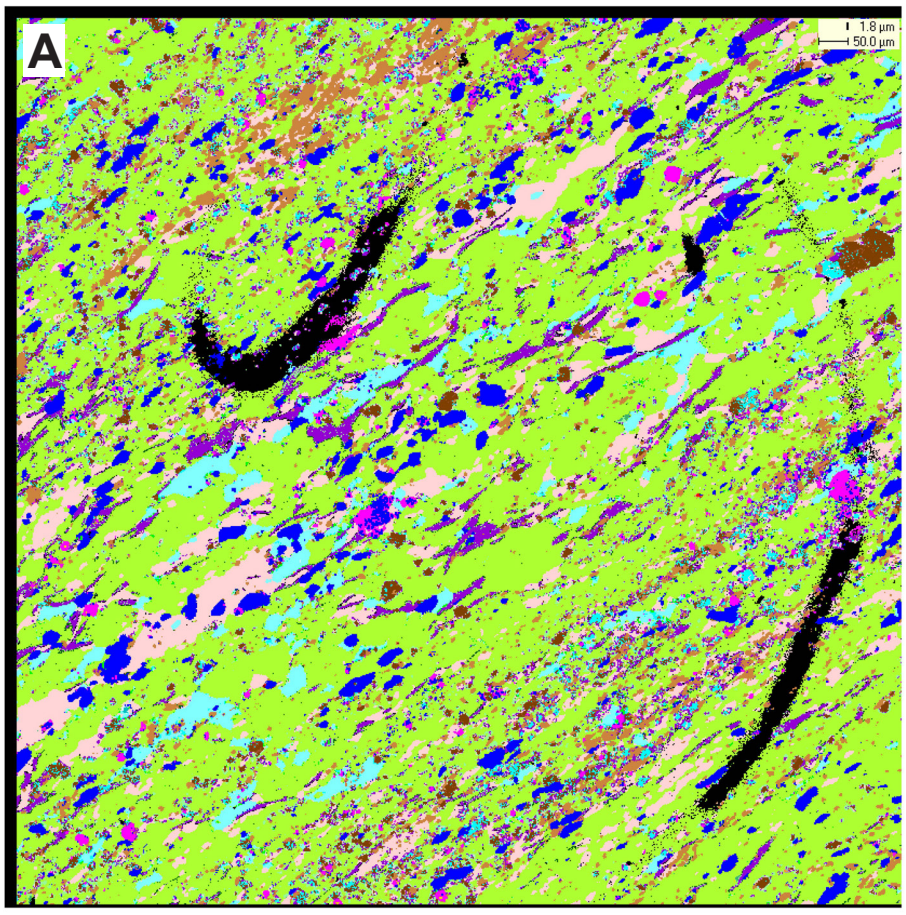

VRD0185-158.8m

- Background
- Brannerite
- Coffinite
- Uraninite
- Uranium-carbonate intergrowths
- Uranium-silicate intergrowths
- U-Intergrowths
- Zircon + U
- Zircon
- Apatite
- Ankerite
- Dolomite
- Calcite
- Other Carbonates
- Albite
- Other Feldspars
- Mica and chlorite
- Epidote
- Quartz
- Riebeckite
- Other Silicates
- REE
- Ti (Fe) Oxides
- Hematite
- Magnetite
- Chalcopyrite
- Galena
- Pyrite
- Others

Figure 21.47. Located QEMSCAN images from Valhalla drillhole VRD0185. A. Low grade strongly foliated albitite, with albite, quartz and ilmenite, as well as lesser zircon, riebeckite, biotite and chlorite. B. Foliated albitite with albite, riebeckite, quartz, magnetite and zircon. C. Massive ore with unfoliated albite, magnetite, ilmenite, riebeckite, quartz and pyrite. Coffinite is the main uranium mineral. D. Brecciated ore type. Main gangue minerals are zircon (18.5%) riebeckite, apatite albite and quartz. Approximately 4.7% magnetite, as well as significant ilmenite and a smaller amount of hematite. Uranium is in fine unidentified uranium mineral intergrowths, coffinite and uraninite.

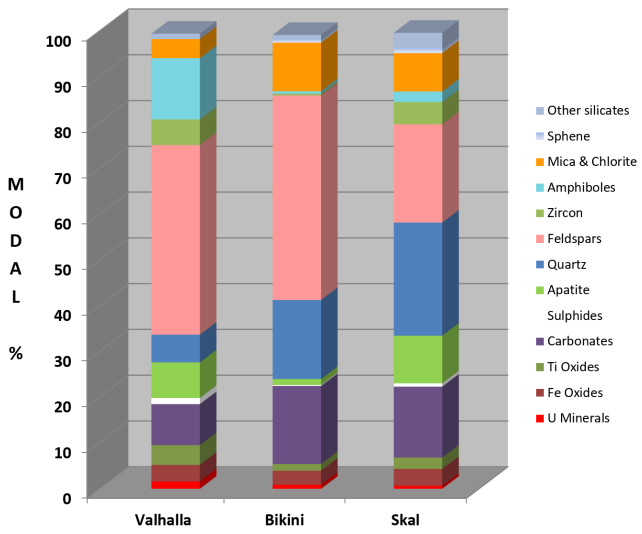

Figure 21.48. Gangue mineralogy from quantitative QEMSCAN analysis of ore frpom the Valhalla region (AMDEL, 2009).

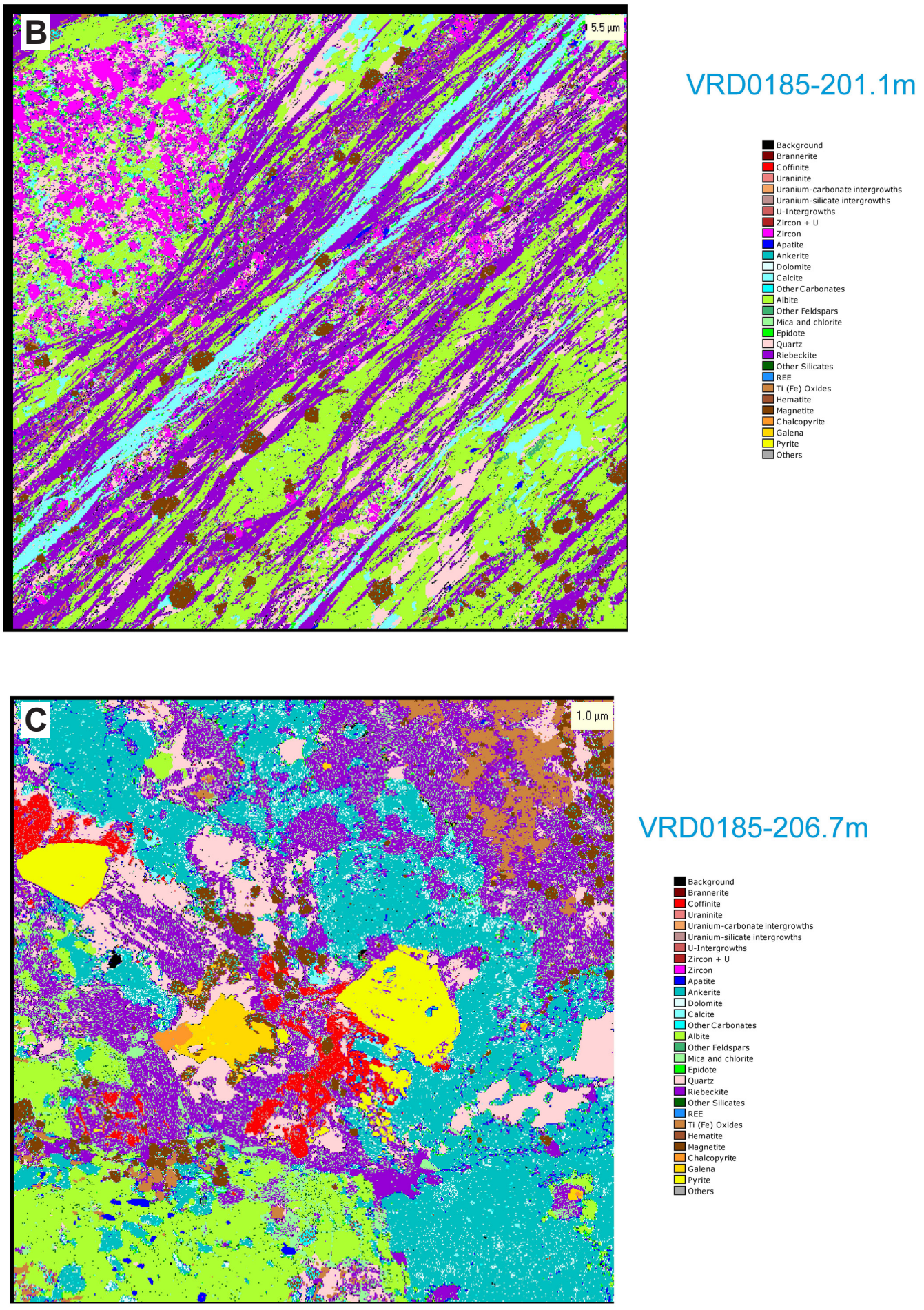

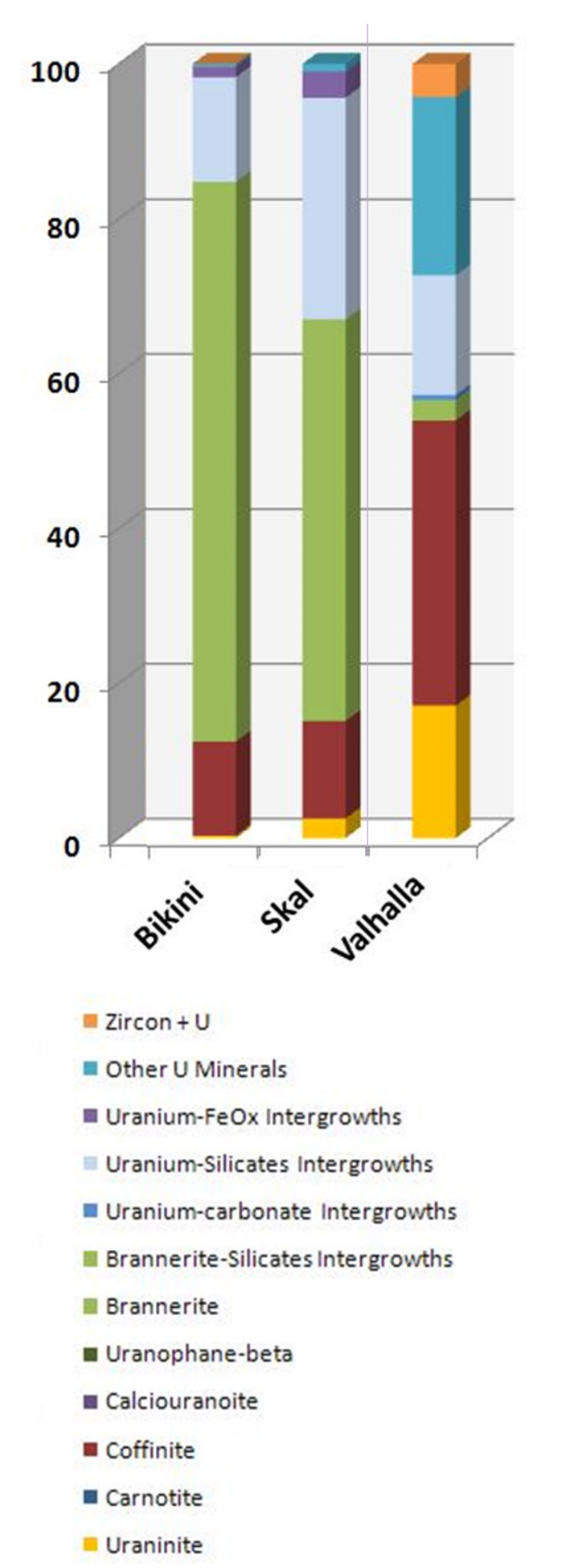

Figure 21.49. Proportions of uranium minerals in Valhalla area deposits based on quantitative QEMSCAN analysis (Wilde et al, 2013).

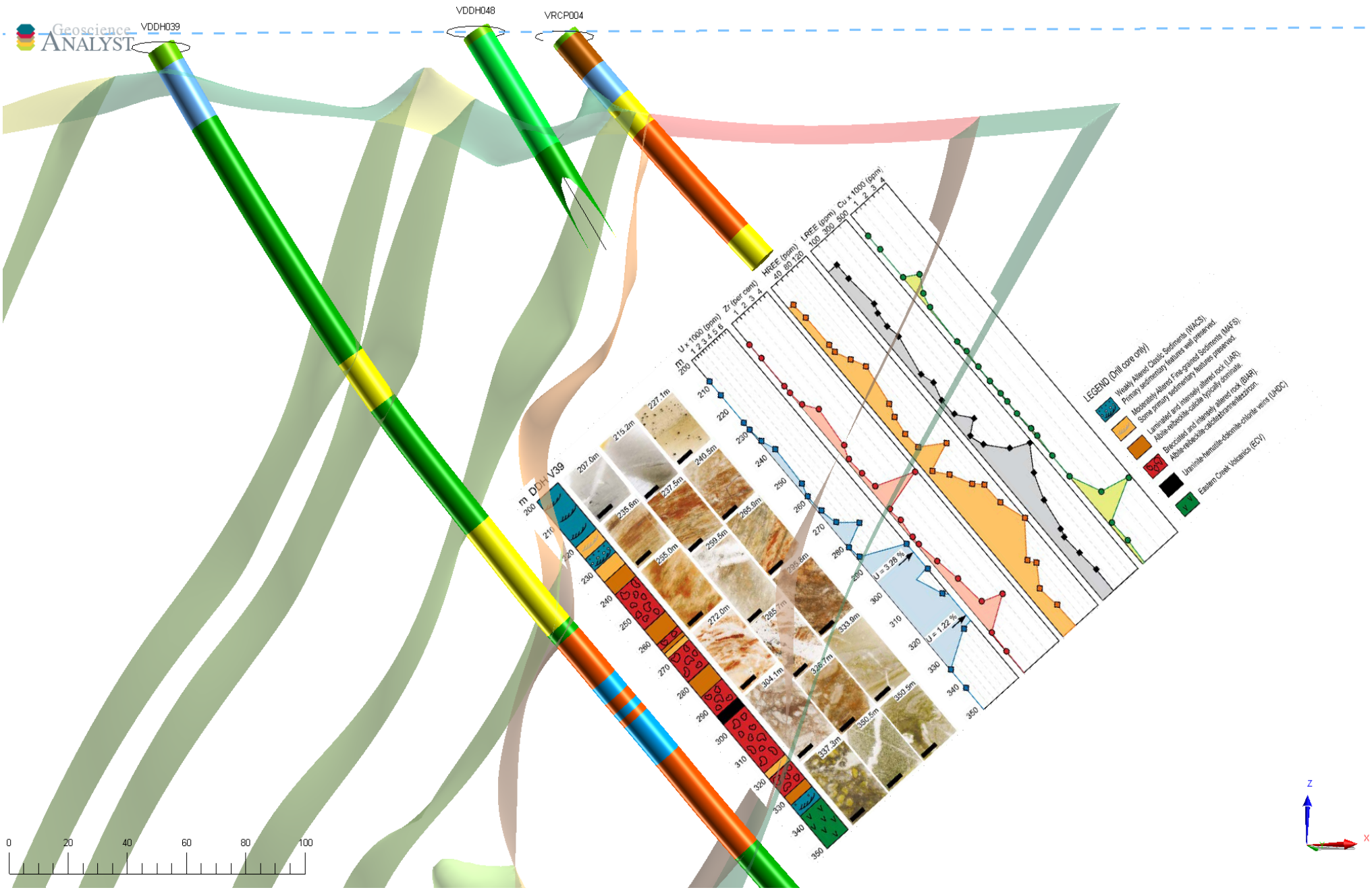

Figure 21.50. W-E cross section through the Valhalla deposit showing the location of drillhole VDDH039. Log, photographs and geochemical graphs sourced from Polito et al, 2009.

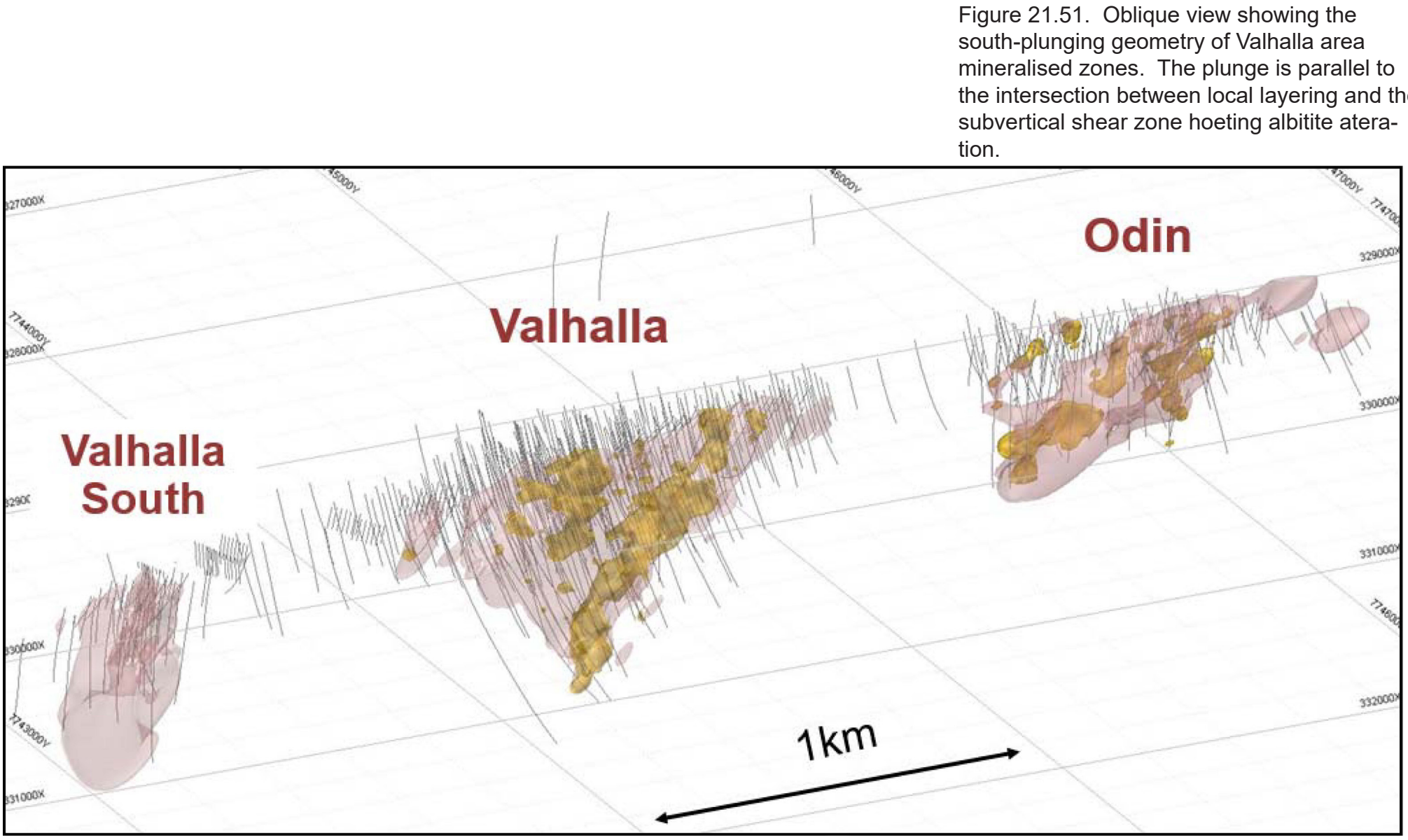

Figure 21.51. Oblique view showing the south-plunging geometry of Valhalla area mineralised zones. The plunge is parallel to the intersection between local layering and the subvertical shear zone hoeting albitite atera-tion.

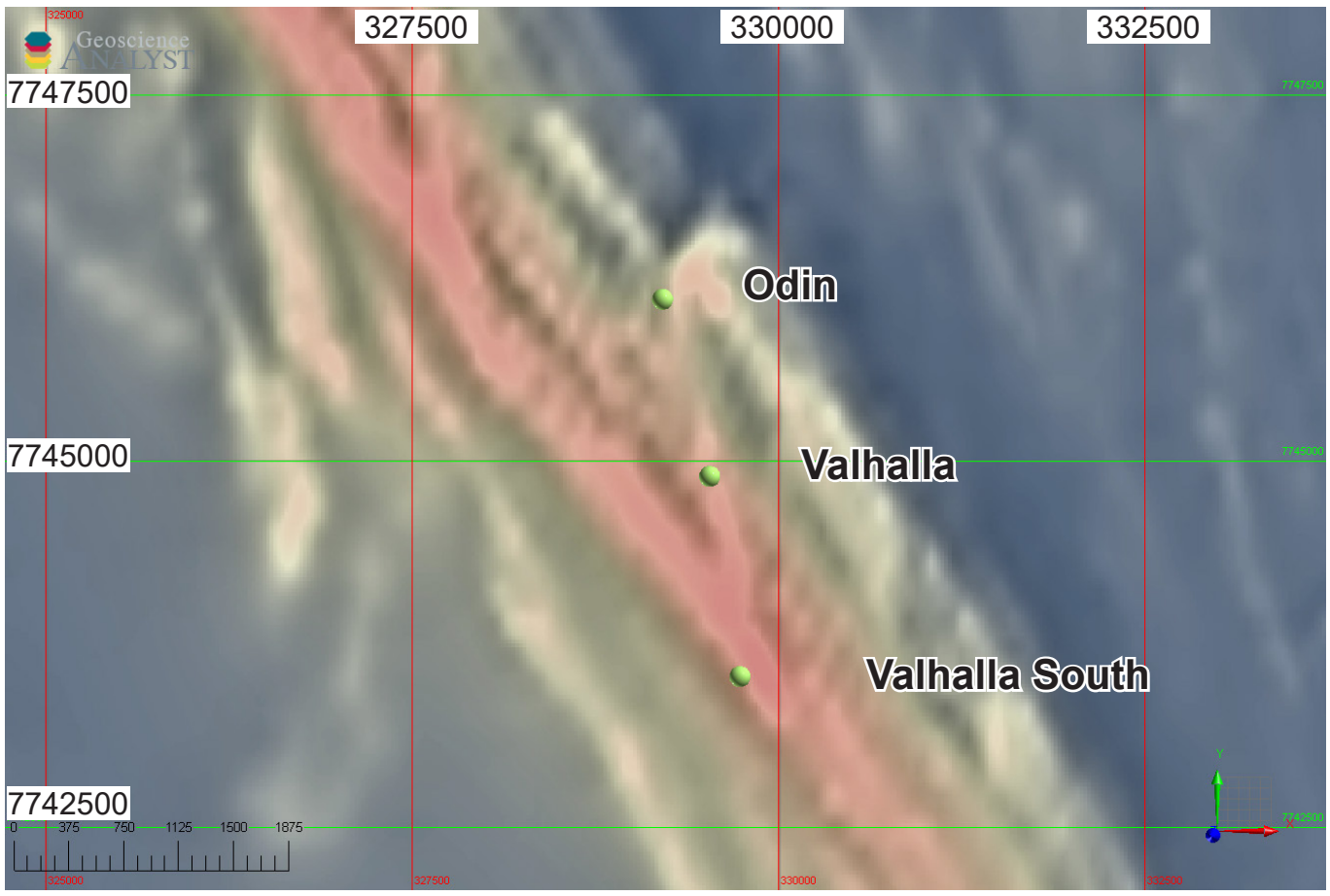

Figure 21.52. Detail of magnetic data over the Valhalla trend, Colour - RTP; Greyscale - RTP vertical derivative. Map Projection AGD84, AMG54.

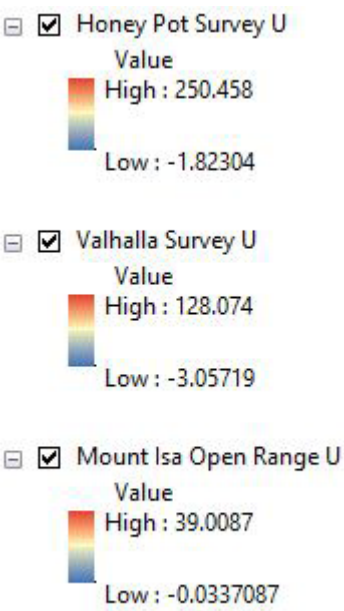

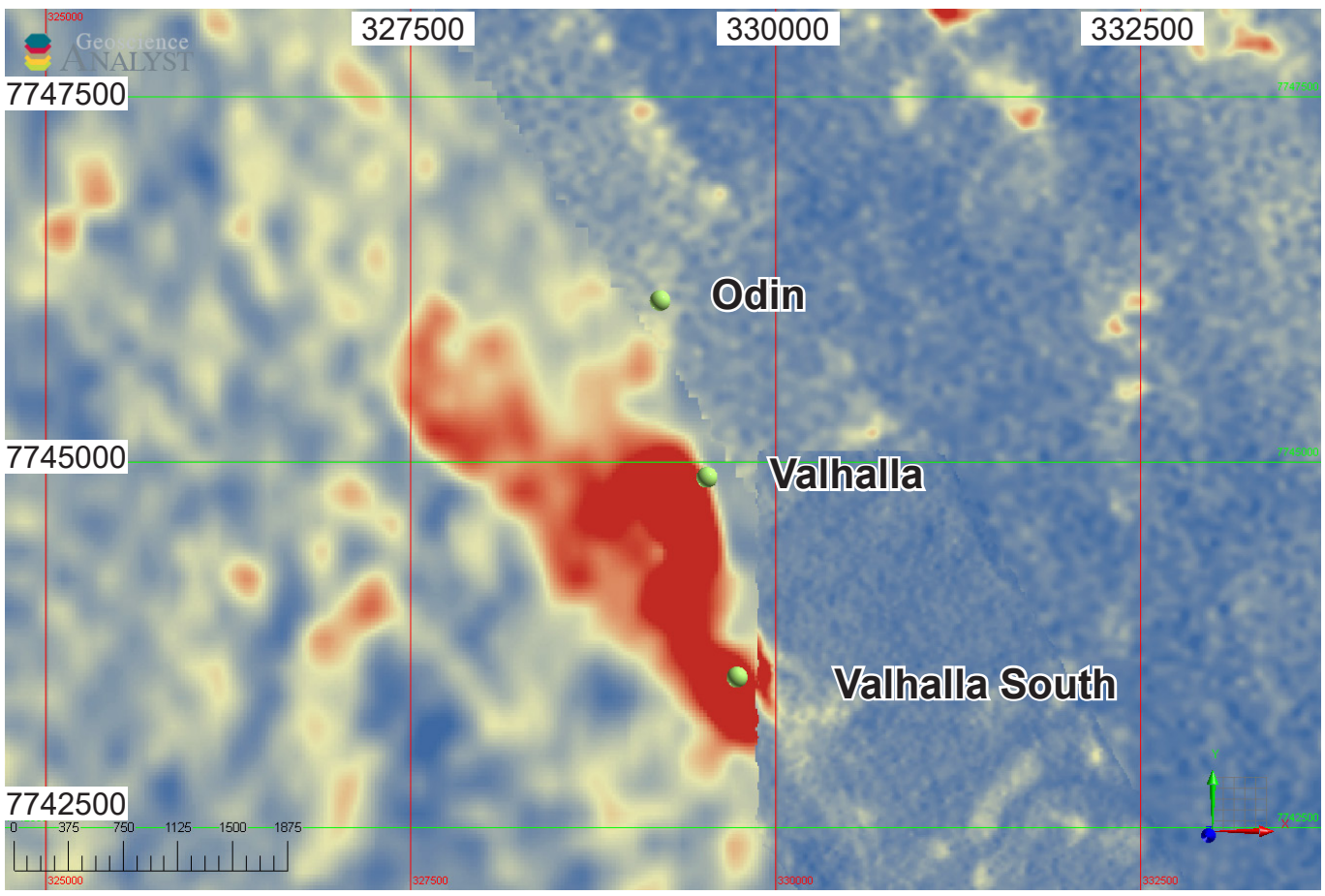

Figure 21.53. Uranium radiometric image over the Valhalla trend. Map Projection AGD84, AMG54.

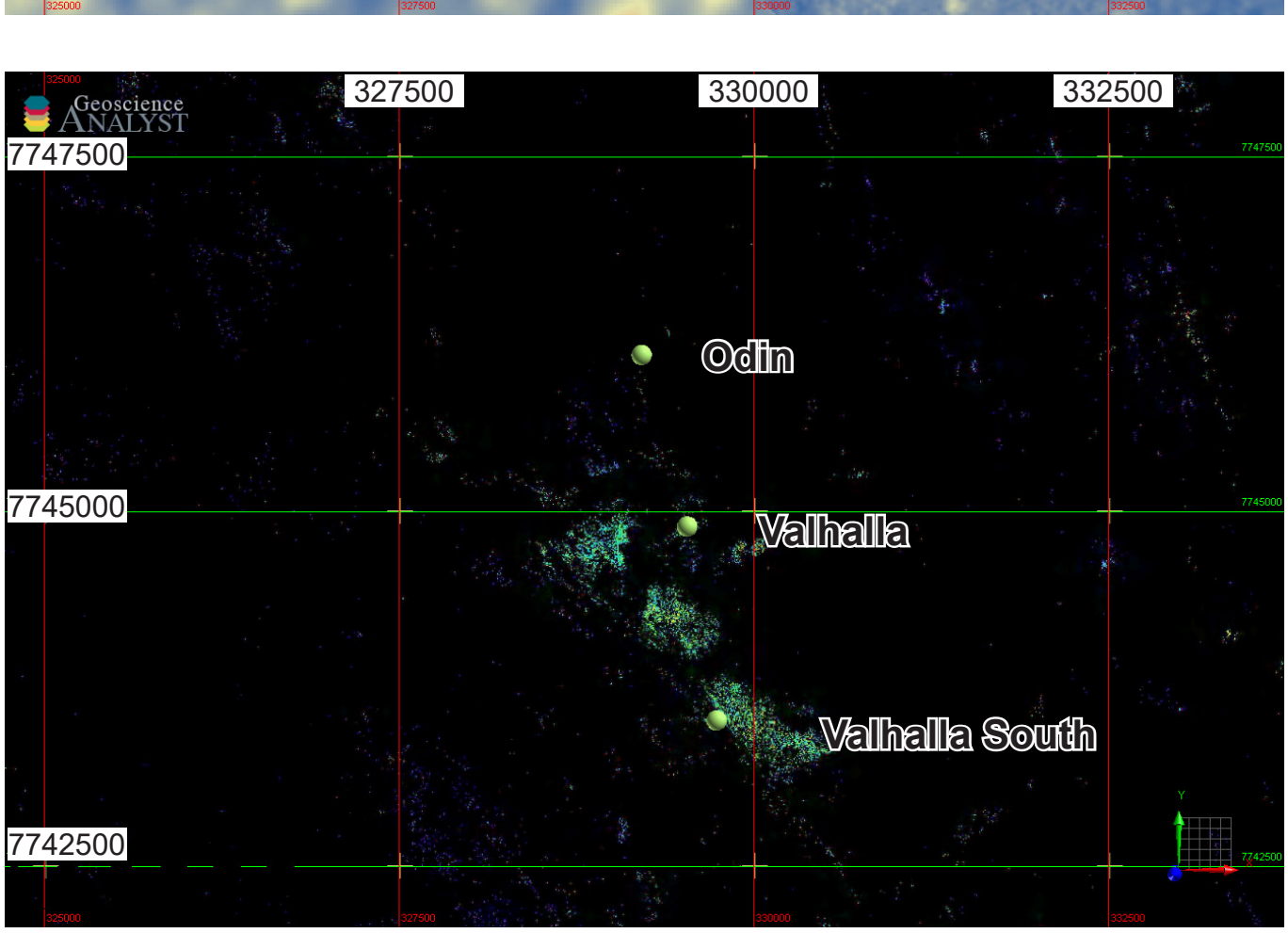

Figure 21.54. Hymap Data over the Valhalla trend - Ferrous iron and MgOH: Attempts to map Fe^{2++}-bearing minerals like actinolite, some chlorites, ankerite and siderite. Blue to red represent low to high content of ferrous iron in pixels with MgOH (+carbonate) mineralogy (black is below threshold). Moderate confidence. There is a zone with anomalous appearance at the south end of the Valhalla trend. For legend see figure 21.31. Map Projection AGD84, AMG54.

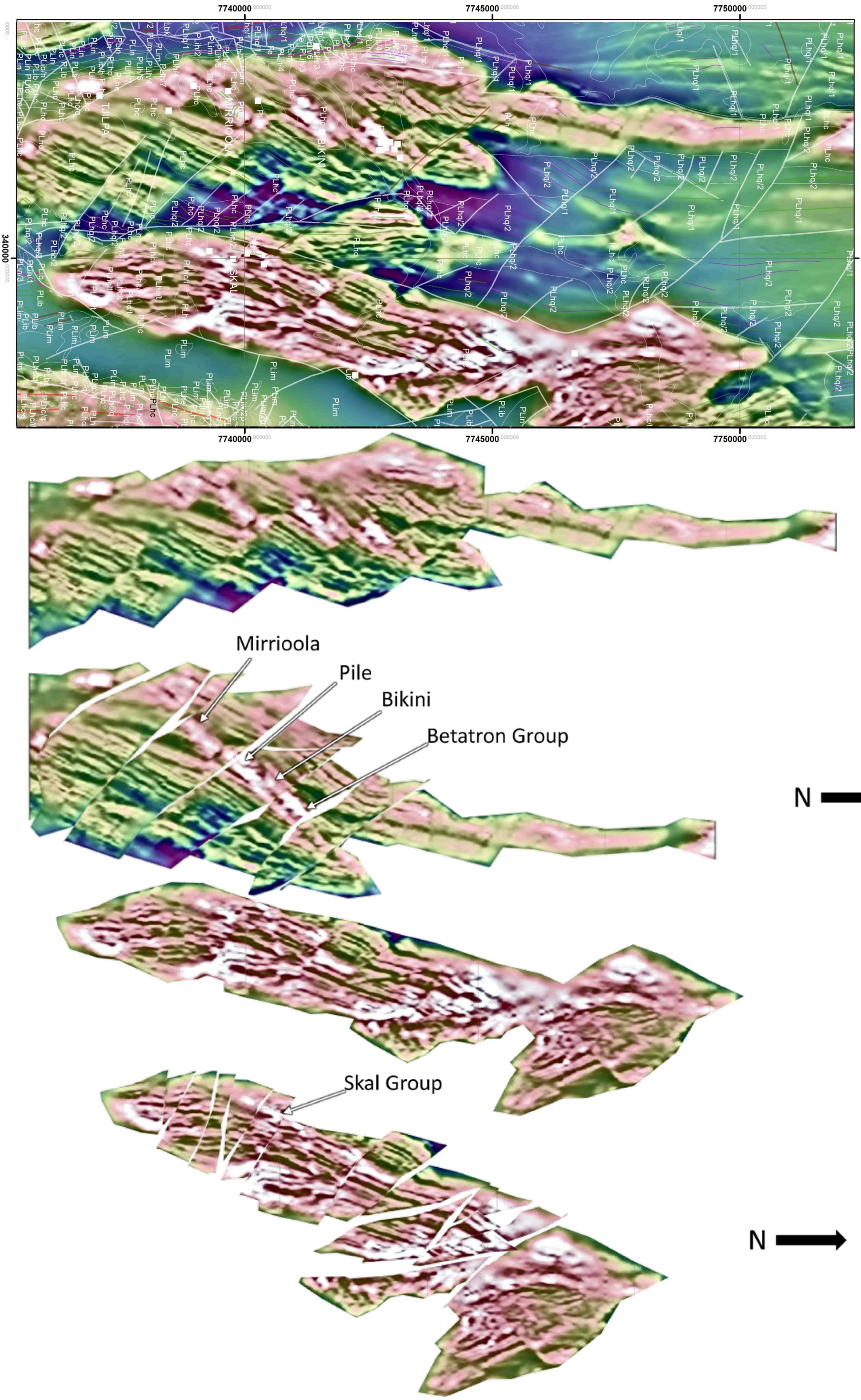
7740000
7745000
7750000
340000
TJILPA
MIRRIOOLA
BIKINI
SKAL
Mirrioola
Pile
Bikini
Betatron Group
Skal Group
N
N

Figure 21.55. Attempted removal of D3 displacement from blocks of ECV metabasalts correlated on the basis of magnetics, for the “belts” hosting the Mirrioola-Bikini and Skal trends. Reconstructions in both cases suggest a >5km zone of albitite alteration which hosts uranium mineralisationMap Projection AGD84, AMG54.

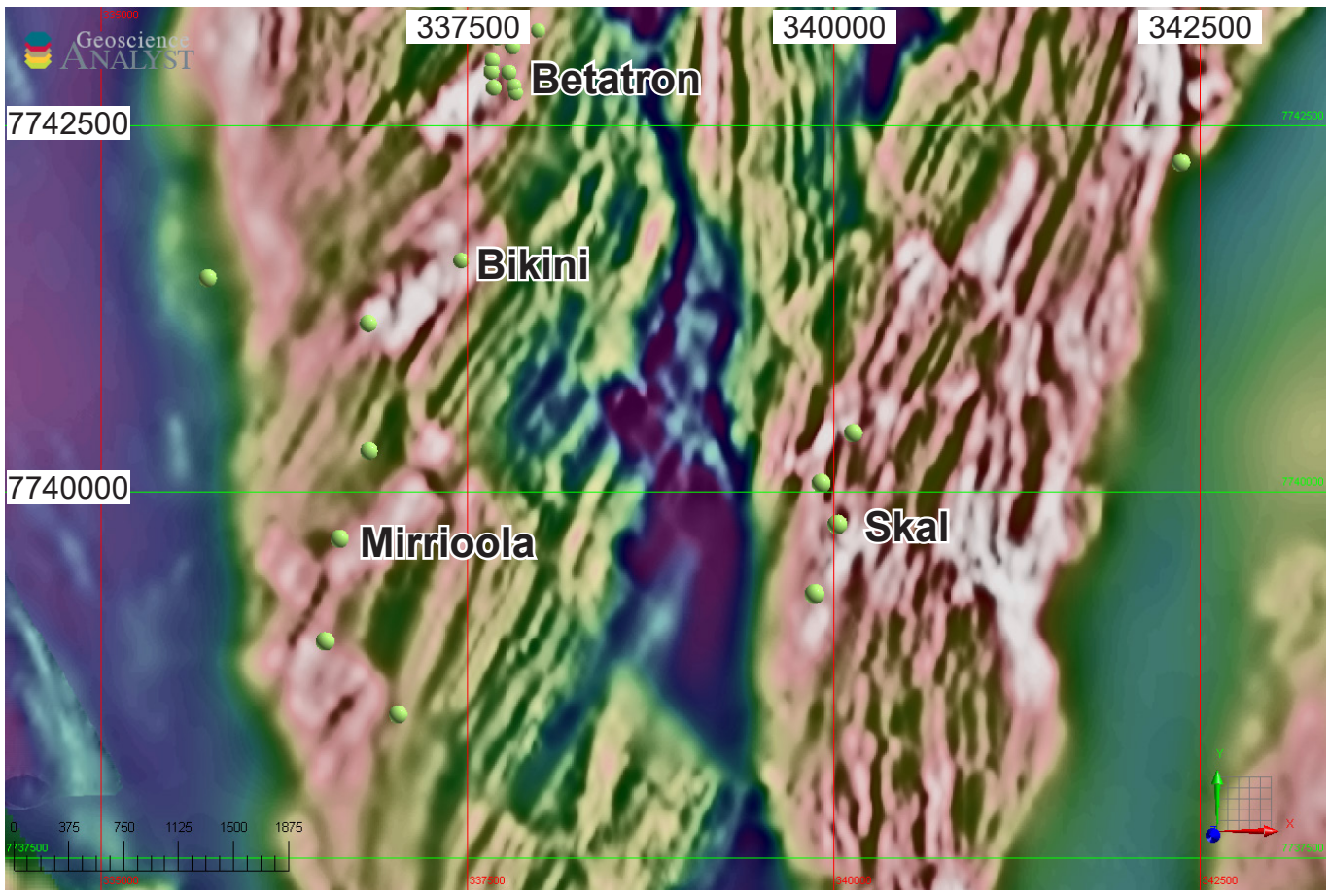

Figure 21.56. Detailed magnetics over the Mirrioola-Bikini-Skal areas. Colour - RTP; Greyscale - RTP VD. Map Projection AGD84, AMG54.

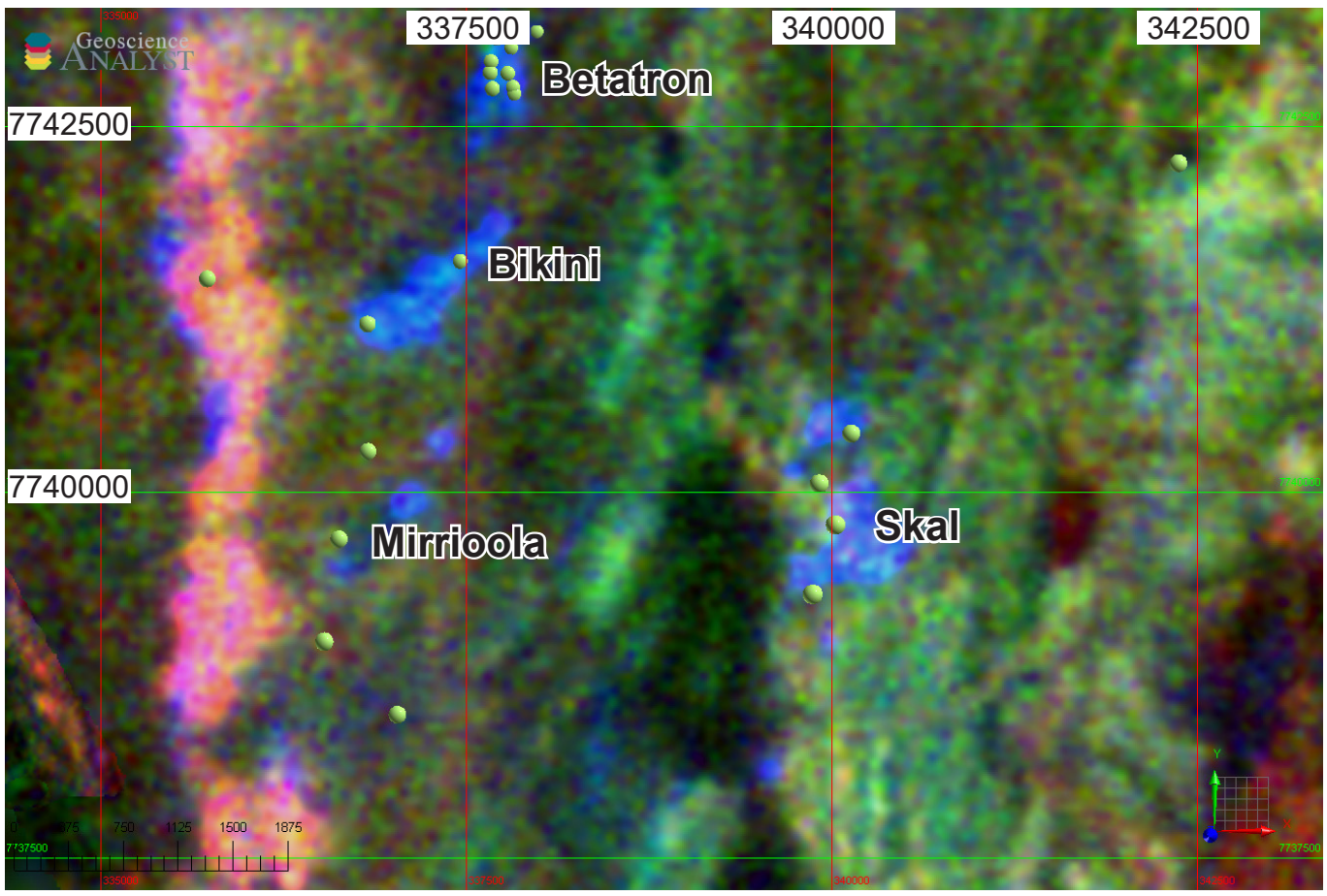

Figure 21.57. Ternary radiometric image over the Mirrioola-Bikini-Skal areas, KThU = RGB. Map Projection AGD84, AMG54.

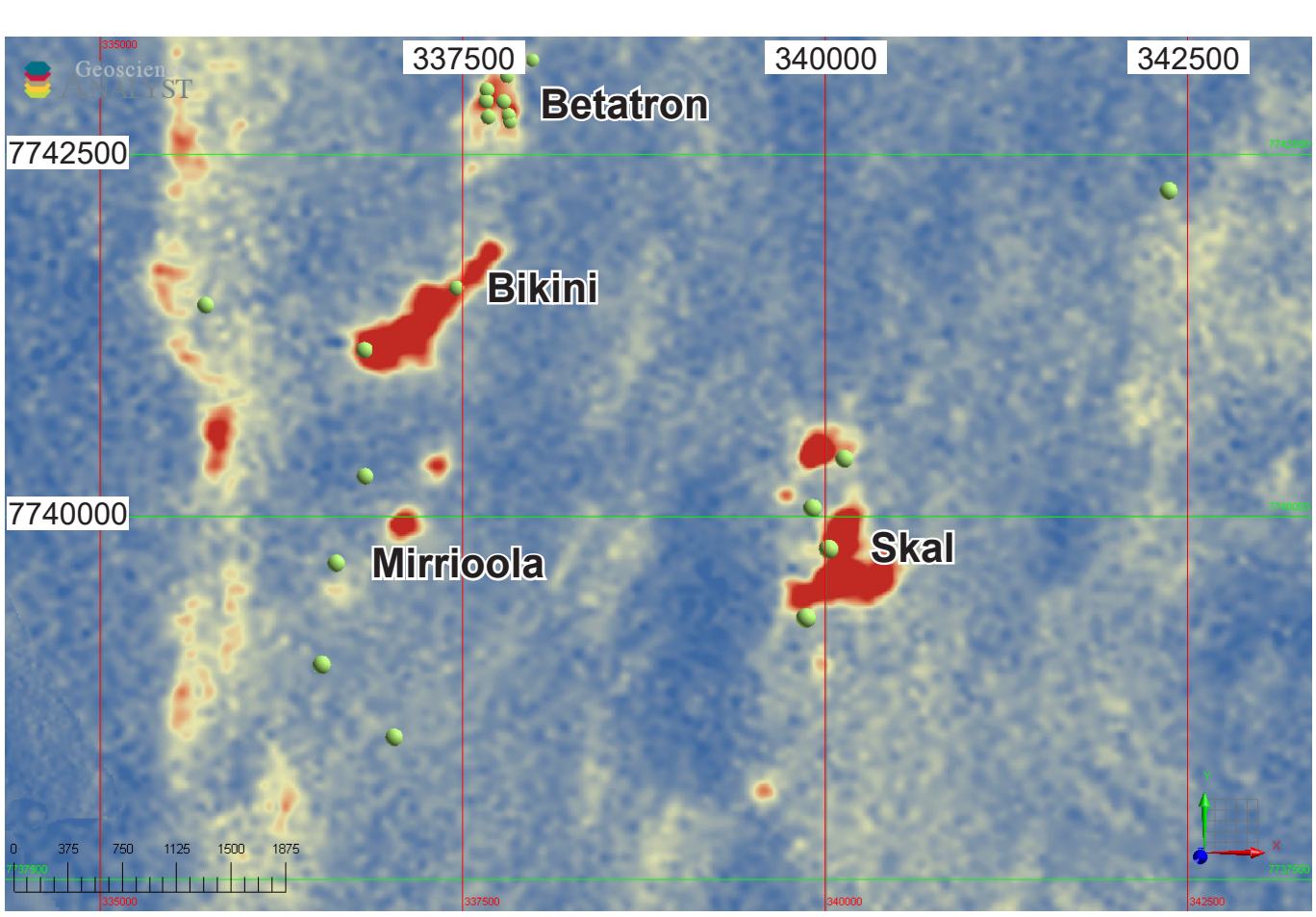

Figure 21.58. Uranium radiometric image over the Mirrioola-Bikini-Skal area. Map Projection AGD84, AMG54.

GENETIC MODEL

Both Both Polito et al (2009) and Wilde et al (2013) proposed that Valhalla and other uranium deposits in the area were representatives of Albitite-type Uranium deposits (Wilde, 2013). Previous authors had noted similarities between these deposits and unconformity-type uranium deposits (Gregory et al, 2005) and IOCG deposits (Hitzman and Valenta, 2005). Common characteristics of this proposed class include (Wilde, 2013):

- Hosted in albitites which are more extensive than mineralisation
- Albitites controlled by brittle-ductile structures
- U mineralisation is post albitisation and associated with dilatant sites along hosting albitised structures
- No host rock preference in class, though ECV clearly important in the Valhalla area
- Abundant fluorapatite and hydrothermal zircon
- Mineralogy - riebeckite, aegirine, garnet, magnetite, hematite, hydrothermal zircon and apatite
- Bulk gain Na; loss of SiO2, K2O, REE, Nb, Hf, Ta. Little Fe addition which is why IOCG interpretations are often discredited
- No obvious magmatic fluid source, though chemical signature suggests carbonatite or alkaline source
- Uranium possibly transported in F, PO4, CO2 complexes
- Chemical controls proposed include:
    - Cooling (Wilde, 2013)
    - Drop in CO2 (Wilde, 2013)
    - Fluid-rock interaction. (Eg Xing et al 2018) – saline, oxidised F-rich fluids reacting with pre-existing magnetite-bearing alteration precipitates uranium

POST-FORMATION MODIFICATION

Both Polito et al (2009) and Wilde et al (2013) noted a late stage of mineralisation which was more uraninite-rich, vein-associated and richer in sulphides. Polito et al (2009) proposed that the approximately 1200 Ma ages derived from geochronological investigations may be indicating the age of the younger uraninite mineralisation

EXPLORATION

Discovery Method

The Valhalla and Skal deposits were both discovered by prospectors in 1954 as part of a period of intense uranium exploration between 1954 and 1956 which involved both airborne and ground-based scintillometer surveying

(McKay and Miezitis, 2001)

REFERENCES

Anonymous. QEMSCAN Analysis Valhalla Uranium Thin Sections, 2009. Unpublished AMDEL Report N3437QS09.

Bain, J.H.C., Heinrich, C.A., Henderson, G.A.M. 1992. Stratigraphy, Structure and Metasomatism of the Haslingdon Group, East Moondarra Area, Mt Isa: A Deformed and Mineralised Proterozoic Multistage Rift-sag Sequence. In Detailed Studies of the Mount Isa Inlier, Australian Geological Survey Organisation Bulletin 243, Stewart, A.J., Blake, D.H., Eds., Australian Geological Survey Organisation: Canberra, Australia, pp. 125–136.

Gregory, M., Wilde, A., Jones, P., 2005. Uranium deposits of the Mount Isa region and their relationship to deformation metamorphism and copper deposition. Econ. Geol. 100, 537–546.

Gregory, M.J., Schaefer, B.F., Keays, R.R., Wilde, A.R., 2008. Rhenium-Osmium systematics of the Mount Isa copper orebody and the Eastern Creek volcanics, Queensland: Implications for ore genesis. Miner. Depos. 43, 553–573.

Hannan, K., Golding, S.D., Herbert, H.K., Krouse, H.R., 1993. Contrasting alteration assemblages in metabasites from Mount Isa, Queensland: Implications for copper ore genesis. Econ. Geol. 88, 1135–1175.

Heinrich, C.A., Bain, J.H.C., Mernagh, T.P., Wyborn, L.A.I., Andrew, A.S., Waring, C.L., 1995. Fluid and mass transfer during metabasalt alteration and copper mineralization. Econ. Geol. 90, 705–730.

Hitzman, M. W., & Valenta, R. K., 2005. Uranium in iron oxide-copper-gold (IOCG) systems. Economic Geology and the Bulletin of the Society of Economic Geologists, 100(8), 1657-1661. doi:10.2113/100.8.1657

McKay, A.D. & Miezitis, Y., 2001. Australia's uranium resources, geology and development of deposits. AGSO – Geoscience Australia, Mineral Resource Report 1.

McPhie, J., Kamenetsky, V., Allen, S., Ehrig, K., Agangi, A., & Bath, A., 2011. The fluorine link between a supergiant ore deposit and a silicic large igneous province. Geology, 39(11), 1003-1006. doi:10.1130/g32205.1

O'Dea, M. G., Lister, G. S., Betts, P. G., & Pound, K. S., 1997a. A shortened intraplate rift system in the Proterozoic Mount Isa Terrane, NW Queensland, Australia. Tectonics, 16(3), 425-441. doi:10.1029/96TC03276

O'Dea, M. G., Lister, G. S., Maccready, T., Betts, P. G., Oliver, N. H. S., Pound, K. S., Huang, W., Valenta, R. K., 1997b. Geodynamic evolution of the Proterozoic Mount Isa terrain. Geological Society Special Publication, 121(1), 99-122. doi:10.1144/GSL.SP.1997.121.01.05

Polito, P., Kyser, K., Stanley, C., 2009. The Proterozoic, albitite-hosted, Valhalla uranium deposit, Queensland, Australia: A description of the alteration assemblage associated with uranium mineralisation in diamond drill hole V39. Miner. Depos. 44, 11–40.

Smith, R. and P. Annan, 1998. "The use of B-field measurements in an airborne time-domain system: Part I. Benefits of B-field versus dB/dt data." Exploration Geophysics 29(1-2): 24-29.

Wilde, A.R., 2013. Towards a model for albitite-type uranium. Minerals 3, 36–48.

Wilde, A., Otto, A., Jory, J., MacRae, C., Pownceby, M., Wilson, N., & Torpy, A., 2013. Geology and Mineralogy of Uranium Deposits from Mount Isa, Australia: Implications for Albitite Uranium Deposit Models. Minerals, 3(3), 258-283. doi:10.3390/min3030258

Xing, Y., Mei, Y., Etschmann, B., Liu, W., & Brugger, J., 2018. Uranium Transport in F-Cl-Bearing Fluids and Hydrothermal Upgrading of U-Cu Ores in IOCG Deposits. Geofluids, 2018, 1-22. doi:10.1155/2018/6835346